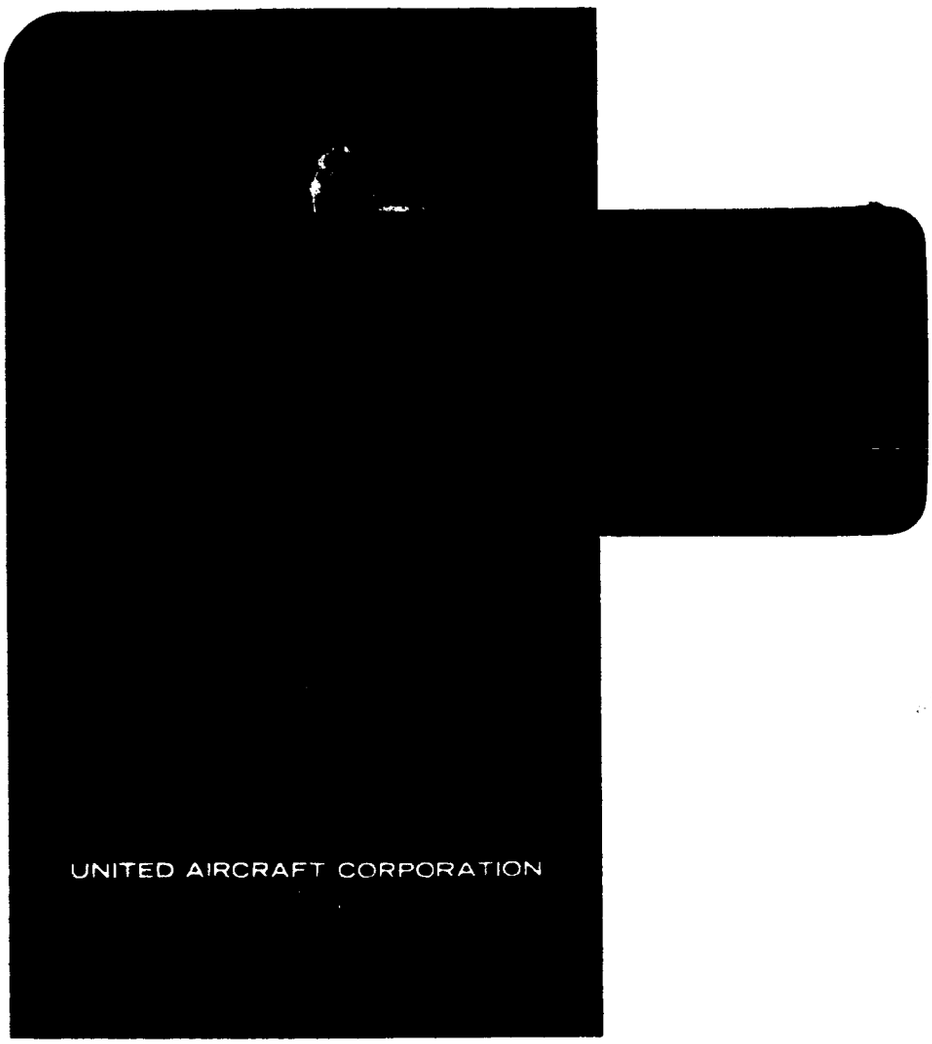

United Aircraft Research Laboratories

EAST HARTFORD, CONNECTICUT

SQT-64207

1 mp

United Aircraft Research Laboratories

UNITED AIRCRAFT CORPORATION

EAST HARTFORD, CONNECTICUT

Report G-110058-28

Handbook for the Study of
Electric Propulsion Systems

UNCLASSIFIED

REPORTED BY _____
R. V. Ragsac

APPROVED BY _____
J. L. Cooley
Assistant Manager of
Advanced Systems Research

DATE November 22, 1968

NO. OF PAGES 141

COPY NO. 32

Report G-110058-28

Handbook for the Study of Electric Propulsion Systems

TABLE OF CONTENTS

TABLE OF CONTENTS (Contd.)

Report G-110058-28

Handbook for the Study of Electric Propulsion Systems

SECTION I

SUMMARY

This report is essentially a compendium of techniques and basic information useful to the preliminary performance analysis of power-limited (low-acceleration, electric) propulsion systems applied to space missions. The material is presented in handbook form and is reasonably complete within itself insofar as a basic understanding of the techniques and procedures is required for one to acquire facility in computing performance. This, in essence, is the objective of the handbook. The accumulation and organization of the material selected for inclusion was guided by the desire for simplicity and computational ease while maintaining a sufficient level of completeness for a general understanding (i.e., to avoid a "cookbook" approach).

Use of Handbook

It is intended that two specific purposes be served. The first is that the preliminary analysis of low-thrust, electric propulsion systems could be accomplished quickly by anyone experienced in calculating vehicle system performance. The second is the long-range desire to have electric propulsion applied to as many concepts of missions, flight and propulsion modes, and objectives as possible, a condition presently deficient when compared to high-thrust (chemical and nuclear) systems. Of particular importance, however, is not only the evaluation of mission concepts but also the immediate problem of investigating the related technology requirements of the major subsystems such as the powerplant, the electric propulsion units, and the associated surface launch vehicles.

The jet power that an electric propulsion system is capable of producing is limited by the maximum power available from the power supply. This power limitation, in addition to the mass of the power system and the long-duration thrusting times, enters into the performance evaluation through the necessary optimization of the powered flight trajectory. This coupling between the system parameters and the powered-trajectory optimization necessarily causes the analysis of power-limited

systems to be more complex than the study of high-acceleration (impulsive-thrust) propulsion systems. Consequently, the present effort was centered about two aspects: first, to uncouple the influence of the system parameters from the trajectory optimization by suitable approximate techniques and to reduce the performance evaluation to a series of equations; second, to present as much appropriate heliocentric and planetocentric trajectory information as is currently available along with auxiliary information related to the application of these trajectories.

Because of certain necessary restrictions, the contents herein are neither complete in terms of depth of analytical development nor of sufficiently large scope to include all possible types of interplanetary flight modes and vehicle subsystems. Enough graphical data and study aids are presented, however, to allow immediate estimates to be made for the simplest power-limited system and trajectory model. For more complicated cases (e.g., expanded definition of propulsion system constituents and vehicle payload) fairly complete equations and related graphs are offered. Generally, initial approximations to system performance can be made given the proper trajectory information; such results are usually regarded as sufficiently accurate for estimating payload potential and overall vehicle mass requirements.

The important mission modes not included in this handbook are trips to a heliocentric position and velocity (e.g., solar orbiter, 1-AU inclined orbiter, solar flyby). The variation of power system output as a function of heliocentric position or of time was also omitted. It should be pointed out, however, that the analytical approaches discussed herein are independent of flight and power modes; they are still applicable provided the proper heliocentric trajectory data are utilized.

Sections II, III, and IV deal primarily with the mass equations of power-limited systems, the related graphs, and heliocentric and planetocentric trajectory information. The basic methods and data necessary for estimating the performance of power-limited systems are presented in these first three sections. Extensions of the background theory which encompasses certain flight modes are presented in Section V; the application of these extensions is discussed in Section VI through several sample analyses. Not all necessary trajectory information is presented in this handbook; thus a description of the major UARL trajectory computer programs as well as related mass optimization decks are briefly given in Section VIII. The Appendices in Section VIII offer more detailed information on some of the aspects covered in the text.

The majority of the information presented herein was extracted from three basic sources: a) Contract NAS8-11309, Study of Low-Acceleration Space Transportation Systems, performed for the Advanced Systems Office, G. C. Marshall Space Flight Center; b) Contract NAS2-2928, Study of Trajectories and Upper Stage Propulsion Requirements for Exploration of the Solar System, performed for the Mission Analysis Division, OART; and c) United Aircraft Research Laboratories' Corporate-sponsored programs. The preparation of this report was also under Corporate sponsorship.

SECTION II

MASS EQUATIONS OF POWER-LIMITED SYSTEMS

Basic Relationships

The power in the exhaust jet of an electric propulsion system is derived from a separate power supply which is limited in its output. Vehicles employing these types of propulsion systems therefore undergo power-limited flight and are restricted to thrust accelerations of not more than 10^{-3} g. The rocket equation for power-limited systems must include the mass, m_w, and maximum power rating, P, of the powerplant. The parameter usually employed to denote power system capability is the powerplant specific mass,

$$\alpha_w \equiv \frac{m_w}{P}$$

The thrust from the exhaust jet is given by

$$F = \dot{m}_p C$$

where $\dot{m}_p$ is the propellant flow rate and C is the exhaust velocity. The power in the beam is

$$p = \frac{1}{2} \dot{m}_p C^2$$

The thrustor converts the power supply output into jet power, and its ability to do so efficiently is accounted for through the thrustor efficiency, η.

$$p = \eta P$$

In general, η is a function of the exhaust velocity delivered by the thrustor (i.e., the specific impulse for a particular thrustor type and design).

Using the fact that the thrust acceleration, a, at any time is the jet thrust over the instantaneous mass of the vehicle, m(t), and using the foregoing relationships, then

$$\frac{1}{m(t)} = \frac{1}{m_0} + \frac{1}{2}\int_0^t \frac{a^2}{\eta P}\, dt$$

It can be seen that to maximize vehicle mass relative to the initial mass, m_0, requires a thrusting program with time which minimizes the integral. This is contrasted to high-acceleration systems for which minimum $\int(a/c)\, dt$ is sought.

Two general types of thrusting programs have been of interest in the analysis of power-limited flight. The first mode considers the thrust magnitude and direction to be completely unconstrained during the flight, ("variable-thrust" operation). The second mode fixes the thrust magnitude but allows the direction to be unconstrained ("constant-thrust" operation). Generally, constant-thrust operation gives rise to heliocentric coast periods. In terms of propulsion system design, the latter mode is desired, since the powerplants and thrustors need not operate over a wide range of output. In terms of payload, however, the variable-thrust mode yields higher values than the constant-thrust case because the thrust vector is completely unconstrained.

In general the power supply output is assumed to be constant with time and may be removed from the integral. However, the outputs of radioisotope and solar power systems are functions of heliocentric position and/or time, and thus the determination of a thrusting program using these types of systems must account for the output variations. For the case of variable thrust, the efficiency must be included in the integral since it varies with exhaust velocity.

By referencing the vehicle mass at the end of powered flight to the initial mass, the rocket equation in nondimensional form becomes

$$\frac{1}{\mu_1} = 1 + \frac{1}{2}\,\frac{a_w J}{\eta \mu_w} \qquad (1)$$

where $\mu_1 \equiv m_1/m_0$, the terminal mass fraction,

$\mu_w \equiv m_w/m_0$, the powerplant fraction,

$J \equiv \int a^2 dt$, the trajectory characteristic.

For convenience and for preliminary mission and system study purposes, η and P were assumed constant.

The minimization of J for a particular flight is a calculus-of-variations problem wherein the integral must be minimized subject to the equations of motion and to certain conditions specified at the boundaries of the trajectory and other points if required. A minimum value of J assures only maximum final mass fraction and does not imply maximum payload.

Maximization of Payload Fraction

For a given minimum-J trajectory, the payload is maximized by properly selecting the powerplant fraction in the case of variable-thrust operation (exhaust velocity is unconstrained). In the constant-thrust mode, both the optimum exhaust velocity and powerplant fraction must be determined. Relationships may be derived to give the optimum parameters; the actual values they take on depend on the definition of the payload fraction that is used.

Payload Definitions

The payload fraction, μ_L, could simply be defined as the mass left over at the end of flight, excluding the powerplant. Thus

$$\mu_L = \mu_1 - \mu_w \qquad (2)$$

Under this definition the payload may be interpreted as consisting of the actual payload and the miscellaneous and tie-in structure, while the thrustor and propellant tanks may be considered part of the powerplant. In the latter instance the definition of α_w is changed to mean the propulsion system specific mass, part of which consists of the powerplant specific mass.

In a first approximation, the mass of the inert tanks depends on the amount of propellant required and the type of design employed, whereas the tie-in structure depends to some extent on the mass of the various subsystems which form the propulsion system. The thrustor mass depends, generally, on the power input and exhaust velocity

it is required to accommodate. Thus an expanded definition of payload should include these dependencies. The basic definition for payload mass can be written

$$m_L = m_1 - (m_W + m_F + m_T + m_S)$$

where the masses of the powerplant, thrustor, tanks, and structure, respectively, are subtracted from the final mass at the end of thrusting.

The tank mass can be determined by defining a tank propellant mass fraction, ρ, similar to that used in high-thrust rocket technology.

$$\rho \equiv \frac{m_P}{m_P + m_T}$$

The structure mass is assumed to be proportional to the mass of the thrustor, tank, propellant, and powerplant, in which case a proportionality constant, σ, may be defined

$$\sigma \equiv \frac{m_S}{m_F + m_T + m_P + m_W}$$

Normalizing with respect to initial mass and defining a thrustor specific mass $\alpha_F(C) \equiv m_F/P$ (a function of C), the nondimensional payload becomes

$$\mu_L = 1 - \left(\frac{1+\sigma}{\rho}\right)(1 - \mu_1) - (1+\sigma)\left[1 + \frac{\alpha_F(C)}{\alpha_W}\right]\mu_W \qquad (3)$$

Both definitions are now analyzed for maximum payload under the two types of modes.

Variable-Thrust Payload Maximization

Substituting the rocket equation into the simplified payload equation and setting the derivative of μ_L with respect to μ_W equal to zero, the optimum powerplant fraction can be determined.

$$\mu_{W_{OPT}} = \beta(1-\beta) \tag{4}$$

and the corresponding maximum payload is

$$\mu_{L_{MAX}} = (1-\beta)^2 \tag{5}$$

with propellant mass

$$\mu_p = \beta, \tag{6}$$

where, for convenience

$$\beta^2 \equiv \frac{a_w J}{2\eta},$$

which is a fixed quantity for a particular minimum-J trajectory and type of powerplant.

For the improved payload definition, the same procedure yields

$$\mu_{W_{OPT}} = \beta\left[\frac{1}{\sqrt{\rho\left(1+\frac{a_F}{a_w}\right)}} - \beta\right] \tag{7}$$

and the corresponding maximum payload is

$$\mu_{L_{MAX}} = 1 - 2(1+\sigma)\sqrt{\frac{1}{\rho}\left(1+\frac{a_F}{a_w}\right)}\beta + (1+\sigma)\left(1+\frac{a_F}{a_w}\right)\beta^2 \tag{8}$$

with propellant mass

$$\mu_p = \sqrt{\rho\left(1 + \frac{\alpha_F}{\alpha_W}\right)}\,\beta \tag{9}$$

Note that if $\rho = 1$, $\alpha_F = 0$, and $\sigma = 0$, then Eqs. (7), (8), and (9) revert back to the original set based on the simplified payload fraction definition, Eqs. (4), (5), and (6).

The maximum value of powerplant specific mass for a given (variable-thrust) minimum-J trajectory can be found by requiring that Eq. (8) be greater than or equal to zero. Hence

$$\beta^2 = \frac{\alpha_W J}{2\eta} \leq \frac{1}{\rho}\left[1 - \sqrt{1 - \frac{\rho}{1+\sigma}}\right]^2 - \frac{\alpha_F J}{2\eta}$$

In contrast to the simple condition that $\beta^2 \leq 1$, as implied from Eq. (5), the highest value of β^2 is directly reduced by the thrustor specific mass but is also increased by lowering the value of ρ, the tank propellant mass fraction. However, lower values of ρ, of course, decrease the maximum value of payload fraction attainable for a given trajectory.

In developing the foregoing equations it has been tacitly assumed that the power and thrustor efficiency are constant with time. The first assumption appears to be reasonable for mission study purposes, while the second is strictly a convenience, since the exhaust velocity varies with time for variable-thrust operation. The payload values derived under these circumstances therefore represent an upper limit.

Constant-Thrust Payload Maximization

If the exhaust velocity, C, and powerplant fraction, μ_w, are fixed for a specific flight, a steering program (which may involve coast periods) must be found that minimizes J, thereby assuring that the final mass is a maximum. Thus the resulting value of J depends on the initial values of C and μ_w and the steering program based on these values. Consequently, the overall optimization problem is to determine C, μ_w, and the proper steering program (and hence J) which maximize the payload fraction.

Substituting the rocket equation, Eq.(1), into the simplified payload definition, Eq. (2), yields

$$\mu_L = \frac{1}{1 + \frac{\gamma^2}{\eta \mu_w}} - \mu_w$$

where $\gamma^2 \equiv \alpha_w J/2$, and η is some function of C. Since constant-thrust operation is employed, the exhaust velocity is constant and η can be removed from the integral.

The total derivative of μ_L with respect to C, μ_w, and γ^2 must be set equal to zero in order to maximize payload. The approach employed here for both payload definitions closely follows that developed by Melbourne and Sauer, Ref. II-1. Thus,

$$d\mu_L = \frac{\mu_1^2 \gamma^2}{\eta^2 \mu_w} \eta' dC + \left(\frac{\mu_1^2 \gamma^2}{\eta \mu_w^2} - 1 \right) d\mu_w - \frac{\mu_1^2}{\eta \mu_w} d\gamma^2 = 0 \qquad (11)$$

where $\eta' = d\eta/dC$.

A characteristic of power-limited systems is that the vehicle at the end of flight has essentially most of its initial mass. Thus it is expected that changes in the powerplant mass do not influence, significantly, the final mass or the thrust acceleration time history. This consideration leads to two important assumptions (Ref. II-1): first, the minimum value of J is independent of μ_w, and second, the average thrust acceleration over a minimum-J trajectory is independent of μ_w. The former assumption implies that $d\gamma^2/d\mu_w = 0$, while the latter permits a relation to be obtained between C and μ_w.

The thrust acceleration at any time, in terms of the propulsion system parameters, is given by

$$a = \frac{2 \eta \mu_w}{\alpha_w C \mu} \qquad (12)$$

where μ is the vehicle mass fraction at any time ($\mu_0 = 1$). For a known minimum-J, constant-thrust trajectory the average thrust acceleration may be written either as an arithmetic mean (AM) or geometric mean (GM). Thus

$$\bar{a} = \frac{a_0 + a_1}{2} \text{ AM}, \quad \bar{a} = (a_0 a_1)^{1/2} \text{GM},$$

where $\bar{a}$ is a constant. These expressions may be rewritten using the equation for thrust acceleration.

$$\bar{a} = \frac{a_0}{2}\left(1 + \frac{1}{\mu_1}\right) \text{ AM}, \quad \bar{a} = \left(\frac{J}{T_c}\right)^{1/2} \text{ GM}, \tag{13}$$

where T_c is the total thrusting time. Using Eqs. (1), (12), and (13) it can be shown that

$$\frac{dC}{d\mu_w} = \frac{C}{\mu_w}\left[\frac{1+\mu_1}{2\mu_1} - \frac{\eta' C}{\eta}\right]^{-1} \text{ AM}, \tag{14}$$

$$\frac{dC}{d\mu_w} = \frac{C}{\mu_w}\left[\frac{2}{1+\mu_1} - \frac{\eta' C}{\eta}\right]^{-1} \text{ GM},$$

If the total derivative of μ_L is taken with respect to μ_w in Eq. (11) and use is made of Eq. (14), then the optimum μ_w is found to be

$$\mu_{w_{OPT}} = \begin{cases} \dfrac{\mu_1(1-\mu_1)}{1 - \left(\frac{2\mu_1}{1+\mu_1}\right)\left(\frac{\eta' C}{\eta}\right)} & \text{AM} \\ \dfrac{\mu_1(1-\mu_1)}{1 - \left(\frac{1+\mu_1}{2}\right)\left(\frac{\eta' C}{\eta}\right)} & \text{GM} \end{cases} \tag{15}$$

The solution of these equations requires an iterative procedure between Eqs. (1), (12), (13), and (15) and a thrustor efficiency function. If the functional form of the thrustor efficiency is given by

$$\eta = \frac{1}{1 + \left(\frac{d}{C}\right)^2}$$

where d, the efficiency parameter, is to be specified, then the use of the geometric-mean equations results in closed-form expressions. Figure II-1 demonstrates the form of η compared to typical thrustors. The optimum values for C and μ_w and the corresponding maximum for μ_L are given by

$$C_{OPT} = \left\{ \frac{J T_c}{\gamma^2} \left(1 + \frac{\gamma^2 d^2}{J T_c} \right) \left[1 - \frac{\gamma}{\left(1 + \frac{\gamma^2 d^2}{J T_c} \right)^{1/2}} \right] \right\}^{1/2} \tag{16}$$

$$\mu_{w_{OPT}} = \gamma \left[\frac{1 + \frac{2\gamma^2 d^2}{J T_c}}{\left(1 + \frac{\gamma^2 d^2}{J T_c} \right)^{1/2}} - \gamma \right] \tag{17}$$

$$\mu_1 = 1 - \frac{\gamma}{\left(1 + \frac{\gamma^2 d^2}{J T_c} \right)^{1/2}} \tag{18}$$

$$\mu_{L_{MAX}} = 1 - 2\gamma \left(1 + \frac{\gamma^2 d^2}{J T_c} \right)^{1/2} + \gamma^2 \tag{19}$$

From Ref. II-1, the agreement between the results from an iterative procedure for Eq. (15) and exact variational calculus solutions is very good and is more than sufficient for mission and system study purposes. The results from the arithmetic mean of Eq. (15) are only slightly more accurate than those obtained from the closed-form expressions Eq. (16) to (19).

If the arithmetic mean in Eq. (15) is desired for a particular form of η, the corresponding iterative procedure could use Eqs. (16) to (19) to obtain initial solutions for the desired parameters. As long as the general trend of the particular efficiency function approximates those of Fig. II-1, such starting guesses will prove to be well within the region of convergence.

By setting Eq. (19) equal to zero, the value of γ^2, and hence α_w, may be determined which causes the maximum payload to vanish.

$$\frac{\alpha_{w_{MAX}} J}{2} = \frac{1}{1 + \sqrt{\frac{4d^2}{J T_c}}} \tag{20}$$

For a given mission (represented by J and T_c) and a particular thrustor (given by d), the maximum allowable value of powerplant specific mass can thus be estimated. This equation is quite helpful, since it may be evaluated prior to a trajectory or system calculation, thereby avoiding negative or zero payloads. In actuality, the value of J computed for a trajectory depends in part on the value of α_w used (see Eq. (12)). However, the coupling between the propulsion system parameters and the steering program (determined for minimum J) is quite weak; this is partially confirmed by the excellent results Melbourne and Sauer obtained from the solutions of Eqs. (15) and Eqs. (16) to (19). Thus, Eq. (20) yields accurate results based on a constant-thrust J which was computed using any initial value of α_w.

Precisely the same assumptions and procedures as used for the simplified payload definition could be employed in the case of the improved payload definition. Hence

$$\mu_{w_{OPT}} = \begin{cases} \dfrac{\mu_1(1-\mu_1)/\rho}{\left[1 + \dfrac{\alpha_F(C)}{\alpha_w}\right]\left[1 - \left(\dfrac{2\mu_1}{1+\mu_1}\right)\left(\dfrac{\eta' C}{\eta}\right)\right] + \left(\dfrac{2\mu_1}{1+\mu_1}\right)\left(\dfrac{\alpha_F' C}{\alpha_w}\right)} & \text{AM} \\ \dfrac{\mu_1(1-\mu_1)/\rho}{\left[1 + \dfrac{\alpha_F(C)}{\alpha_w}\right]\left[1 - \left(\dfrac{1+\mu_1}{2}\right)\left(\dfrac{\eta' C}{\eta}\right)\right] + \left(\dfrac{1+\mu_1}{2}\right)\left(\dfrac{\alpha_F' C}{\alpha_w}\right)} & \text{GM} \end{cases} \tag{21}$$

where, in general, the functional dependence of α_F and η on C must be specified. In addition, the following equations, which are based on the appropriate average thrust-acceleration definition are required to complete the set along with the rocket equation.

$$C = \frac{1 + \mu_1}{1 - \mu_1} \cdot \frac{J}{\bar{a}} \quad \text{AM}$$

$$C = \frac{\sqrt{\mu_1 J T_c}}{1 - \mu_1} \quad \text{GM} \tag{22}$$

Suggested Computational Procedure

Except for the closed-form expressions based on the specified form of the efficiency function, the solution for optimum exhaust velocity and powerplant fraction requires an iterative procedure. The technique discussed below is based on actual numerical cases and the attendant problems encountered.

Regardless of the payload definition and the type of thrustor efficiency curve, the optimum powerplant fraction is derived as a function of the burnout mass fraction and exhaust velocity, Eqs. (15) and (21). Thus, in general,

$$\mu_{w_{OPT}} = f(\mu_1, C) \tag{23}$$

where the rocket equation gives

$$\mu_1 = \frac{1}{1 + \frac{\gamma^2}{\eta \mu_w}} \tag{1}$$

and, functionally, $\eta = \eta(C)$ and if required, $\alpha_f = \alpha_f(C)$.

J and $\bar{a}$ are obtained from a constant-thrust acceleration or constant-thrust (with or without coast periods) trajectory corresponding to the mission. The powerplant defines α_w and the thrustor type the form of η and α_f.

As stated in the development of the initial constant-thrust equations, a power-limited system retains most of its original mass, and, consequently, the dependence of μ_1 on μ_w is quite weak. This relative insensitivity suggests that an iteration between Eqs. (23) and (1) should be employed for a given guess of C, since convergence is practically assured regardless of the type of iteration procedure used. Successive substitution has been found to be quite useful, although the method of false position has been noted to yield an improvement in convergence rate. This latter method is also quite useful in the iteration for the exhaust velocity. Thus the iteration between μ_1 and μ_w is nested inside the iterative loop for C.

A guess is given for C to initiate the iteration between μ_1 and μ_w, i.e., Eqs. (23) and (1). By using the method of false position, any initial reasonable guess for μ_1 will converge rapidly to the appropriate μ_w. With the converged value of μ_1 and μ_w, Eq. (22) is employed to update C. False-position is applied to the C-loop

to obtain a C which is used in the nested iteration for μ_1 and μ_w. This procedure has been found to be quite stable for many cases. If C is employed as part of the nested iteration, multiple solutions to C arise and, in addition, divergence occurs.

If the functional form of the particular thrustor efficiency curve being utilized approximates the equation of Fig. II-1, then appropriate starting guesses for the above suggested technique may be obtained from Eqs. (16), (17), and (18).

Definitions

a = thrust acceleration

C = exhaust jet velocity

d = thrustor efficiency parameter

F = thrust

J = $\int a^2 dt$

m = mass

m_F = thrustor

m_L = payload

m_P = propellant

m_S = structure

m_t = propellant tank

m_w = powerplant

m_0 = initial

m_1 = terminal

p = jet power

P = powerplant output power

T_c = constant thrust powered time

α_F = thrustor specific mass = m_F/P

α_w = powerplant specific mass = m_w/P

β^2 = $\alpha_w J/2\eta$

γ^2 = $\alpha_w J/2$

η = thrustor efficiency = p/P

ρ = tank propellant mass fraction = $m_p/(m_p + m_t)$

σ = structure proportionality constant = $m_s/(m_F + m_t + m_p + m_w)$

μ = mass fraction = m/m_0

μ_L = payload fraction

μ_0 = initial mass fraction = 1

μ_p = propellant fraction

μ_w = powerplant fraction

μ_1 = terminal fraction

Summary of Equations

General

Terminal mass fraction:

$$\mu_1 = \frac{1}{1 + \frac{1}{2}\frac{\alpha_w J}{\eta \mu_w}}$$

Simplified payload fraction:

$$\mu_L = \mu_1 - \mu_w$$

Improved payload fraction:

$$\mu_L = 1 - \left(\frac{1+\sigma}{\rho}\right)\left(1-\mu_1\right) - \left(1+\sigma\right)\left[1+\frac{\alpha_F(C)}{\alpha_W}\right]\mu_W$$

Hypothetical thrustor efficiency:

$$\eta = \frac{1}{1+\left(\frac{d}{C}\right)^2}$$

Variable Thrust, Simplified Payload

Optimum powerplant fraction:

$$\mu_{W_{OPT}} = \beta\left(1-\beta\right)$$

Maximum payload:

$$\mu_{L_{MAX}} = \left(1-\beta\right)^2$$

Propellant:

$$\mu_P = \beta$$

Variable Thrust, Improved Payload

Optimum powerplant fraction:

$$\mu_{W_{OPT}} = \beta\left[\frac{1}{\sqrt{\rho\left(1+\frac{\alpha_F}{\alpha_W}\right)}} - \beta\right]$$

Maximum payload:

$$\mu_{L_{MAX}} = 1 - 2(1+\sigma)\sqrt{\frac{1}{\rho}\left(1+\frac{\alpha_F}{\alpha_W}\right)}\beta + (1+\sigma)\left(1+\frac{\alpha_F}{\alpha_W}\right)\beta^2$$

Propellant:

$$\mu_p = \sqrt{\rho\left(1+\frac{\alpha_F}{\alpha_W}\right)}\beta$$

Constant Thrust, Simplified Payload

Optimum powerplant fraction:

$$\mu_{W_{OPT}} = \begin{cases} \dfrac{\mu_1(1-\mu_1)}{1-\left(\frac{2\mu_1}{1+\mu_1}\right)\left(\frac{\eta' C}{\eta}\right)} & \text{AM} \\ \dfrac{\mu_1(1-\mu_1)}{1-\left(\frac{1+\mu_1}{2}\right)\left(\frac{\eta' C}{\eta}\right)} & \text{GM} \end{cases}$$

$$\eta = \eta(C)$$

Closed form: geometric mean, hypothetical thrustor efficiency:

$$C_{OPT} = \left\{ \frac{J T_c}{\gamma^2}\left(1+\frac{\gamma^2 d^2}{J T_c}\right)\left[1-\frac{\gamma}{\left(1+\frac{\gamma^2 d^2}{J T_c}\right)^{1/2}}\right]\right\}^{1/2}$$

$$\mu_{W_{OPT}} = \gamma\left[\frac{1+\frac{2\gamma^2 d^2}{J T_c}}{\left(1+\frac{\gamma^2 d^2}{J T_c}\right)^{1/2}} - \gamma\right]$$

$$\mu_1 = 1 - \frac{\gamma}{\left(1 + \frac{\gamma^2 d^2}{J T_c}\right)^{1/2}}$$

$$\mu_{L_{MAX}} = 1 - 2\gamma\left(1 + \frac{\gamma^2 d^2}{J T_c}\right)^{1/2} + \gamma^2$$

At zero maximum payload:

$$\frac{\alpha_{w_{MAX}} J}{2} = \frac{1}{1 + \sqrt{\frac{4 d^2}{J T_c}}}$$

Constant Thrust, Improved Payload

$$\mu_{w_{OPT}} = \begin{cases} \dfrac{\mu_1(1-\mu_1)/\rho}{\left[1 + \dfrac{\alpha_F(c)}{\alpha_w}\right]\left[1 - \left(\dfrac{2\mu_1}{1+\mu_1}\right)\left(\dfrac{\eta' c}{\eta}\right)\right] + \left(\dfrac{2\mu_1}{1+\mu_1}\right)\left(\dfrac{\alpha_F' c}{\alpha_w}\right)} & \text{AM} \\ \dfrac{\mu_1(1-\mu_1)/\rho}{\left[1 + \dfrac{\alpha_F(c)}{\alpha_w}\right]\left[1 - \left(\dfrac{1+\mu_1}{2}\right)\left(\dfrac{\eta' c}{\eta}\right)\right] + \left(\dfrac{1+\mu_1}{2}\right)\left(\dfrac{\alpha_F' c}{\alpha_w}\right)} & \text{GM} \end{cases}$$

$\eta = \eta(c)$

$\alpha_F = \alpha_F(c)$

REFERENCE

II-1. Melbourne, W. G., and C. G. Sauer, Jr.: "Payload Optimization for Power-Limited Vehicles". JPL Space Programs Summary No. 37-17, Vol. IV, October 1962.

FIG. II - 1

DEPENDENCE OF THRUSTOR EFFICIENCY ON EXHAUST VELOCITY

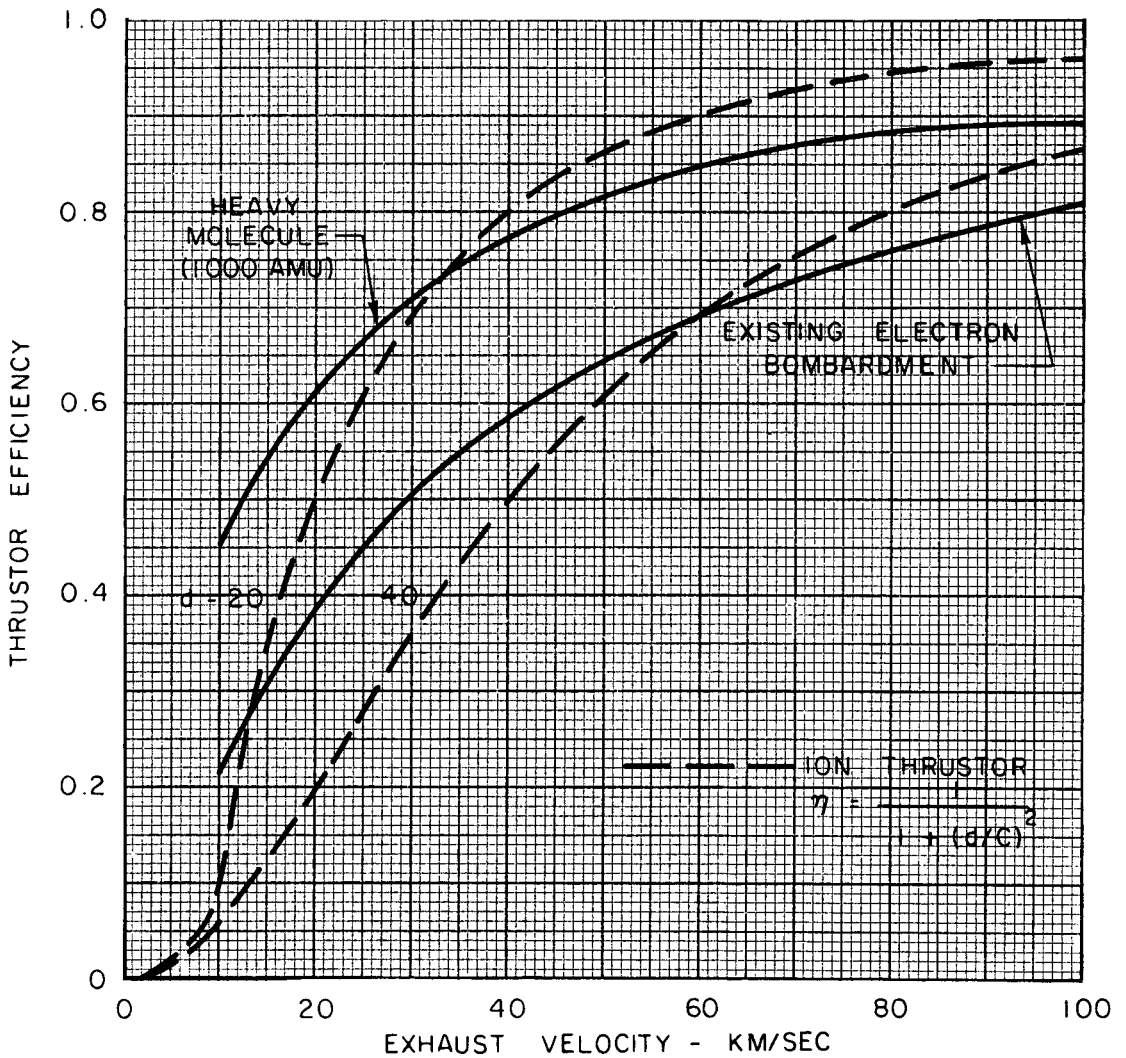

SECTION III

DATA FOR OPTIMUM SYSTEM PARAMETERS

Contained in this section are graphical and numerical data for estimating power-limited system performance under constant-thrust and variable-thrust operation. In general the requirements for utilizing these data are variable-thrust J or the constant-thrust J and powered time for the corresponding heliocentric interplanetary mission. Methods and data for estimating these requirements are presented in Section IV, following.

Constant-Thrust Operation

Equations (16) to (20) of Section II are quite useful, since the system parameters are given by simplified expressions. Accordingly, based on these equations, Figs. III-1 to -8 present optimum C and μ_W, and resulting μ_1 and maximum μ_L for values of γ^2, the product $J_c T_c$, and d = 10, 20, 30, and 40 km/sec (the efficiency parameter). The maximum power plant specific mass that yields zero payload for the given J_c and T_c can be easily found from the nomograph of Fig. III-9. All of these figures are based on the simplified payload definition and hypothetical efficiency function, Eqs. (1) and Fig. 1 of Section II, respectively. The notation J_c is employed to emphasize constant-thrust operation and to distinguish it from the variable-thrust J to be given later.

The graphs require J_c and T_c based on a constant-thrust or constant-thrust-acceleration heliocentric trajectory. The powerplant defines α_W and the thrustor type gives d. The efficiency parameter, d, is estimated by fitting (approximately) the hypothetical efficiency functions to the given thruster curve. The appropriate units for the parameters are given in the figures.

The use of the improved payload fraction definition requires a functional relationship between thrustor specific mass and exhaust velocity. An example of empirical data obtained from Ref. 2 is illustrated in Fig. III-10 for electron bombardment and contact type thrustors. The two curves for each thrustor type indicate "current" and "improved" technology levels. The curves have been smoothed and extrapolated to an exhaust velocity of 20 km/sec for purposes of deriving an analytic fit.

Two analytic fits to the data presented in Fig. III-10 have been employed, first a sum of exponentials and, second, a fourth-degree polynomial. The former method yields a smooth fit to the data throughout the entire range of C and also produces a smooth curve for the first derivative. These results are presented in Table III-1. The fourth-degree polynomial yields exact results at the evenly

spaced data points, although the general form is wavy both in the reproduced curve and its first derivative. Table III-2 presents the basic method, and Table III-3 gives the coefficients for the curves of Fig. III-10.

For an accurate reproduction of curves of this type, the sum-of-exponentials fit is preferred. However, the numerical procedure necessary to obtain the coefficients is quite complicated and does not appear justified in view of the contribution of thrustor mass to the total vehicle mass. Consequently, the polynomial approximation is preferred for the foregoing reason and further, because the appropriate coefficients are easily determined, as shown by Table III-2. Any other thrustor curve may be quickly approximated by the polynomial if input data points are specified at exhaust velocities of 20, 40, 60, 80, and 100 km/sec.

Variable-Thrust Operation

For the simplified payload fraction definition, the optimum powerplant mass fraction and other parameters are obtained from Eqs. (4), (5), and (6) of Section II. For convenience, the maximum payload fraction as a function of powerplant fraction is plotted in Fig. III-11 with β a parameter. The points of maximum payload and optimum powerplant fractions are indicated for any value of β.

Corresponding plots for the improved payload definition (variable-thrust) are given in Fig. III-12 with the parameters X and M identified as

$$X \equiv \rho\left(1 + \frac{\alpha_F}{\alpha_W}\right)$$

and

$$M \equiv \frac{\rho}{1+\sigma}\left(1 - \mu_{L\,MAX}\right)$$

Note that, insofar as the powerplant and propellant fractions are concerned, precisely the same results are obtained for the simplified and improved payload cases provided the values of ρ, α_F, and α_W are such that X is 1.0. Under these circumstances the maximum payload is given simply by

$$\mu_{L\,MAX} = 1 - \frac{2(1+\sigma)}{\rho}\beta + \frac{(1+\sigma)}{\rho}\beta^2$$

TABLE III - 1

EXPONENTIAL APPROXIMATION TO THRUSTOR SPECIFIC MASS FUNCTION

$$\alpha_F(C) = a_1 e^{-\sigma_1\left(\frac{C}{20}-1\right)} + a_2 e^{-\sigma_2\left(\frac{C}{20}-1\right)}$$

α_F, KG/KW C, KM/SEC

	a_1	σ_1	a_2	σ_2
ELECTRON BOMBARDMENT, 1	1.63542	0.406626	2.46479	1.92452
" " , 2	0.429867	0.403804	1.05991	1.06851
CONTACT, 1	−0.0197516	−0.357073	1.10985	0.342079

CONTACT, 2 :

$$\alpha_F(C) = e^{-0.600736\left(\frac{C}{20}-1\right)}\left\{0.590562\cos\left[\left(13^\circ\,14.428'\right)\left(\frac{C}{20}-1\right)\right] + 0.275432\sin\left[\left(13^\circ\,14.428'\right)\left(\frac{C}{20}-1\right)\right]\right\}$$

TABLE III-2

DETERMINATION OF COEFFICIENTS FOR THRUSTOR SPECIFIC MASS FUNCTION

$$\alpha_F(C) = a_0 + a_1\left(\frac{C}{20}\right) + a_2\left(\frac{C}{20}\right)^2 + a_3\left(\frac{C}{20}\right)^3 + a_4\left(\frac{C}{20}\right)^4$$

α_F, KG/KW

C, KM/SEC

INPUT:

C	20	40	60	80	100
α_F	α_{F0}	α_{F1}	α_{F2}	α_{F3}	α_{F4}

$$\begin{pmatrix} a_0 \\ a_1 \\ a_2 \\ a_3 \\ a_4 \end{pmatrix} = D \times \begin{pmatrix} \alpha_{F0} \\ \alpha_{F1} \\ \alpha_{F2} \\ \alpha_{F3} \\ \alpha_{F4} \end{pmatrix}$$

WHERE

$$D = \begin{pmatrix} 5 & -10 & 10 & -5 & 1 \\ -6.41665 & 17.83331 & -19.50 & 10.16667 & -2.08333 \\ 2.95833 & -9.83333 & 12.25 & -6.83333 & 1.45833 \\ -0.58333 & 2.16667 & -3.0 & 1.83333 & -0.41667 \\ 0.041667 & -0.16667 & 0.25 & -0.16667 & 0.041667 \end{pmatrix}$$

TABLE III - 3

POLYNOMIAL APPROXIMATION FOR THRUSTOR SPECIFIC MASS

$$\alpha_F(C) = a_0 + a_1\left(\frac{C}{20}\right) + a_2\left(\frac{C}{20}\right)^2 + a_3\left(\frac{C}{20}\right)^3 + a_4\left(\frac{C}{20}\right)^4$$

α_F, KG/KW

C, KM/SEC

THRUSTOR TYPE	a_0	a_1	a_2	a_3	a_4
ELECTRON BOMBARDMENT, I	11.73	−11.467	4.6271	−0.84750	0.057916
2	3.44	−2.68666	0.88670	−0.13833	0.008333
CONTACT, I	1.55	−0.54083	0.089583	−0.091662	0.0004167
2	1.00	−0.53167	0.14333	−0.023333	0.0016667

PAYLOAD AND POWERPLANT FRACTIONS FOR CONSTANT—THRUST OPERATION

d = 10 KM/SEC

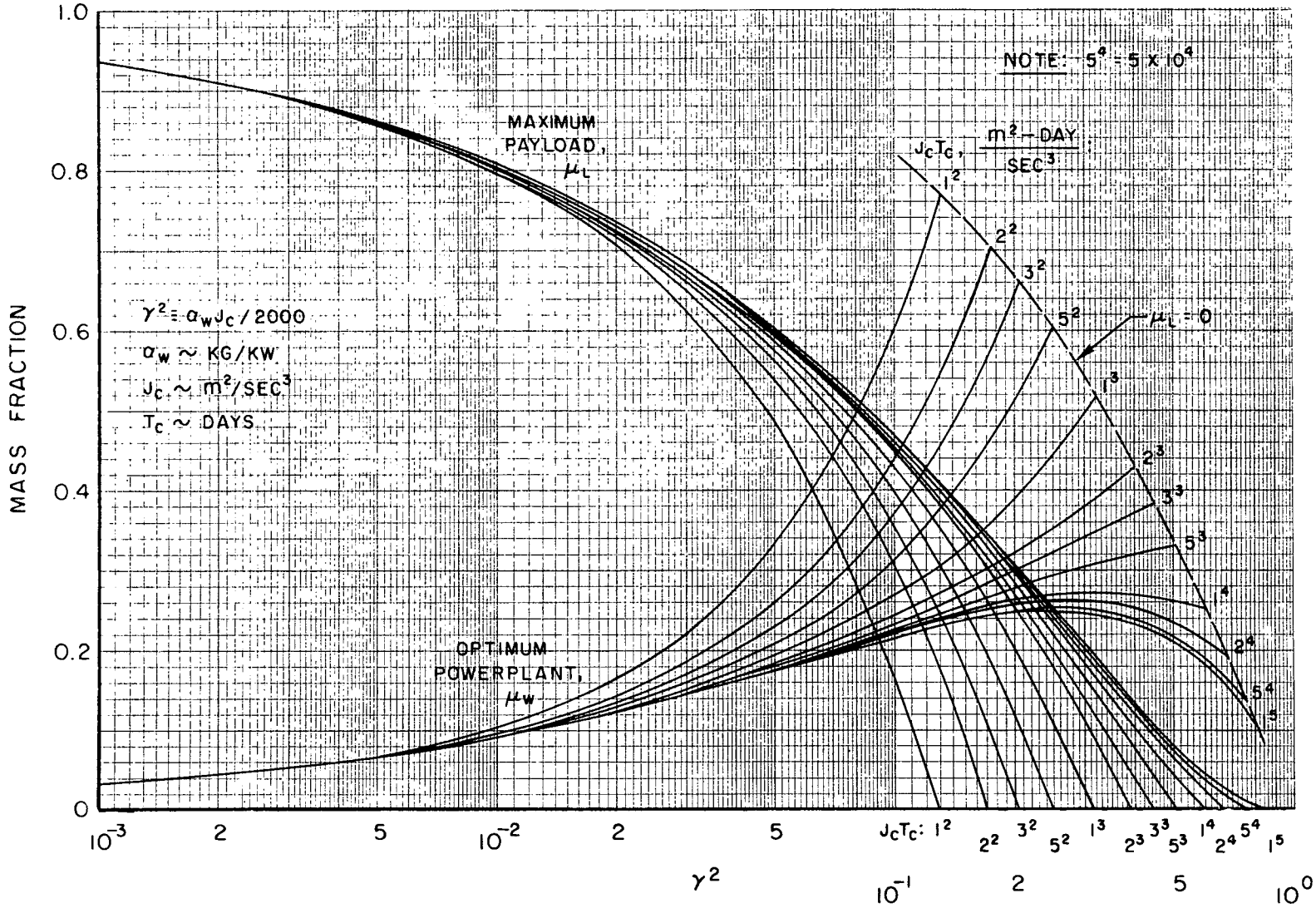

OPTIMUM EXHAUST VELOCITY FOR CONSTANT-THRUST OPERATION

d = 10 KM/SEC

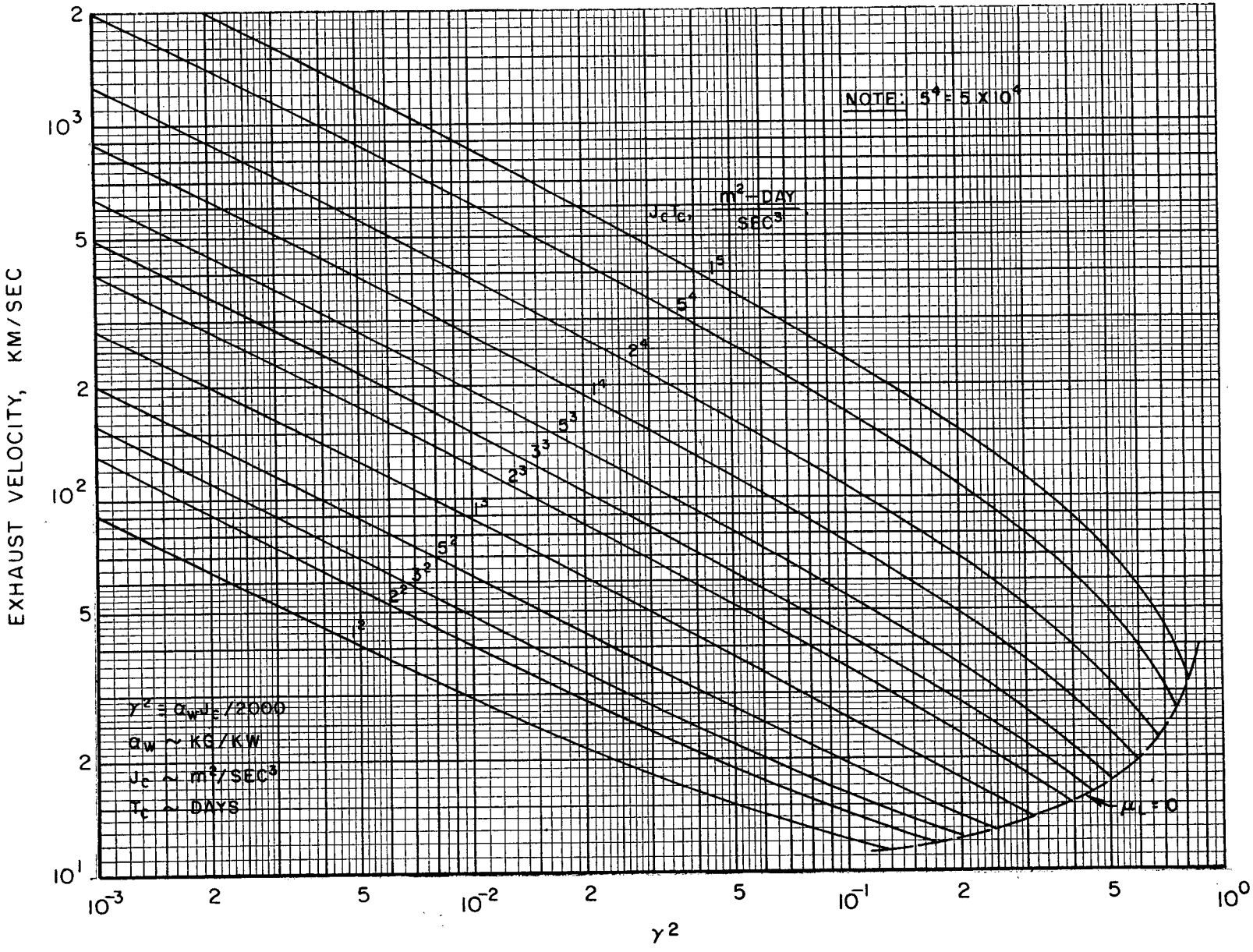

PAYLOAD AND POWERPLANT FRACTIONS FOR CONSTANT-THRUST OPERATION

d = 20 KM/SEC

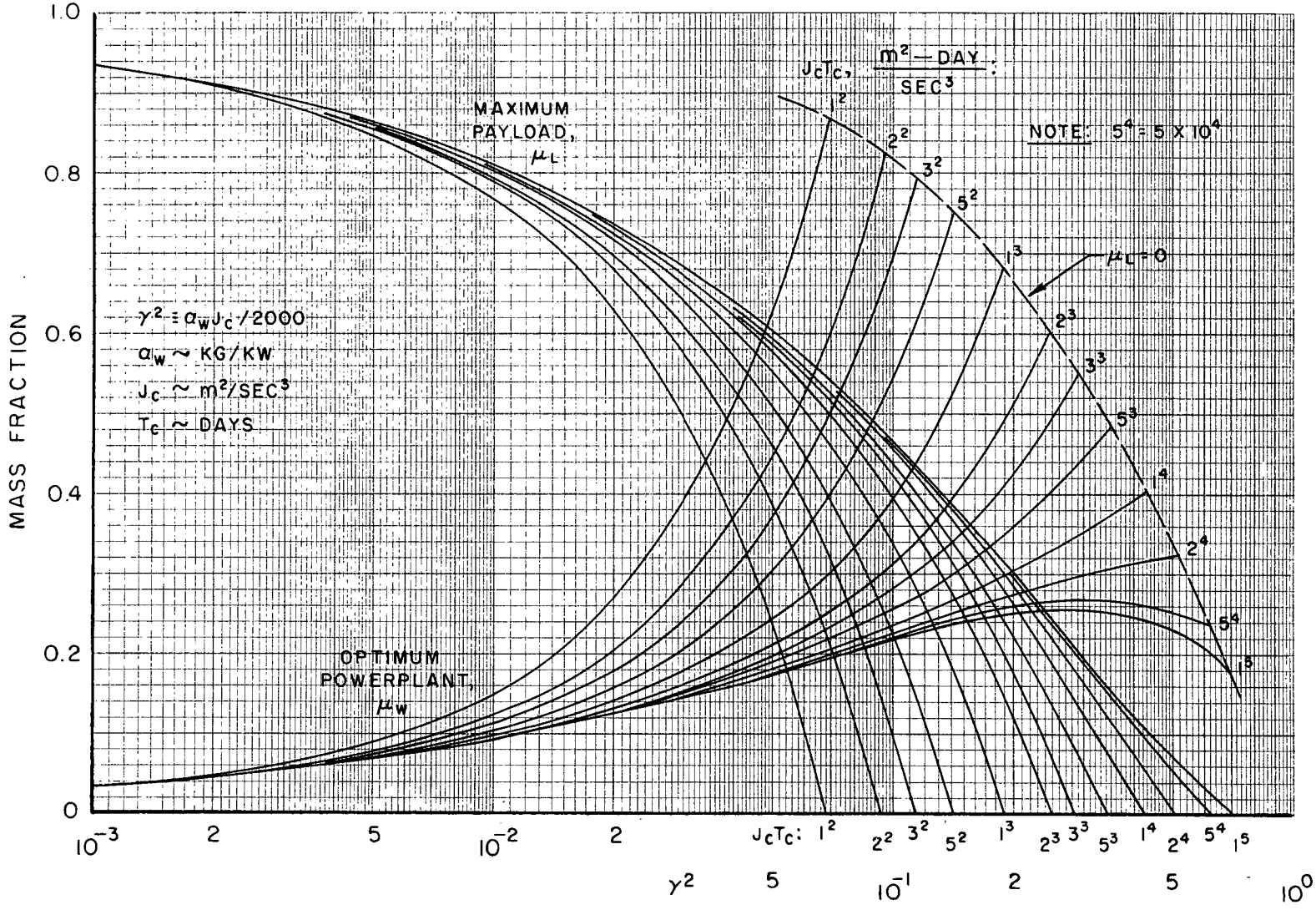

OPTIMUM EXHAUST VELOCITY FOR CONSTANT—THRUST OPERATION

d = 20 KM/SEC

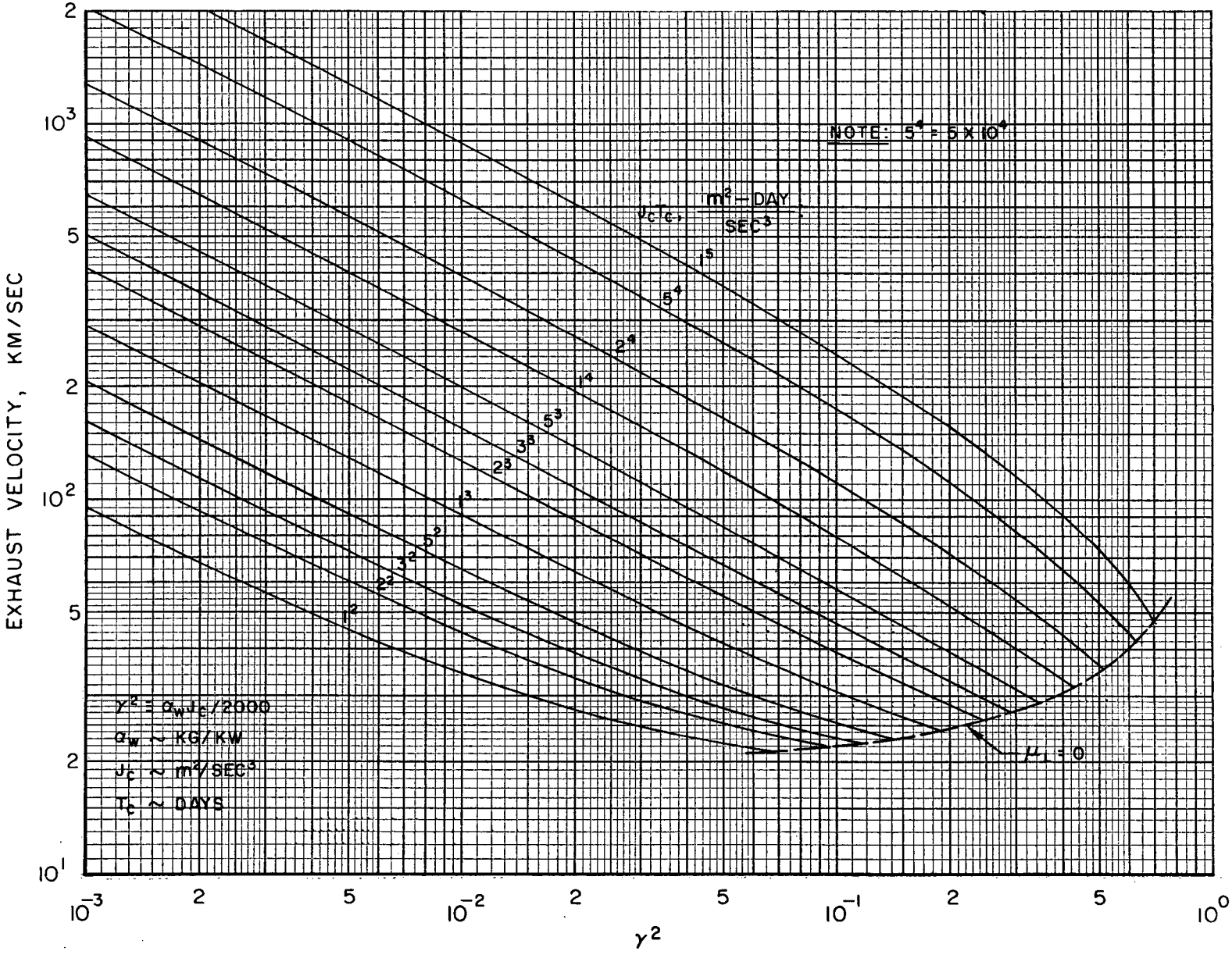

PAYLOAD AND POWERPLANT FRACTIONS FOR CONSTANT-THRUST OPERATION

d = 30 KM/SEC

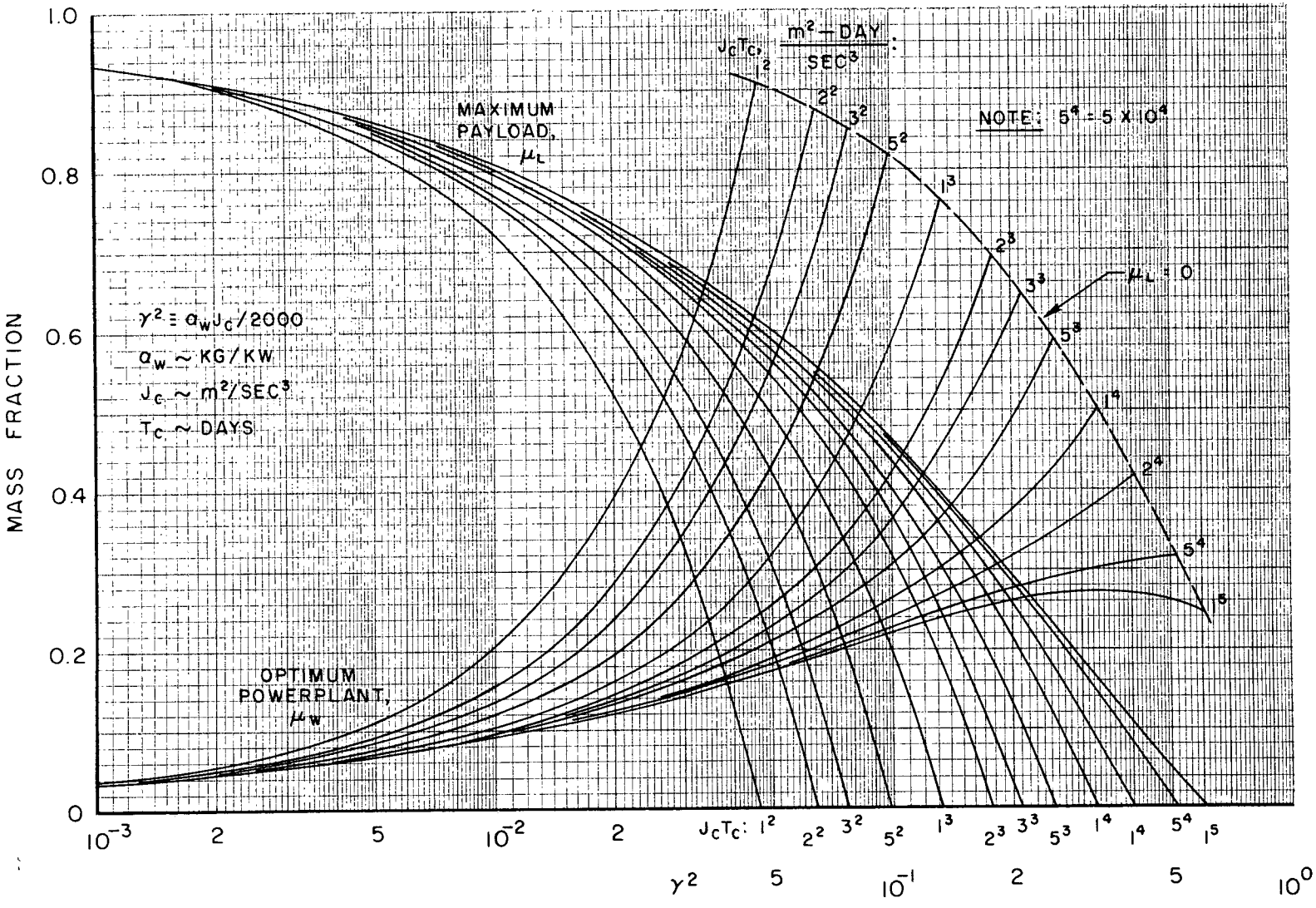

OPTIMUM EXHAUST VELOCITY FOR CONSTANT-THRUST OPERATION

d = 30 KM/SEC

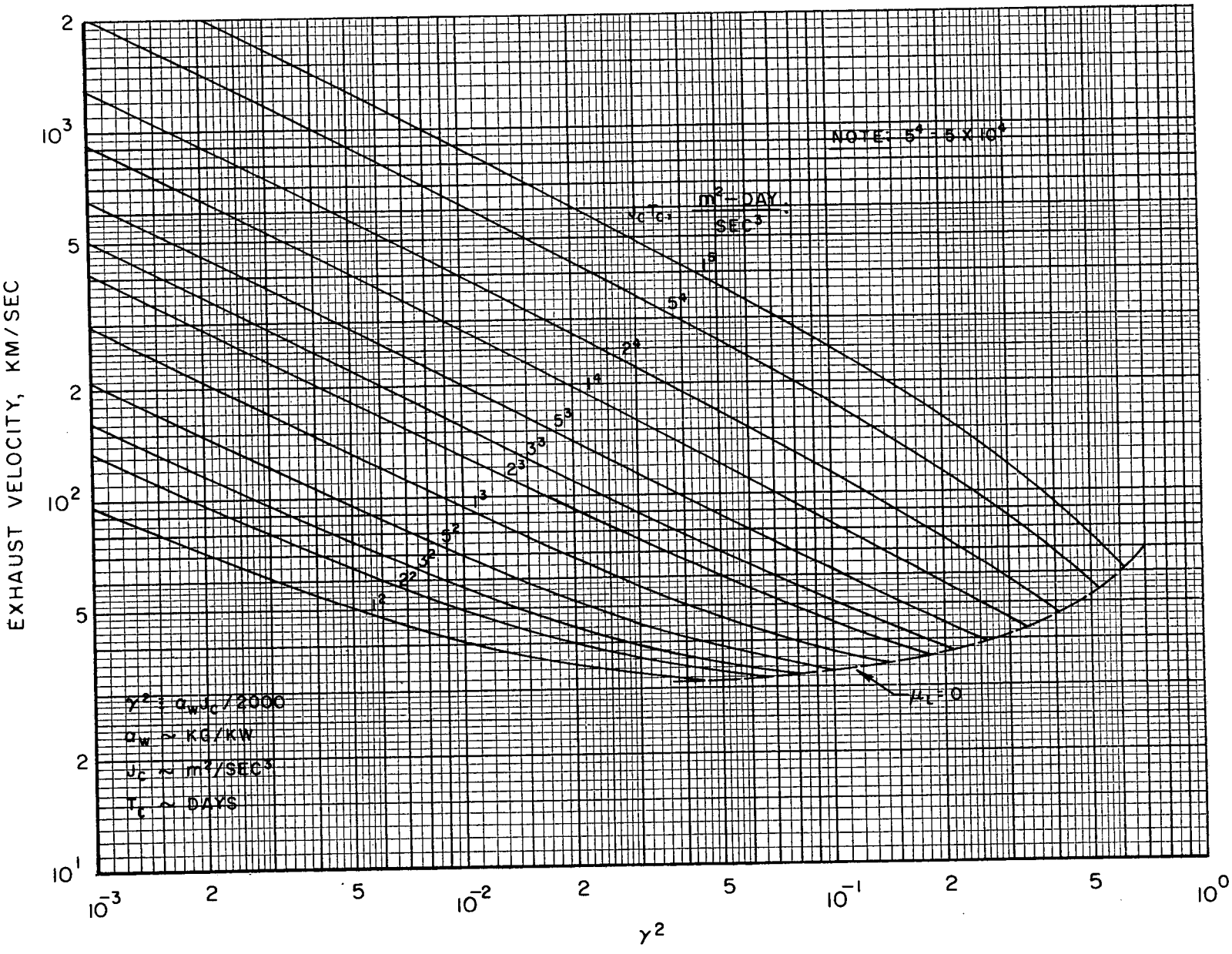

FIG. III-6

PAYLOAD AND POWERPLANT FRACTIONS FOR CONSTANT-THRUST OPERATION

d = 40 KM/SEC

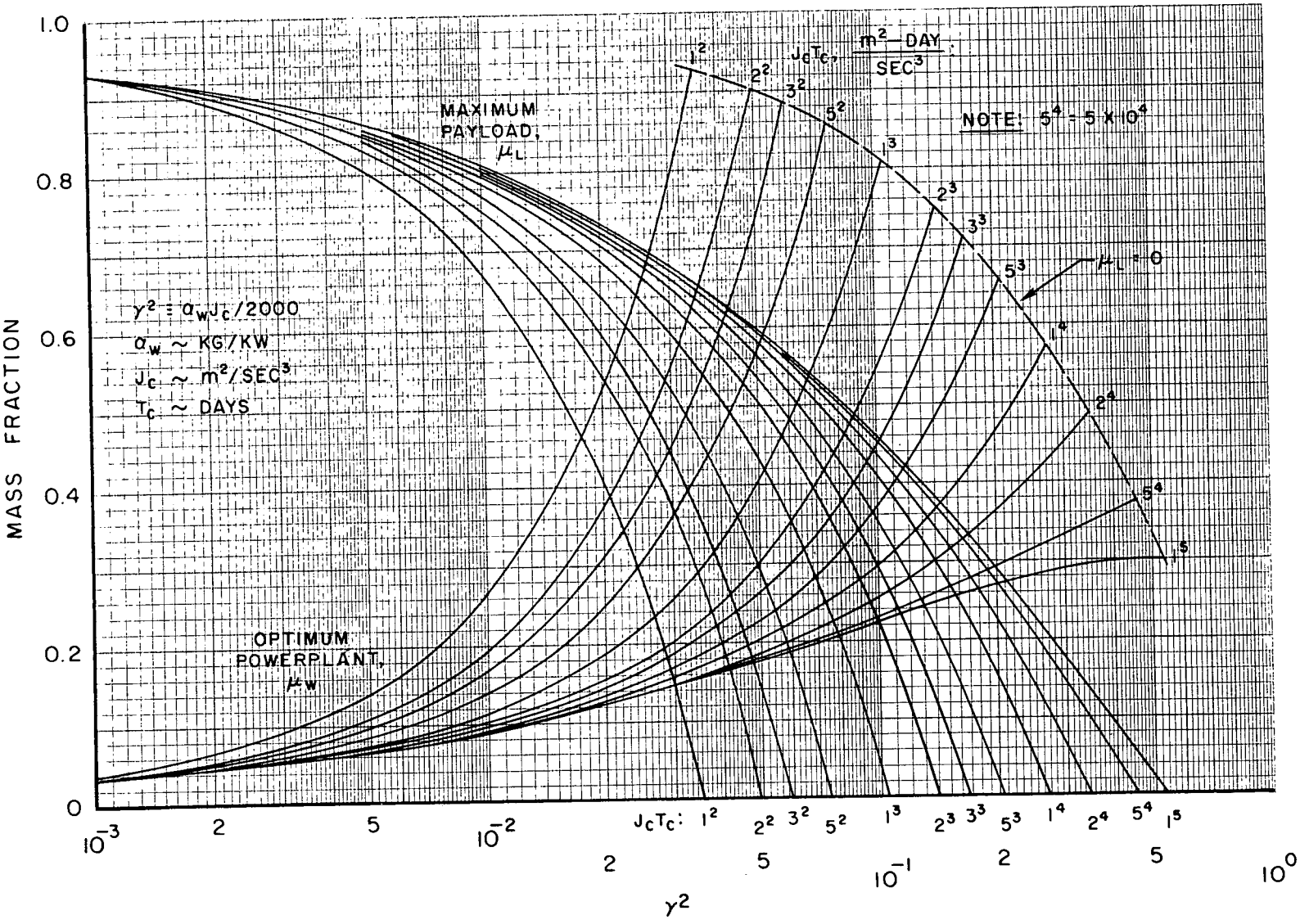

OPTIMUM EXHAUST VELOCITY FOR CONSTANT—THRUST OPERATION

d = 40 KM/SEC

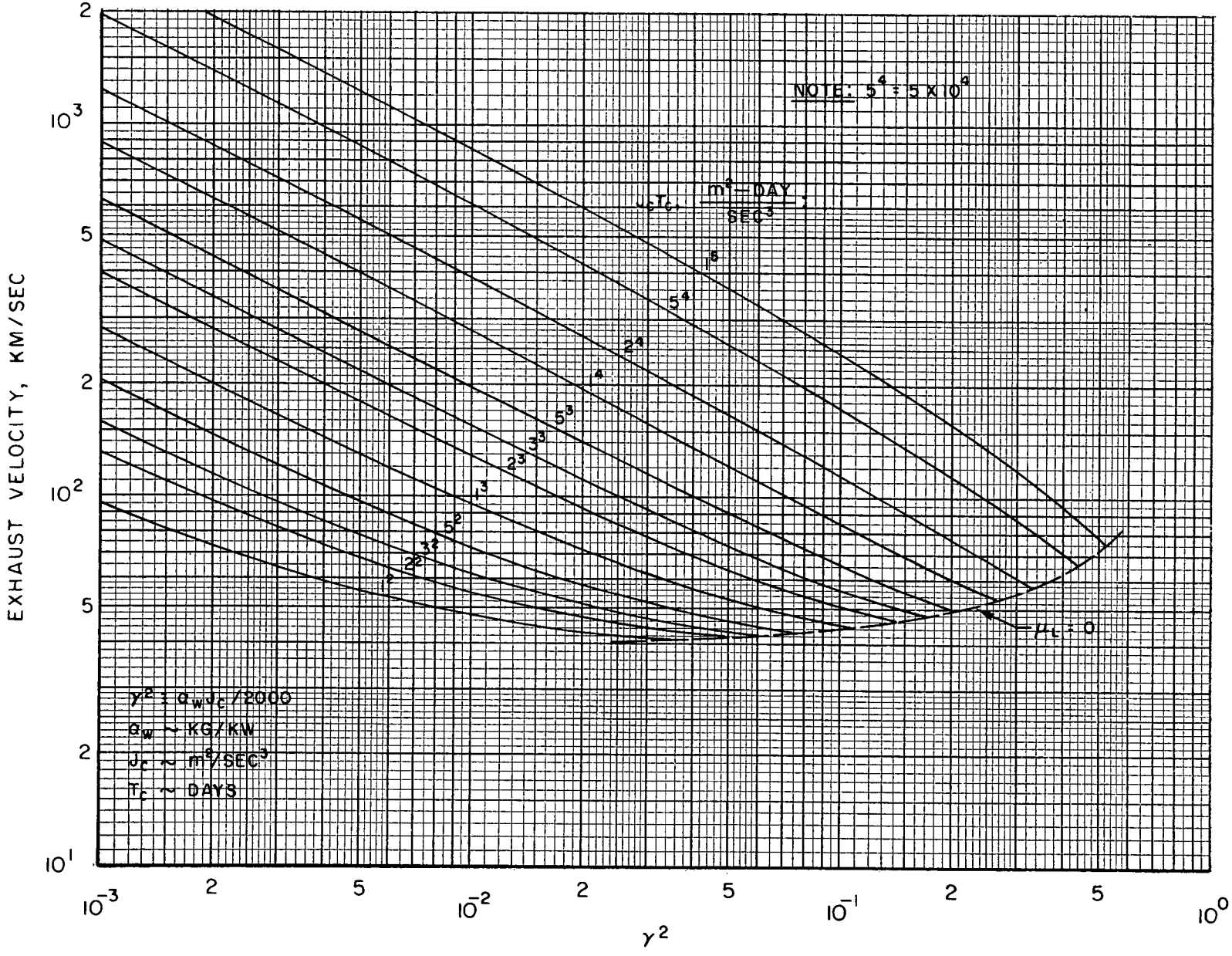

FIG. III-8

G - 110058 - 28

FOLDOUT FRAME 1

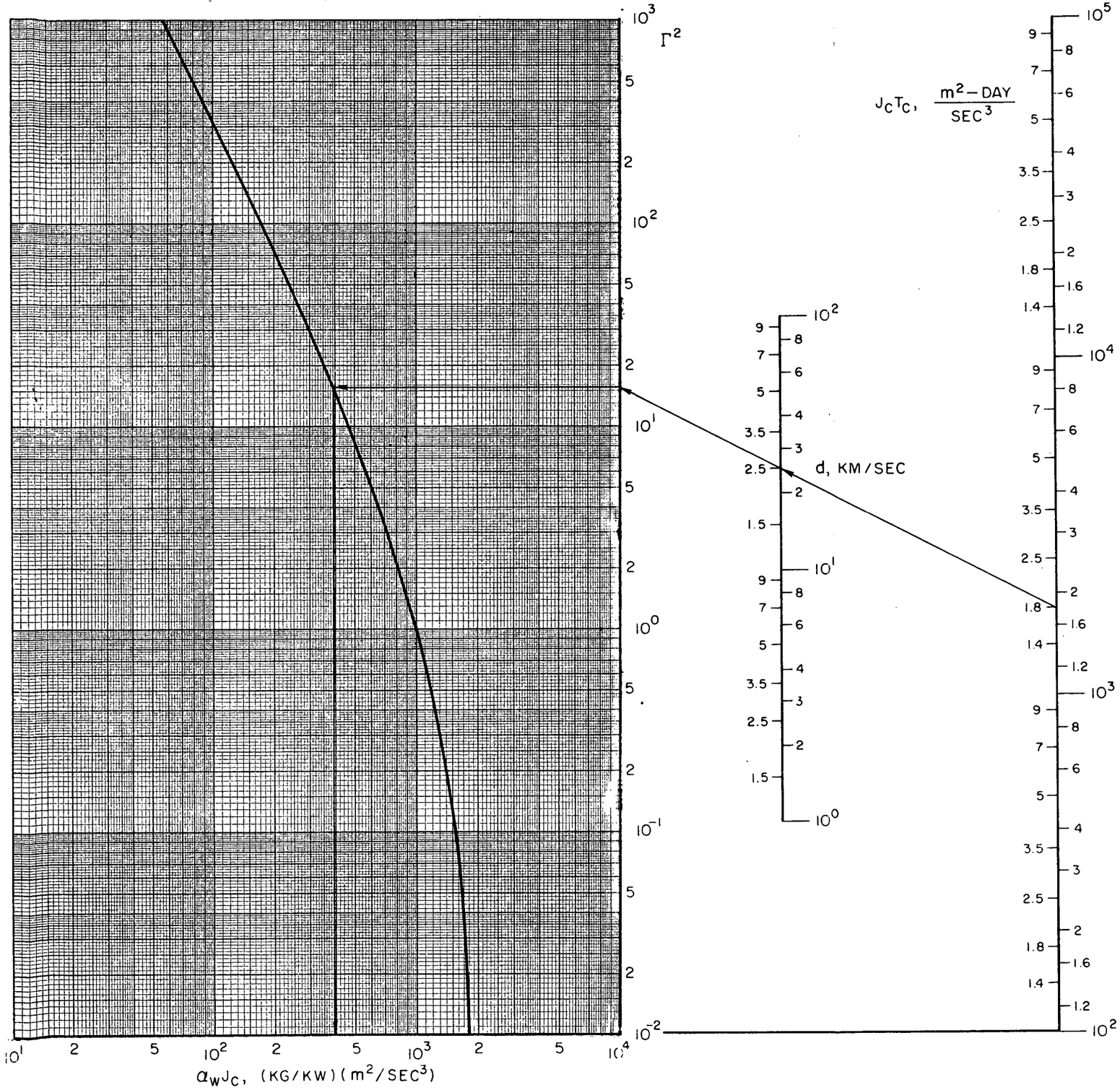

FOLDOUT FRAME 2

FIG. III-9

POWERPLANT SPECIFIC WEIGHT AT ZERO PAYLOAD FRACTION

d = THRUSTOR EFFICIENCY PARAMETER, KM/SEC

J_C = CONSTANT THRUST J, m^2/SEC^3

T_C = POWERED TIME, DAYS

EXAMPLE:

d = 25, $J_C T_C = 1.8 \times 10^3$;

$\therefore \Gamma^2 = 15.7$,

& $\alpha_{WMAX} = \frac{3.95 \times 10^2}{J_C}$, KG/KW

FIG. III – 10

THRUSTOR SPECIFIC MASS

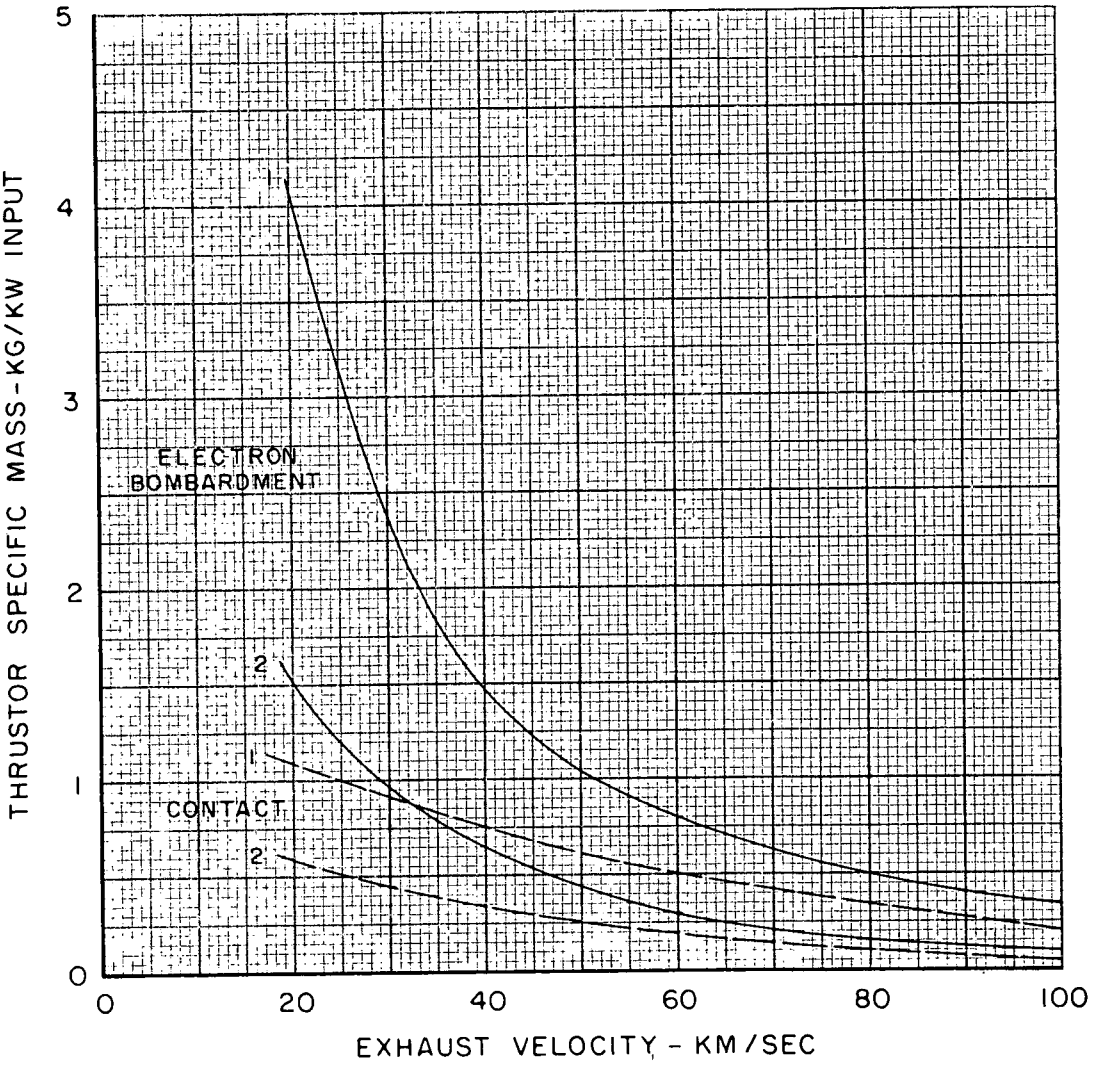

FIG. III-11

DEPENDENCE OF PAYLOAD FRACTION ON POWERPLANT FRACTION

SIMPLIFIED PAYLOAD DEFINITION

$$\mu_L = \mu_1 - \mu_W$$

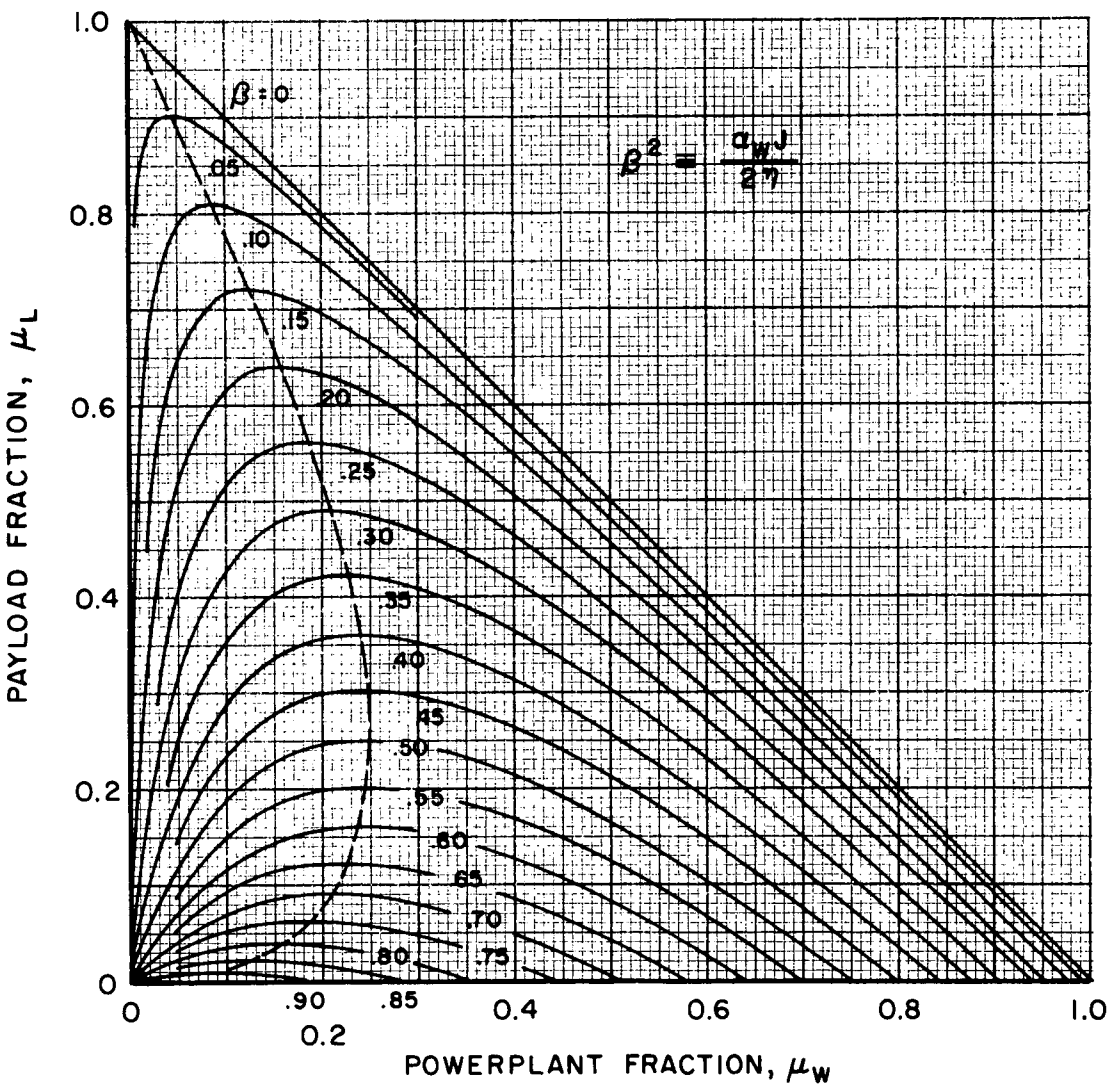

FIG. III-12

MAXIMUM PAYLOAD AND POWERPLANT FRACTIONS

IMPROVED PAYLOAD DEFINITION

$$\mu_L = 1 - \left(\frac{1+\sigma}{\rho}\right)(1-\mu_1) - (1+\sigma)\left(1+\frac{a_F}{a_W}\right)\mu_W$$

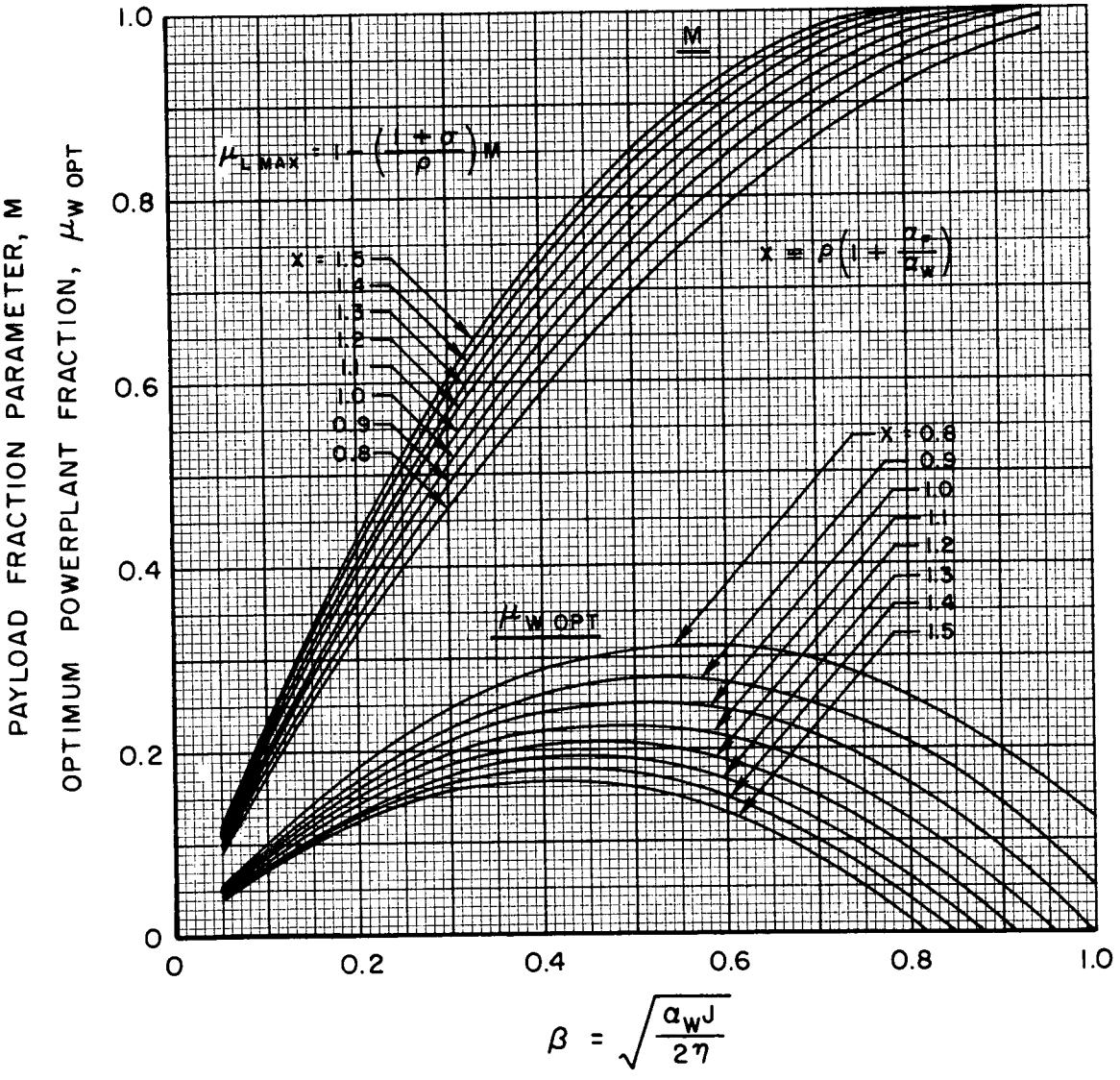

SECTION IV

HELIOCENTRIC AND PLANETOCENTRIC TRAJECTORIES

The presentation of constant-thrust trajectory information to be used in the analysis of power-limited space vehicles relies on the assumptions that variations in powerplant specific mass and either specific impulse (exhaust velocity C) or powerplant fraction, μ_W, do not significantly affect the value of J over an optimally steered trajectory and, further, that the power system output is invariant with either spatial position or time, or both. Under these assumptions, it is possible to organize the power-limited trajectory information by computing a constant-thrust-with-coast trajectory such that the vehicle is optimally steered (i.e., J is minimized) and the payload fraction, μ_L, is maximized for either given C and optimized μ_W or given μ_W and optimized C, all for a given powerplant specific mass and travel time. The J so computed is therefore characteristic of the particular trajectory and could be considered an indication of the flight propulsion requirements with only the proper selection of exhaust velocity and powerplant fraction needed to maximize the space vehicle's payload carrying capability at any other given powerplant specific mass (see Section II, pg. 3).

The foregoing approach was employed in the computation of heliocentric and planetocentric trajectory requirements for selected planets. Not all planets were considered for the heliocentric missions simply because of the expense involved. The data listed herein were available from a series of previous company and NASA funded studies. Only constant-thrust, constant-power trajectories with optimal coast were employed in the heliocentric flights; similarly for the planetocentric spirals, except that no coast periods arise in this type of flight. As implied by the constant-power assumption, the trajectory information is not applicable to vehicles powered by solar-electric or radioisotope power systems since the powerplant is a function of heliocentric position or time, respectively. In the case of the radioisotope systems, this limitation need not hold if the power decay is not significant over the operating time.

In the case of mixed-thrust trajectories in which the boundary conditions on the heliocentric trajectory include nonzero hyperbolic excess speeds, the transition region between the two gravitational fields encompasses low-thrust operation within the planet's sphere of influence. Because the heliocentric trajectory optimization assumes, as part of the boundary conditions, that the planets are massless points, it is necessary to develop corrections to account for the realistic case in which the low-thrust vehicle is affected by the planet's mass. This aspect is discussed in the final part of this section and in detail in Section VIII, Appendix B.

Heliocentric Trajectories

Figure IV-1 displays the characteristic trajectory requirement, J, as a function of heliocentric travel time to each of four planets. Rendezvous trajectories are shown for trips to Mercury, Jupiter, and Saturn, and flyby trips to these three planets as well as to Uranus. All of the information shown was obtained using a computer program which computes constant-thrust, constant-power, fixed-time trajectories with optimum coast periods (see Section VII for description). The trajectories are all two-dimensional with the planets moving in elliptical orbits. A fixed powerplant specific mass of 5 kg/kw was used and the exhaust velocity and powerplant fraction were simultaneously optimized for maximum payload fraction (simplified definition, Section II, pg. 3). The hypothetical thrustor efficiency function given at the bottom of pg. 8, Section II, was used with d = 20 km/sec.

The planets and types of trajectories chosen were those presently felt to be missions appropriate to first-generation, unmanned, electrically propelled, interplanetary probes. Because only one-way probe missions were considered, the J's are accordingly the lowest value possible for the corresponding trip time; i.e., the heliocentric central angle through which the probe traverses is optimum. Although all of the trajectory data were computed for a certain planetary alignment year occurring in the early 1980's, the information is considered applicable to other years for preliminary systems analysis and mission studies.

Trips labeled "rendezvous" are those for which the departure and arrival conditions are the appropriate planet's heliocentric orbital position and velocity; with respect to the planet the probe is at escape conditions. The flyby trips are trajectories which leave Earth with its heliocentric position and velocity and pass through the massless point representing the destination planet. Because of this terminal condition, the trajectory may also be interpreted as an impacter.

The total time that thrusting is necessary for both rendezvous and flybys trips is illustrated in Fig. IV-2. Since coasting periods arise in optimum constant-thrust trajectories, the powered time (or operating time) is always less than the heliocentric travel time. The hyperbolic excess velocity for planetary flybys is given in Fig. IV-3. To an observer on the surface of the planet, the probe would appear to be closing along a radius vector with a speed given by

$$V = \sqrt{V_\infty^2 + V_e^2} \ ,$$

where V_∞ is the hyperbolic excess velocity, and V_e is the escape velocity at the planet's surface.

For the systems analysis of some types of flight modes (described in Section V) it is convenient to assume that the J-curves of Fig. IV-1 and the powered times in Fig. IV-2 are approximately linear functions of travel time. The motivation is to quickly obtain trajectory information which may be directly applied to Eqs. 16 to 19 of Section II. Assuming a linear relationship, then the characteristic J and corresponding powered time are given, respectively, by

$$J_H = \hat{J}_H \left(\frac{T_H}{\hat{T}_H} \right)^{m_H} \quad \text{and} \quad T_{HP} = \hat{T}_{HP} \left(\frac{T_H}{\hat{T}_H} \right)^{m_H},$$

where J_H, T_H, and T_{HP} are the heliocentric J, travel time, and powered time, respectively. The quantities topped by a caret are reference values. The necessary information for these equations is given in Table IV-1 for both rendezvous and flybys. Data for Uranus rendezvous were not available. Also indicated at the bottom of each column is the range of trip times from which the corresponding data were derived.

As can be seen from Fig. IV-1, the linear approximation is not strictly correct and tends to be in error at the higher relative trip times, especially in the case of Mercury. However it has been found in most cases of interest that the J so used results in about 10 to 15% error in the mass fractions. This error was considered reasonable for mission study purposes. In any event the data of Figs. IV-1 and IV-2 could be used as plotted for more accurate analysis.

Planetocentric Spiral Trajectories

The trajectory data for planetocentric spirals represent the requirements for a low-thrust spiral between escape conditions and a circular parking orbit. Only constant-thrust outward (departure) and inward (capture) spirals are considered for both optimal and tangential (or circumferential) steering programs. Two methods of computing the trajectory characteristics, J, as well as the appropriate vehicle and propulsion system parameters are given. The first, developed by W. G. Melbourne of JPL (Ref. IV-1), employs tangential steering. The second approach is based on the work of Breakwell and Rauch (Ref. IV-2) as modified by Edelbaum (Ref. IV-3) and is applicable to both tangential and optimal steering programs.

The derivation of the equations in both techniques is given in Section VIII, Appendix A, Planetocentric Low-Thrust Trajectory Equations. The pertinent equations and trajectory data are presented here.

Melbourne's Method

From Appendix A, the time, T, required for a vehicle to reach escape velocity from a circular orbit of radius R_c and with circular velocity V_c is given by

$$T = \frac{C^2}{2\eta} \frac{\Gamma}{\mu_w/\alpha_w} \left(1 - e^{-V_c/C}\right), \tag{1}$$

where $V_c = \sqrt{\mu_p/R_c}$, μ_p being the planet's gravitational parameter. The term Γ is an empirical correction factor designed to give the exact escape time, for tangential steering, as determined from numerically integrated trajectories. It is a function of the initial thrust acceleration (in units of the gravitational acceleration at the parking orbit) and is shown in Fig. IV-4.

If $1-\Gamma$ were plotted against the normalized initial thrust acceleration on log paper the curve would be essentially a straight line. Thus, using the functional form $\Gamma = 1-pA_o^q$, a least-squares fit to the experimental points yields an analytic expression for the correction factor.

$$\Gamma = 1 - 0.76382(A_o)^{0.24323}, \tag{2}$$

where A_o is the initial thrust acceleration in terms of g at the parking orbit. In terms of the familiar system parameters Eqs. (1) and (2) are, respectively,

$$\frac{\mu_w}{\alpha_w} = \frac{1}{172.8} \frac{V_c C}{\eta} \frac{\Gamma}{T} \left(1 - e^{-V_c/C}\right) \tag{3}$$

and

$$\Gamma = 1 - p\left[\frac{1}{500} \frac{(\eta/C)(\mu_w/\alpha_w)}{\mu_p/R_c^2}\right]^q, \tag{4}$$

where V_c and C are in km/sec, T is in days, μ_p is in km^3/sec^2, R_c is in km, and α_w is in kg/kw.

In the usual application of finding J as a function of time for given parking orbit conditions, an iteration is required between Eqs. (3) and (4). From Fig. IV-4 it can be seen that a Γ of about 0.9 corresponds fairly well to thrust accelerations of from 10^{-3} to 10^{-5} g. This is close to the accelerations expected of advanced low-thrust systems and thus a Γ of 0.9 provides a reasonable starting guess for the following procedure. With time and exhaust velocity, C, given, and the parking orbit fixed, Eq. (3) is solved for μ_w/α_w. This value is substituted into Eq. (4) and a new value of Γ is computed which in turn is put into Eq. (3) and the entire process is repeated until Γ between the two equations agrees within some specified tolerance.

Finally the J corresponding to the input quantities is found from

$$J = 2000\eta \frac{\mu_w}{a_w} \frac{\Gamma\left(1 - e^{-V_c/C}\right)}{1 - \Gamma\left(1 - e^{-V_c/C}\right)} .$$

It is assumed that η is given as some function of C, e.g., the hypothetical form at the bottom of pg. 8, Section II. With all other quantities fixed, a range of C's could be introduced to note the effect on J. Fortunately J is essentially independent of C as will be shown later. Consequently, for any given thrusting time a representative C could be used to compute a J which would then be applicable to any C.

The foregoing expressions, which are applicable to departure spirals, may be used to compute capture (inward) trajectories since the latter are equivalent to the former except that vehicle mass increases rather than decreases. Thus by changing the ratio V_c/C to a negative quantity while still measuring time positive from the terminal parking oribt, the above equations apply to capture spirals.

Breakwell-Rauch Method

This method is based on the development of a systematic theory which accounts for the influence of the planet and the sun on the motion of the vehicle as it traverses the two gravitational fields. Using a mathematical perturbation technique on the planetocentric and heliocentric trajectories, the two positions of the overall trajectory are matched in order to define a point at which the computation of vehicle performance for the planet-centered part of the flight ceases for departure or commences for capture. Thus, to the order of accuracy of the perturbation, this switching point will cause the calculation of performance to agree with the actual trajectory profile.

Using the perturbation parameter, μ, the mass ratio of the planet to the sun, the Breakwell-Rauch theory for power-limited spirals is carried out through terms of order $\mu^{1/4}$ and $\mu^{1/2}$ with errors on the order of μ so that it is comparable to the widely used analysis for high-thrust trajectories. The term of order $\mu^{1/4}$ is quite important for all the planets while the term of order $\mu^{1/2}$ is quite small for the inner planets although it may be important for trajectories about the massive planets. The following is based on the analysis carried out to the order of $\mu^{1/4}$ so that there will be some error in applying the results to the massive planets.

The incremental velocity, ΔV_1, required to reach the switching point (or time) is

$$\frac{\Delta V_1}{V_c} = 1 - \zeta\left(\frac{F}{m_1}\mu_p\right)^{1/4}, \qquad (5)$$

where F is thrust, m_1 is the vehicle mass at the switching time, and ζ is a constant whose value depends on the steering program. For tangential steering $\zeta = 1.757$, while for optimal steering it is 1.840.

The mass ratio required between the switch point and the initial (or terminal) parking orbit may be determined by introducing the usual system parameters into Eq. (5). Thus,

$$\mu_1 = \exp\left\{-\frac{V_c}{C}\left[1 - 1.84\left(\frac{1}{500}\,\frac{(\eta/C)(\mu_w/\alpha_w)}{\mu_p/R_c^2}\right)^{1/4}\frac{1}{\mu_1^{1/4}}\right]\right\}, \qquad (6)$$

where μ_1 is the ratio of terminal mass to initial mass. Equation (6) is used as given for spirals leaving a parking orbit and thrusting to the switch point; hence an iteration is required to obtain μ_1. If capture spirals are to be computed, then the term $\mu_1^{1/4}$ in the right-hand side of Eq. (6) is fixed at unity (see Appendix A), thereby eliminating the iteration on μ_1.

For a fixed planet and given C (the functional form for $\eta(C)$) and thrusting time, an iteration is necessary between Eq. (6) and

$$\frac{\mu_w}{\alpha_w} = \frac{1}{172.8}\,\frac{C^2}{\eta}\,\frac{(1-\mu_1)}{T} \qquad (7)$$

in order to obtain μ_w/α_w. The procedure is somewhat complicated in the case of departure spirals since the iteration on μ_1 is required. The basic approach taken here is to nest the iteration for μ_1 inside that for μ_w/α_w. For typical planetocentric trajectories the vehicle retains most of its initial mass so that a reasonable initial guess for μ_1 would be unity.

The trajectory requirement can be calculated from

$$J = 2000\,\eta\left(\frac{\mu_w}{\alpha_w}\right)\left(\frac{1-\mu_1}{\mu_1}\right). \qquad (8)$$

If $\Gamma = 1$ in Eq. (4), then it becomes Eq. (8) since $\mu_1 = e^{-V_c/C}$.

That J is independent of C is shown in Table IV-2 for both outward and inward spirals about Earth. Table IV-2 also indicates the small difference in J between the capture and departure spirals. For all but the most massive planets this difference is insignificant and is not more than about 4% for the larger planets if the parking orbit radius is 10 or more planetary radii. Hence all of the trajectory data have been computed for departure spirals only, and can also be used for capture spirals with little error. Further, only optimal steering of the vehicle was considered since the two steering programs result in J's that differ by approximately 5%.

The Breakwell-Rauch method was favored over the Melbourne approach because of the theoretically more accurate trajectory model employed by the former and the fact that the transition region effects between the gravitational fields were partly accounted for. However, the Melbourne method is simpler, especially for computing departure trajectories by means other than a digital computer. A direct comparison of the two approaches is presented in Appendix A. Briefly, the difference in the J's may be as high as 20 to 30%; however, the net effect in the vehicle mass fractions is much less than 10%.

A sample plot of J vs powered time is shown in Fig. IV-5 for a set of planets and selected parking orbit radii. These data were obtained by the Breakwell-Rauch method using optimal steering. Note that the curves are approximately straight lines except in the vicinity of relatively long powered times. Nevertheless, since the vehicle mass fractions are almost insensitive to some variations in J once a reasonably accurate J is employed, then a linear fit to the curves of Fig. IV-5 would provide a compact technique of presenting numerous planetocentric trajectory data. Assuming the curves are of the form

$$J = \hat{J}\left(\frac{T}{\hat{T}}\right)^{m}, \tag{9}$$

and using a least-squares criterion for fitting the data, then the parameters $\hat{J}$, $\hat{T}$, and m could be tabulated for a particular planet and a given parking orbit radius. The results of this procedure are given in Table IV-3 where $\hat{J}$ and $\hat{T}$ are simply reference values, m is actually the slope of the log plot (Fig. IV-5), and r_p is the circular parking radius in units of the planet's radius. Values of $\hat{J}$ and m at other than the r_p's listed could of course be found by interpolation.

Planetocentric Orbit-to-Orbit Spiral

The computation of trajectory requirements for elevating or lowering a parking orbit about a planet is based on Ref. IV-1. Only tangential steering is considered here since the trajectory requirements are quite low for most planet-centered orbital missions and thrusting times and, as a consequence, the benefits from optimal steering would be relatively slight. Because of the fact that the spiral trajectory and corresponding analysis is confined completely within the planet's sphere of influence and involves no transition region, the performance equations do not contain the correction factor Γ. The development of this aspect of planet-centered spirals is discussed in Appendix A.

The required increment that must be accommodated by the electric propulsion system is precisely the difference in orbital velocities. Thus a vehicle which transfers (outward) from a low orbit of radius ρ_o (normalized by the planet's radius, R_p) to a final high orbit ρ_1, about a planet of gravitational parameter μ_p, will require a terminal mass fraction given by

$$\mu_1 = \exp\left[- \frac{\sqrt{\mu_P / R_P}}{C} \left(\frac{1}{\rho_0^{1/2}} - \frac{1}{\rho_1^{1/2}} \right) \right], \qquad (10)$$

so if the allowed thrusting time is T days and the propulsion system exhaust velocity is C km/sec, then the characteristic trajectory requirement is

$$J = \frac{1}{0.0864} \frac{C^2}{T} \frac{(1 - \mu_1)^2}{\mu_1}, \qquad (11)$$

where it can be seen that J does not depend on the thrustor power conversion efficency. Table IV-4 shows the results of a sample calculation for an Earth-centered spiral which commences from a low orbit of 1.05 and culminates in a series of high orbits, including the case of a synchronous orbit ($\rho_1 = 6.6301$).

An abbreviated form of Eq. (11) may be developed by noting certain characteristics of Table IV-4 which could be assumed to hold for any planet. For a given time and ρ_1, J is essentially independent of C. If this slight variation in J's is acceptable, then an average J over the range of C's would be a highly accurate estimate for the J at the given T and ρ_1. Furthermore it can be seen that, regardless of the thrusting time and terminal orbit, the average J always occurs at an exhaust velocity of approximately 40 km/sec.

Hence, for a transfer between two given orbits, Eq. (10) becomes a constant if C = 40 km/sec and Eq. (11) may be written as a constant divided by the thrusting time T. The J obtained in this manner will be an estimate of the average J which may be used in the performance analysis, i.e., where exhaust velocity and powerplant fraction are varied. Figure IV-6 shows the dependence of J on thrusting time for a transfer between an Earth-centered orbit of radius 1.05 and a series of terminal orbits, including the 24-hr synchronous orbit.

Conversely, if T is fixed, then Eq. (11) may be written as a function of ρ_1 by setting C = 40 and substituting Eq. (10) into Eq. (11). A further simplification of this result may be obtained by noting that a plot of J vs ρ_1 on a semi-log graph, Fig. IV-7, is almost linear for ρ_1 between 2 and 10. A least-squares fit to this plot would yield a simple relation involving only ρ_1 for the assumed T. The general form of the equation would be

$$J = a \rho_1^b,$$

where a and b are constants determined by the least-squares method. This result may be expedient for quick performance analyses of transfers to various orbital radii.

Either the arithmetic-mean, Eq. (15), or geometric-mean, Eqs. (16) to (19), results of Section II may be used to determine the exhaust velocity and powerplant fraction which maximizes net spacecraft mass fraction. Equations (12) and (13) of Section II may be used to compute the initial and average thrust accelerations, respectively, if necessary.

In computing the performance of orbit-changing propulsion systems, it is useful to estimate beforehand the minimum thrusting time which yields zero net mass fraction. As noted above, for transfers between two given orbits, Eq. (11) can be written so that J is inversely proportional to the time. Or, using some reference time, $\hat{T}$, and corresponding J, $\hat{J}$, then

$$J = \hat{J}\left(\frac{\hat{T}}{T}\right). \tag{12}$$

With the use of Eq. (19), Section II, and the corresponding thrustor efficiency function, the desired minimum time may be found by substituting Eq. (12) and setting the result equal to zero. This procedure is essentially accomplished in Eq. (20) of Section II, so that putting Eq. (12) into Eq. (20), Section II, the desired result is obtained.

$$\frac{a_w d^2}{T} = \frac{2}{\frac{\hat{J}\hat{T}}{d^2}\left(1 + \frac{2}{\sqrt{\hat{J}\hat{T}/d^2}}\right)} \tag{13}$$

Note that the dimensionless ratio $\hat{J}\hat{T}/d^2$ (appropriate conversion units are required) contains the reference parameters indicative of the orbital transfer and the thrustor efficiency. Equation (13) may be utilized in two ways. Given the powerplant specific mass, the minimum thrusting time may be found which produces zero maximum net mass fraction, or given a required time, the maximum powerplant specific mass may be computed for the propulsion system. A generalized non-dimensional plot of Eq. (13) is shown in Fig. IV-8. Reasonably accurate results may be obtained from Fig. IV-8 for quick evaluation.

As an example, consider an Earth-centered transfer from an orbit of 1.05 radii to a synchronous orbit. From Table IV-4 selecting the reference time as 5 days, the reference J is 50.046 m^2/sec^3. If d = 20 km/sec, then, with the proper conversion constants for nondimensionality,

$$0.0864\,\frac{\hat{J}\hat{T}}{d^2} = 0.0864\,\frac{(50 \times 5)}{(20)^2} = 0.054.$$

With this value, Fig. IV-8 gives $\alpha_w d^2/T = 3.85$. Again with the proper conversion constants,

$$\frac{\alpha_w d^2}{86.4\,T} = 3.85, \quad \text{and} \quad \frac{\alpha_w}{T} = 0.832.$$

Thus, for example, if α_w = 15 kg/kw, then the minimum allowable thrusting time is 18 days. If T = 12 days, then the maximum allowable specific mass is 10 kg/kw

Corrections for Low-Thrust Hyperbolic Trajectories

For the purpose of computing performance, it is assumed that the electric spacecraft, after being boosted from or onto the parking orbit, initiates or terminates its interplanetary trajectory with the planet's heliocentric position and the velocity resulting from the hyperbolic excess velocity due to high thrust boost and the planet's heliocentric velocity. In actual operation, the high- and low-thrust stages will be ignited sequentially so that the electric system does operate for some period of time within the planet's sphere of influence on a hyperbolic path. Because there currently does not exist a method of exactly determining the precise performance values for an overall interplanetary trajectory, it is necessary to employ velocity and position offsets on the boundaries of the heliocentric trajectory to replace the effect of the planet.

These offsets are based on the velocity-intercept notion of matching the planetocentric trajectory far from the planet with the heliocentric trajectory close to the planet. The vehicle's planetocentric velocity as it recedes from the planet approaches an asymptotic form as the gravitational field of the planet diminishes. By extending this asymptote back to zero velocity, an intercept time, t_1, may be defined as the time at which a vehicle escaping from a heliocentric, massless point planet with zero initial planetocentric velocity would have the foregoing asymptotic behavior as its velocity profile. For the case of hyperbolic low-thrust trajectories, the foregoing approach may be simply implemented by considering the case of purely radial motion. This is justified, heuristically, since hyperbolic trajectories, after a short period, become essentially radial.

This case may be solved analytically for the constant thrust-acceleration trajectory to obtain the required offsets of velocity, δV, and position, δR. The vehicle is assumed to start from the center of the planet with an initial hyperbolic excess speed. If V_{∞_0} is the initial hyperbolic excess speed, F/m the thrust acceleration, and μ_P the planet's gravitational parameter, then:

$$\text{for } V_{\infty_0}\left(\frac{F}{m}\mu_P\right)^{-1/4} \leq 2,$$

$$\delta V = \left[2\sqrt{2}\,E(k) - \sqrt{2}\,K(k)\right]\left(\frac{F}{m}\mu_P\right)^{1/4}, \tag{14}$$

where

$$k^2 = \frac{1}{2} - \frac{1}{8}\left[V_{\infty_0}\left(\frac{F}{m}\mu_P\right)^{-1/4}\right]^2 . \tag{15}$$

for $V_{\infty_0}\left(\frac{F}{m}\mu_P\right)^{-1/4} \geq 2$,

$$\delta V = \left\{ \frac{1}{2}\left[V_{\infty_0}\left(\frac{F}{m}\mu_P\right)^{-1/4}\right]^2 + \sqrt{\frac{1}{4}\left[V_{\infty_0}\left(\frac{F}{m}\mu_P\right)^{-1/4}\right]^4 - 4} \right\}^{1/2} E(k)\left(\frac{F}{m}\mu_P\right)^{1/4}, \tag{16}$$

where

$$k^2 = \frac{2\sqrt{\frac{1}{4}\left[V_{\infty_0}\left(\frac{F}{m}\mu_P\right)^{-1/4}\right]^4 - 4}}{\frac{1}{2}\left[V_{\infty_0}\left(\frac{F}{m}\mu_P\right)^{-1/4}\right]^2 + \sqrt{\frac{1}{4}\left[V_{\infty_0}\left(\frac{F}{m}\mu_P\right)^{-1/4}\right]^4 - 4}} . \tag{17}$$

In either case, the position offset is given by

$$\delta R = \frac{(\delta V)^2 - V_{\infty_0}^2}{2(F/m)} . \tag{18}$$

The detailed development of the foregoing results are presented in Appendix B. The quantities K(k) and E(k) are, respectively, the complete elliptic integrals of the first and second kind with modulus k^2. Because of K and E, which are tabulated data, it is expedient for performance calculations to define correction factors D and C in the velocity and position offsets, respectively, as follows:

$$\delta V - V_{\infty_0} = D\left(\frac{F}{m}\mu_P\right)^{1/4} , \tag{19}$$

and

$$\delta R = C\left(\frac{F/m}{\mu_P}\right)^{-1/2} \tag{20}$$

From these definitions and the previous equations, it can be seen that D and C are functions of $V_{\infty_o}(F\mu_P/m)^{-1/4}$, the initial velocity parameter. These curves are given in Fig. IV-9. The velocity offset is in the direction of the initial heliocentric thrust direction and is always larger than the initial hyperbolic excess velocity. The position offset is a positive quantity in the same direction and is quite small, for the inner planets at least, and is usually neglected in performance estimates.

The foregoing results, although based on constant thrust-acceleration trajectories, apply equally well to constant-thrust flights if the thrust acceleration, F/m, is based on the mass at the juncture of the heliocentric trajectory. In general, F/m would be known beforehand only for the initial and terminal portions of the heliocentric trajectory whereas the mass expenditure during the planetocentric portion would be undetermined. Since $\delta V - V_{\infty_o}$ represents the velocity contribution of the low-thrust system during the planetary phase, an iteration on the planet-centered terminal mass fraction, μ_{1D}, would be necessary according to

$$\delta V - V_{\infty_o} = -C \ln \mu_{1D} = D\left(\frac{F/m_o}{\mu_{1D}}\mu_P\right)^{1/4}, \tag{21}$$

where, functionally,

$$D = D\left[V_{\infty_o}\left(\frac{F/m_o}{\mu_{1D}}\mu_P\right)^{-1/4}\right], \tag{22}$$

and where F/m_o is the initial thrust acceleration upon departure from the parking orbit (after high-thrust burn) and C is the low-thrust exhaust velocity (not correction factor). For high-thrust capture onto a planetary parking orbit after electric thrusting planetocentrically, no iteration is necessary since

$$-C \ln \mu_{1C} = D\left(\frac{F}{m_{1H}}\mu_P\right)^{1/4} = D\left(\frac{F/m_o}{\mu_{1H}}\mu_P\right)^{1/4}, \tag{23}$$

wherein μ_{1H}, the terminal mass fraction for the heliocentric transfer, is known from the heliocentric trajectory optimization program and μ_{1C} is the terminal mass fraction for the capture phase.

A simpler procedure would be to use the initial heliocentric thrust acceleration for F/m in the departure case. This is justified primarily because of the relatively short time the vehicle thrusts in the vicinity of the departure planet and the high specific impulses associated with electric propulsion. Consequently μ_{1D} would be almost unity for departure from Earth.

In practice the foregoing velocity correction, $\delta V - V_{\infty_o}$, i.e., the right-hand side of Eq. (21), would be applied to the high-thrust phase by reducing the assigned initial velocity of the high-thrust system by the amount $D(F\mu_p/m)^{1/4}$. This permits the constant-thrust computer program to optimize the heliocentric trajectory and the propulsion parameters as presently performed with the boundary conditions being the hyperbolic excess speeds and the planets' heliocentric positions (neglecting δR).

Because the optimization of the high- and low-thrust combination will be computerized and since the numerous tabular values of the elliptic integrals are not easily made a part of performance and mass calculations, a simplified functional form of D and C would be most helpful to the routine computations. A least-squares curve fit was applied to obtain D and C as functions of $V_{\infty_o}(F\mu_p/m)^{-1/4}$. In each case the form of the equations used was suggested by the shape of the curves in Fig. IV-9. For D the form was given by

$$y = ar^x + bs^x, \tag{24}$$

which is equivalent to

$$y = ae^{x \ln r} + be^{x \ln s},$$

where a, b, r, and s are parameters to be found such that the sum of the squares of the residuals is a minimum. The quantities y and x are D and $V_{\infty_o}(F\mu_p/m)^{-1/4}$, respectively. The results for the D equation are:

$$a = 0.052688 \qquad r = 0.909470$$

$$b = 1.15207 \qquad s = 0.394237$$

The form used for C was

$$y = ae^{-rx^2} + be^{-sx^2}, \tag{25}$$

where C = y, and a, b, r, and s are as before. The solution gives

$$a = 0.346150 \qquad r = 0.235156$$

$$b = 0.366336 \qquad s = 0.0239258$$

The foregoing curve fits are highly accurate and differ from the exact values by not more than 1% at any given point.

REFERENCES

IV-1. Melbourne, W. G.: "Interplanetary Trajectories and Payload Capabilities of Advanced Propulsion Vehicles". JPL Technical Report 32-68, March 1961.

IV-2. Breakwell, J. V., and H. E. Rauch: "Asymptotic Matching in Power-Limited Interplanetary Transfers". AAS preprint 66-114, 1966.

IV-3. Ragsac, R. V. et al.: "Study of Trajectories and Upper Stage Propulsion Requirements for Exploration of the Solar System". UA Research Laboratories Report F-910352-13, Vol. II, Section VI by T. N. Edelbaum, September 1967.

TABLE IV-1

PARAMETERS FOR HELIOCENTRIC TRAJECTORY

AND POWERED TIME EQUATIONS

$$J_H = \hat{J}_H \left(\frac{T_H}{\hat{T}_H}\right)^{m_H} \qquad T_{HP} = \hat{T}_{HP}\left(\frac{T_H}{\hat{T}_H}\right)^{m_{HP}}$$

	Mercury	Jupiter	Saturn	Uranus
Rendezvous				
T_H, days	80	400	700	
$\hat{J}_H$, m^2/sec^3	181.929	103.478	85.816	
m_H	-2.20382	-2.86920	-2.78780	
$\hat{T}_{HP}$, days	56.161	257.175	437.583	
m_{HP}	1.156017 $80 \le T \le 200$	0.895741 $400 \le T \le 1000$	0.908804 $700 \le T \le 1200$	
Flyby				
$\hat{T}_H$	70	300	600	600
$\hat{J}_H$, m^2/sec^3	59.241	47.092	30.230	131.036
m_H	-2.86384	-2.37067	-2.06470	-2.59108
$\hat{T}_{HP}$, days	43.796	150.890	321.034	329.991
m_{HP}	1.291965 $70 \le T \le 160$	1.056036 $300 \le T \le 800$	0.887848 $600 \le T \le 1200$	0.907105 $600 \le T \le 1400$

TABLE IV-2

INVARIANCE OF J AND COMPARISON OF EARTH

OUTWARD AND (INWARD) SPIRALS

C km/sec	μ_1	μ_w/α_w kw/kg	J m^2/sec^3
20	0.7359 (0.7318)	0.02038 (0.02069)	7.313 (7.583)
40	0.8572 (0.8560)	0.02754 (0.02777)	7.340 (7.473)
60	0.9022 (0.9017)	0.03771 (0.03793)	7.354 (7.443)
80	0.9257 (0.9254)	0.04873 (0.04894)	7.363 (7.429)
100	0.9401 (0.9399)	0.06011 (0.06032)	7.368 (7.422)
120	0.9498 (0.9496)	0.07167 (0.07188)	7.372 (7.416)
140	0.9568 (0.9567)	0.08333 (0.08354)	7.375 (7.413)
160	0.9621 (0.9620)	0.09507 (0.09528)	7.377 (7.410)
180	0.9662 (0.9662)	0.1068 (0.1071)	7.379 (7.408)
200	0.9695 (0.9695)	0.1187 (0.1189)	7.380 (7.407)

TABLE IV-3

PARAMETERS FOR PLANETOCENTRIC SPIRAL TRAJECTORY EQUATION

$$J = \hat{J} \, (T/\hat{T})^m$$

MERCURY

r_p radii	$\hat{J}$, m^2/sec^3	m
1.05	3.5040	-0.86560
2	1.5216	-0.82282
3	0.97289	-0.78826
4	0.57795	-0.75918
5	0.41471	-0.73352
6	0.31343	-0.71024
7	0.24566	-0.68874
8	0.18783	-0.66868

$\hat{T}$ = 15; 15 ≤ T ≤ 90 days

VENUS

r_p radii	$\hat{J}$, m^2/sec^3	m
1.1	10.871	-0.89108
2	5.1611	-0.85981
4	2.0600	-0.81075
6	1.11610	-0.77341
8	0.75733	-0.74193
10	0.53630	-0.71410
12	0.40047	-0.68882
14	0.31042	-0.66547
16	0.24740	-0.64365
18	0.20146	-0.62308
20	0.16691	-0.60355

$\hat{T}$ = 30; 30 ≤ T ≤ 240 days

EARTH

r_p radii	$\hat{J}$, m^2/sec^3	m
1.05	13.588	-0.89256
2	6.1181	-0.86001
4	2.4534	-0.81207
6	1.3874	-0.77555
8	0.90752	-0.74474
10	0.64419	-0.71751
12	0.48206	-0.69277
14	0.37439	-0.66991
16	0.29891	-0.64855
18	0.24383	-0.62840
20	0.20233	-0.60929

$\hat{T}$ = 30; 30 ≤ T ≤ 240 days

MARS

r_p radii	$\hat{J}$, m^2/sec^3	m
1.05	2.7629	-0.89000
2	1.2354	-0.85572
4	0.49032	-0.80526
6	0.27511	-0.76682
8	0.17876	-0.73437
10	0.12615	-0.70565
12	0.093900	-0.67955
14	0.072567	-0.65542
16	0.057676	-0.63291
18	0.046845	-0.61167
20	0.038713	-0.59147

$\hat{T}$ = 30; 30 ≤ T ≤ 240 days

TABLE IV-3 (Contd.)

PARAMETERS FOR PLANETOCENTRIC SPIRAL TRAJECTORY EQUATION

$$J = \hat{J} (T/\hat{T})^m$$

JUPITER

r_p radii	$\hat{J}$, m^2/sec^3	m
1.1	357.54	-0.87011
5	43.328	-0.74747
10	14.140	-0.65012
20	3.9024	-0.50939
30	1.6516	-0.39974

$\hat{T}$ = 30; 30 ≤ T ≤ 240 days

SATURN

r_p radii	$\hat{J}$, m^2/sec	m
1.1	118.80	-0.85841
5	13.928	-0.72128
10	4.3632	-0.61281
20	1.1321	-0.45597
30	0.4567	-0.33433

$\hat{T}$ = 30; 30 ≤ T ≤ 204 days

URANUS

r_p radii	$\hat{J}$, m^2/sec^3	m
1.1	46.545	-0.87273
5	5.8949	-0.75211
10	1.9548	-0.65778
20	0.55017	-0.52164
30	0.23616	-0.41539

$\hat{T}$ = 30; 30 ≤ T ≤ 240 days

NEPTUNE

radii	$\hat{J}$, m^2/sec^3	m
1.1	63.117	-0.88077
5	8.2738	-0.76874
10	2.8224	-0.68156
20	0.82784	-0.55599
30	0.36695	-0.45793

$\hat{T}$ = 30; 30 ≤ T ≤ 240 days

PLUTO

r_p radii	$\hat{J}$, m^2/sec^3	m
1	20.791	-0.87007
2	8.4338	-0.82489
5	2.2691	-0.73632
10	0.73379	-0.63553
20	0.19900	-0.48984

$\hat{T}$ = 15; 15 ≤ T ≤ 120 days

2A

TABLE IV-4

REQUIRED J FOR EARTH-CENTERED ORBITAL TRANSFERS

Initial Orbit = 1.05 radii

C, km/sec	Terminal Orbit = 4 radii Thrusting Time, Days 5	15	30	C, km/sec	Terminal Orbit = 8 radii Thrusting Time, Days 5	15	30
	J, m^2/sec^3				J, m^2/sec^3		
20	32.895	10.965	5.4826	20	56.374	18.791	9.3956
30	32.841	10.947	5.4736	30	56.216	18.739	9.3693
40	32.823	10.941	5.4704	40	56.161	18.720	9.3602
50	32.814	10.938	5.4690	50	56.135	18.712	9.3559
60	32.809	10.936	5.4682	60	56.122	18.707	9.3536
70	32.806	10.935	5.4677	70	56.113	18.704	9.3522
80	32.804	10.935	5.4674	80	56.108	18.703	9.3513
90	32.803	10.934	5.4672	90	56.104	18.701	9.3507
100	32.802	10.934	5.4670	100	56.101	18.700	9.3502
Avg. J	32.822	10.941	5.4703	Avg. J	56.159	18.720	9.3599
	Synchronous Orbit = 6.630 radii				Terminal Orbit = 10 radii		
20	50.216	16.739	8.3693	20	63.378	21.126	10.563
30	50.091	16.697	8.3485	30	63.179	21.060	10.530
40	50.047	16.682	8.3412	40	63.109	21.036	10.518
50	50.027	16.676	8.3378	50	63.077	21.026	10.513
60	50.016	16.672	8.3359	60	63.060	21.020	10.510
70	50.009	16.670	8.3348	70	63.049	21.016	10.508
80	50.005	16.668	8.3341	80	63.042	21.014	10.507
90	50.002	16.667	8.3336	90	63.038	21.013	10.506
100	50.000	16.667	8.3333	100	63.034	21.011	10.506
Avg. J	50.046	16.682	8.3409	Avg. J	63.104	21.031	10.517

HELIOCENTRIC TRAJECTORY REQUIREMENTS

☿ MERCURY
♃ JUPITER
♄ SATURN
♅ URANUS

R = RENDEZVOUS
F = FLYBY (IMPACTER)

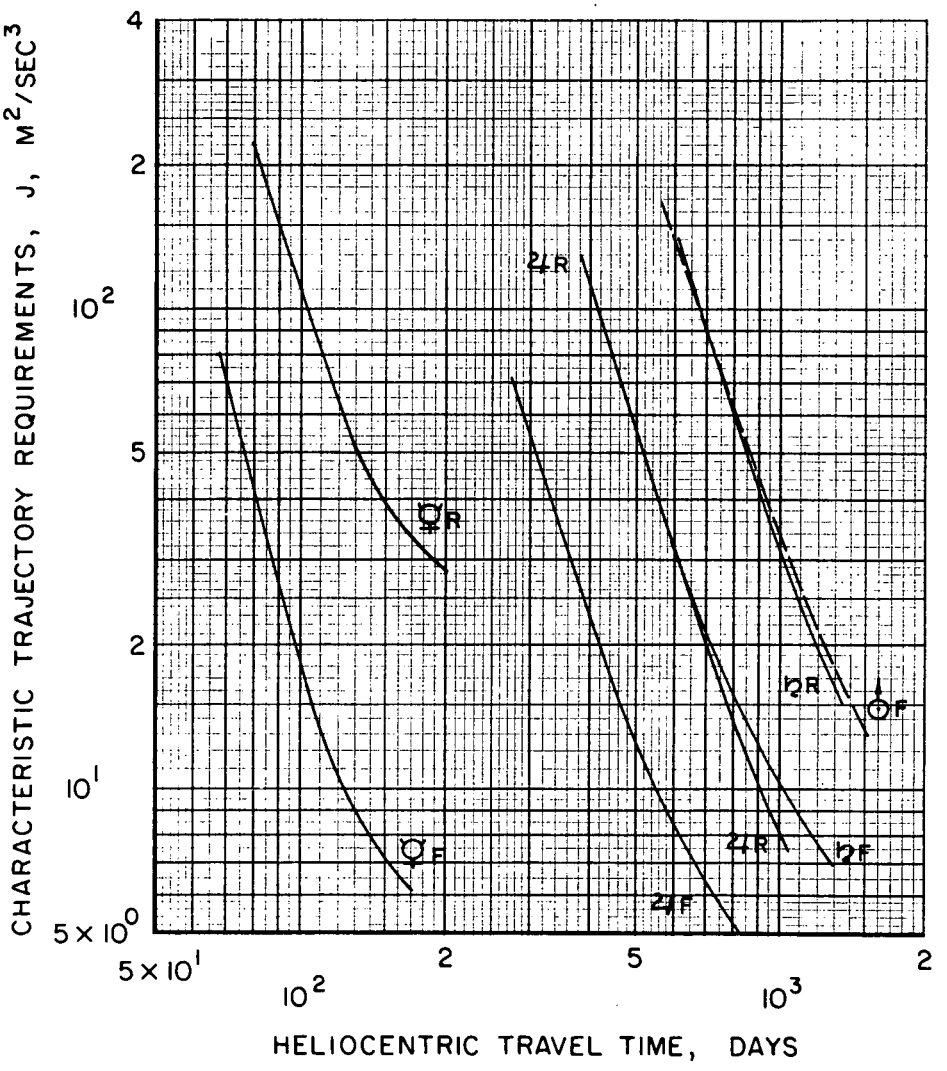

FIG. IV-2

HELIOCENTRIC POWERED TIME REQUIREMENTS

☿ MERCURY
♃ JUPITER
♄ SATURN
♅ URANUS

R = RENDEZVOUS
F = FLYBY (IMPACTER)

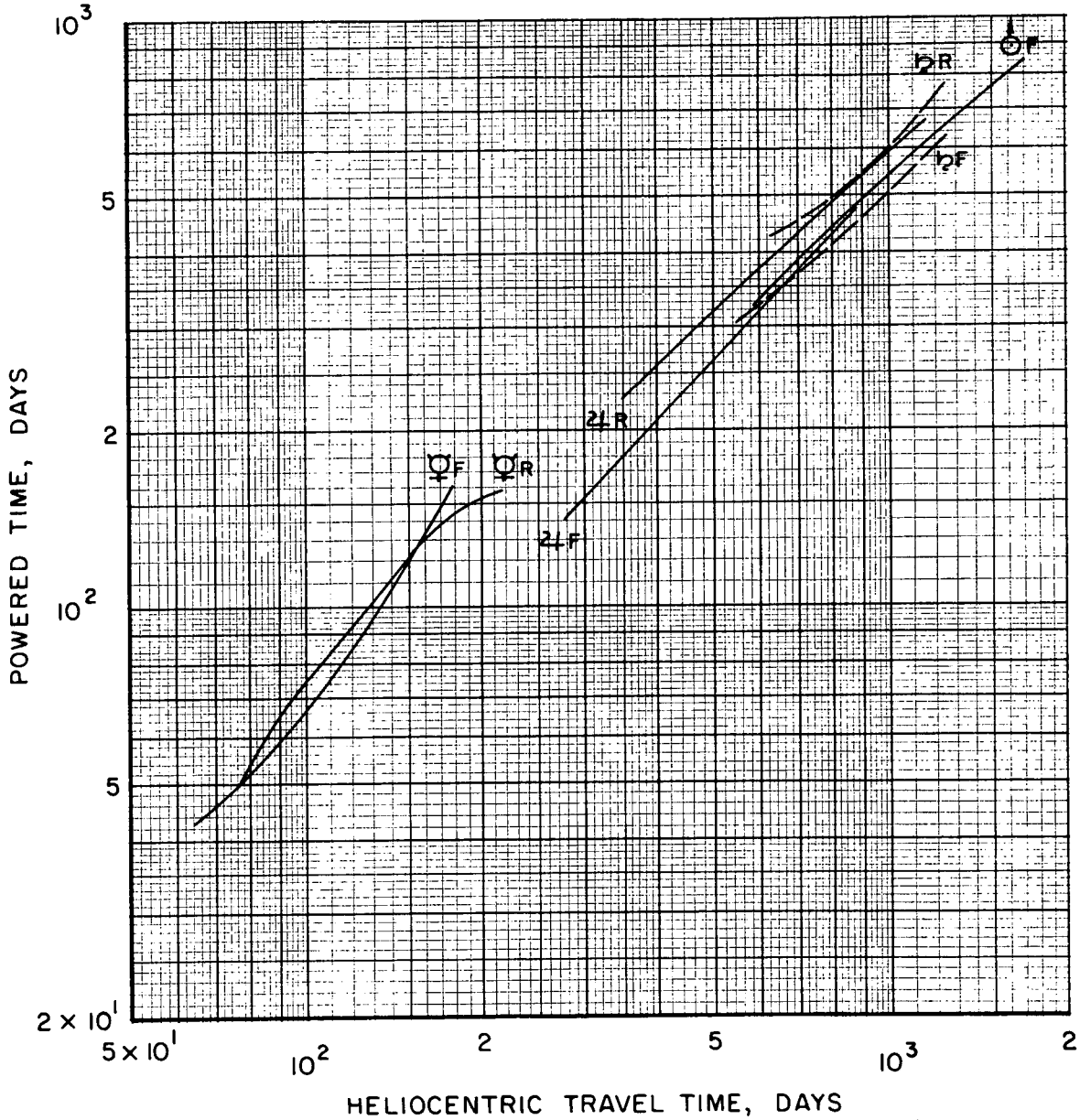

FLYBY VELOCITIES AT THE PLANETS

☿ MERCURY
♃ JUPITER
♄ SATURN
⊙ URANUS

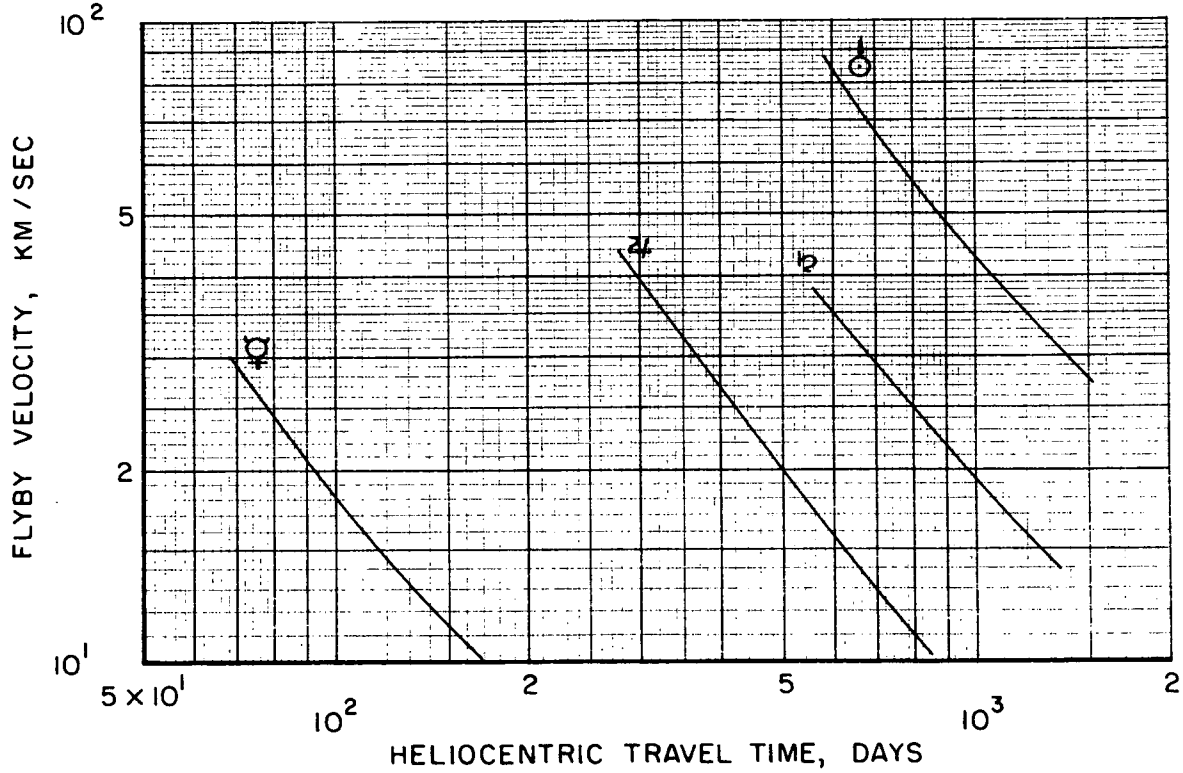

G-110058-28

FIG. IV-3

CORRECTION FOR PLANETARY SPIRAL ESCAPE TIME

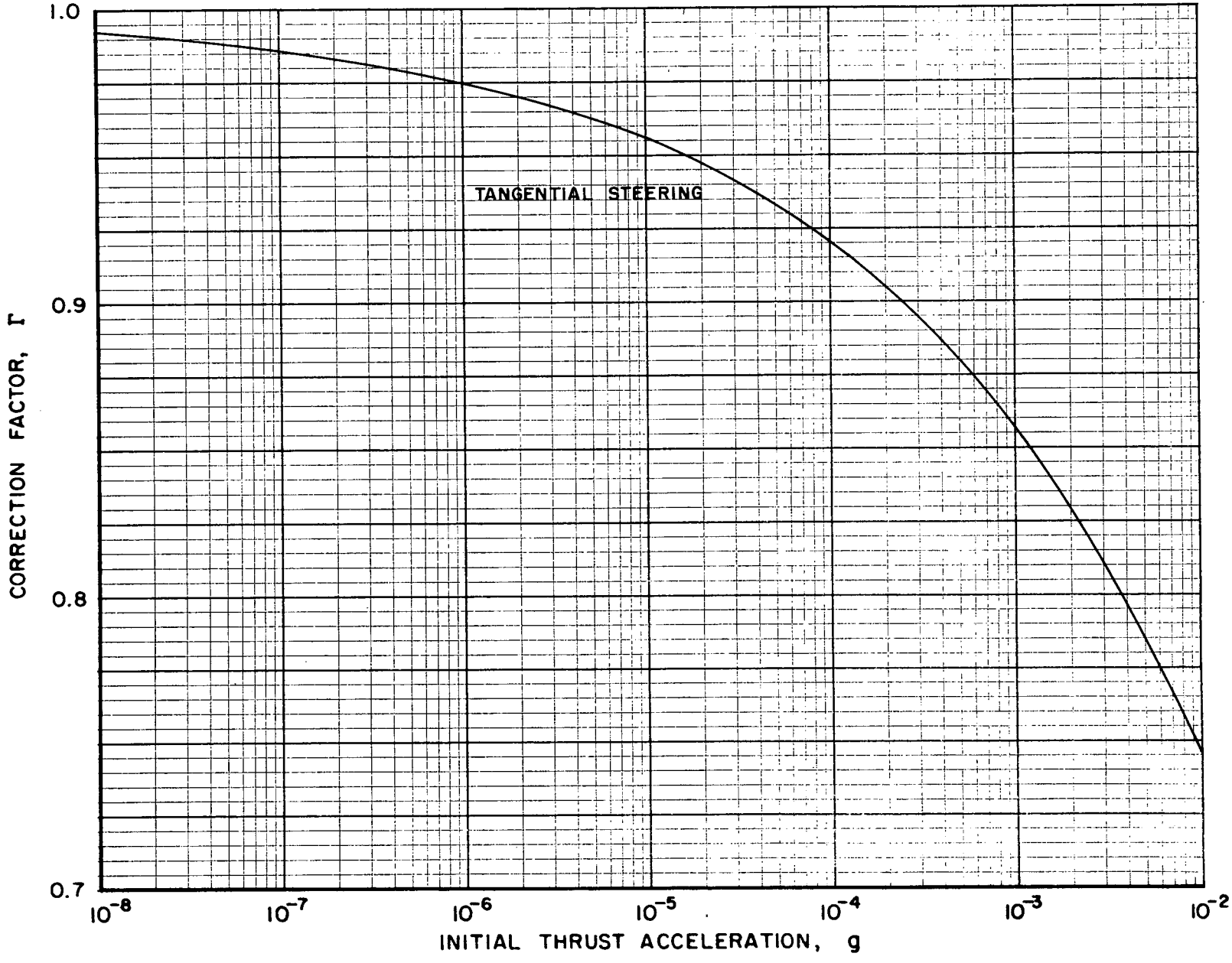

G-110058-28

FIG. IX-4

FIG. IV - 5

PLANETOCENTRIC SPIRAL TRAJECTORY REQUIREMENTS

☿ MERCURY
♄ SATURN
♃ JUPITER
♅ URANUS
⊕ EARTH

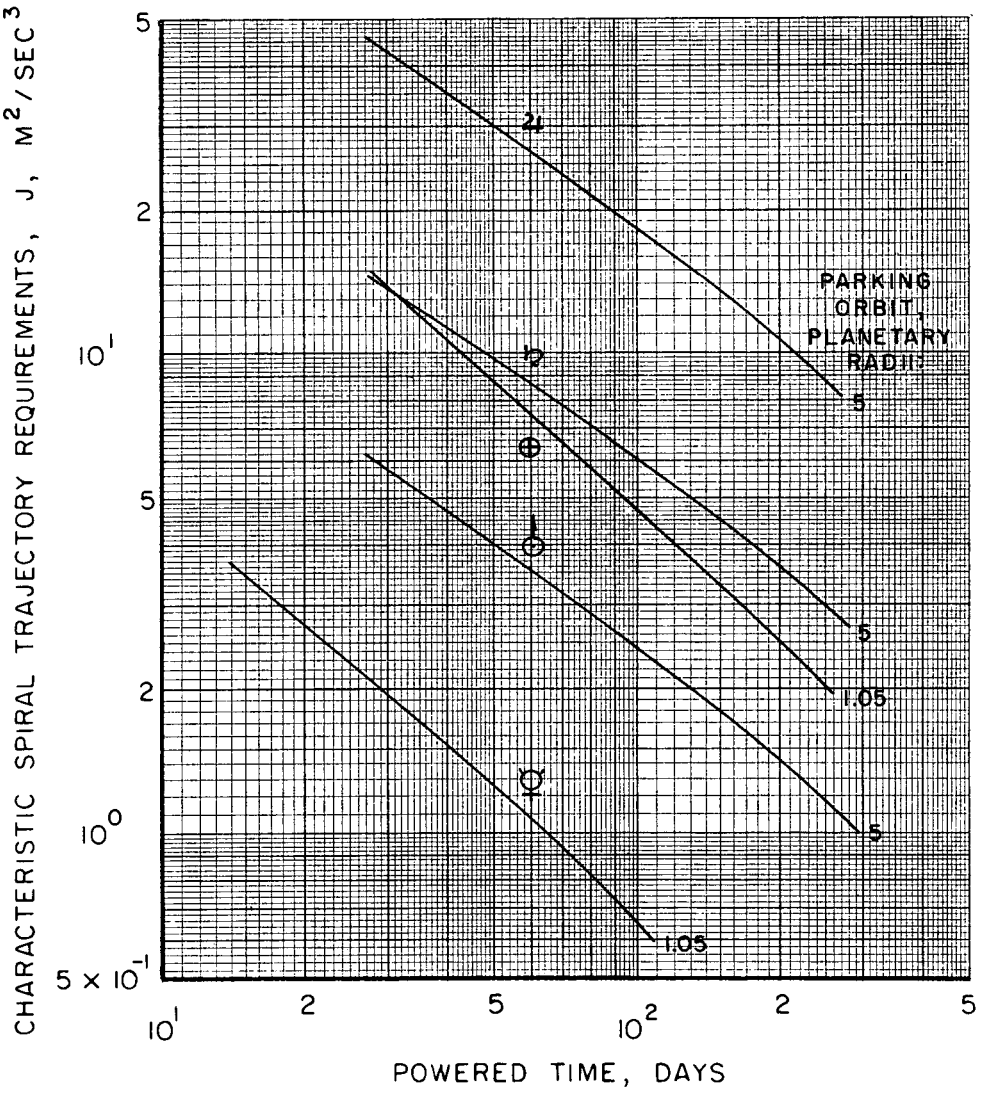

TRANSFERS BETWEEN EARTH-CENTERED ORBITS

INITIAL ORBIT = 1.05 RADII

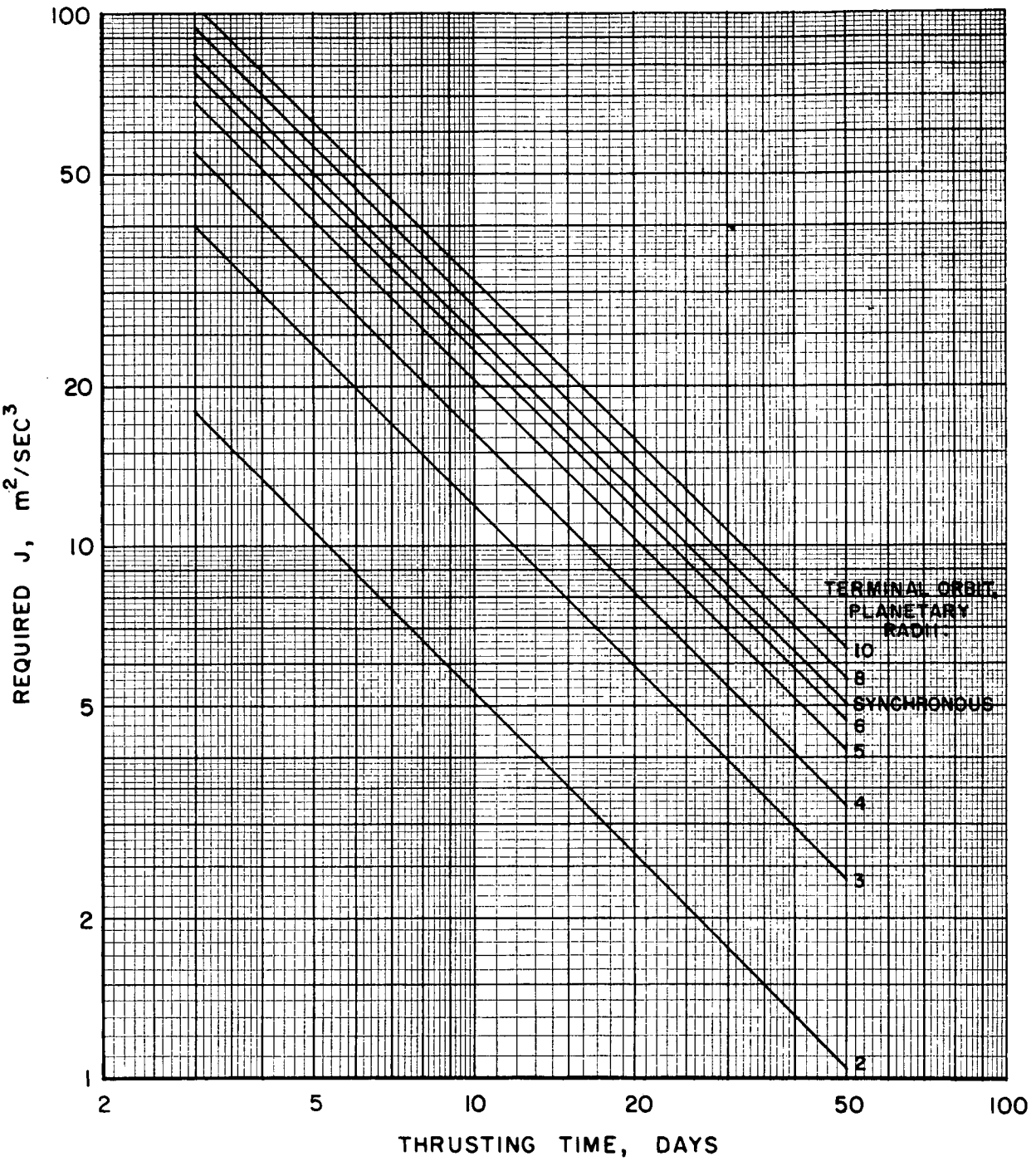

FIG. IV-7

TRANSFERS BETWEEN EARTH-CENTERED ORBITS

INITIAL ORBIT = 1.05 RADII

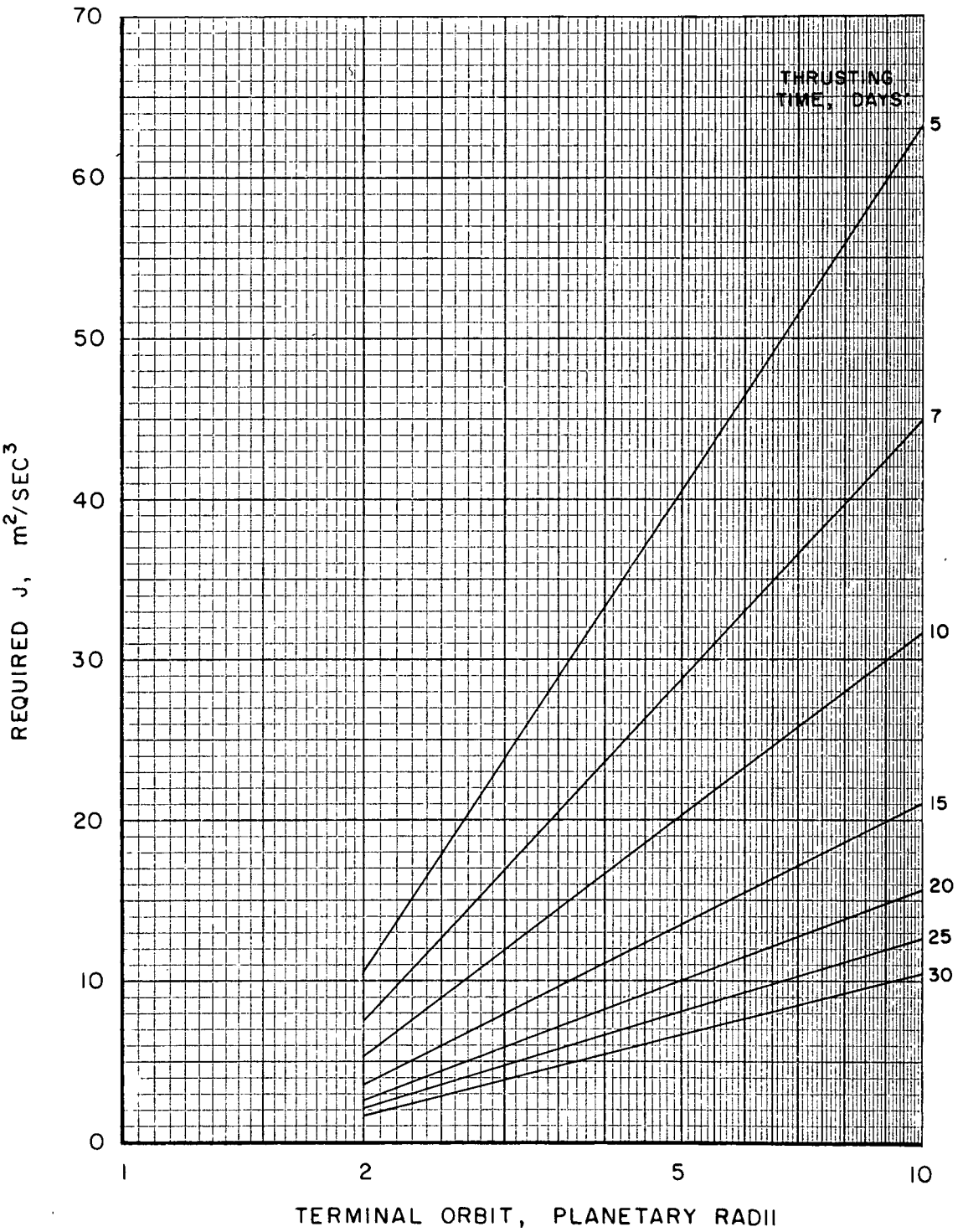

FIG. IV-8

MAXIMUM POWERPLANT SPECIFIC MASS OR MINIMUM TIME FOR ZERO NET MASS FRACTION

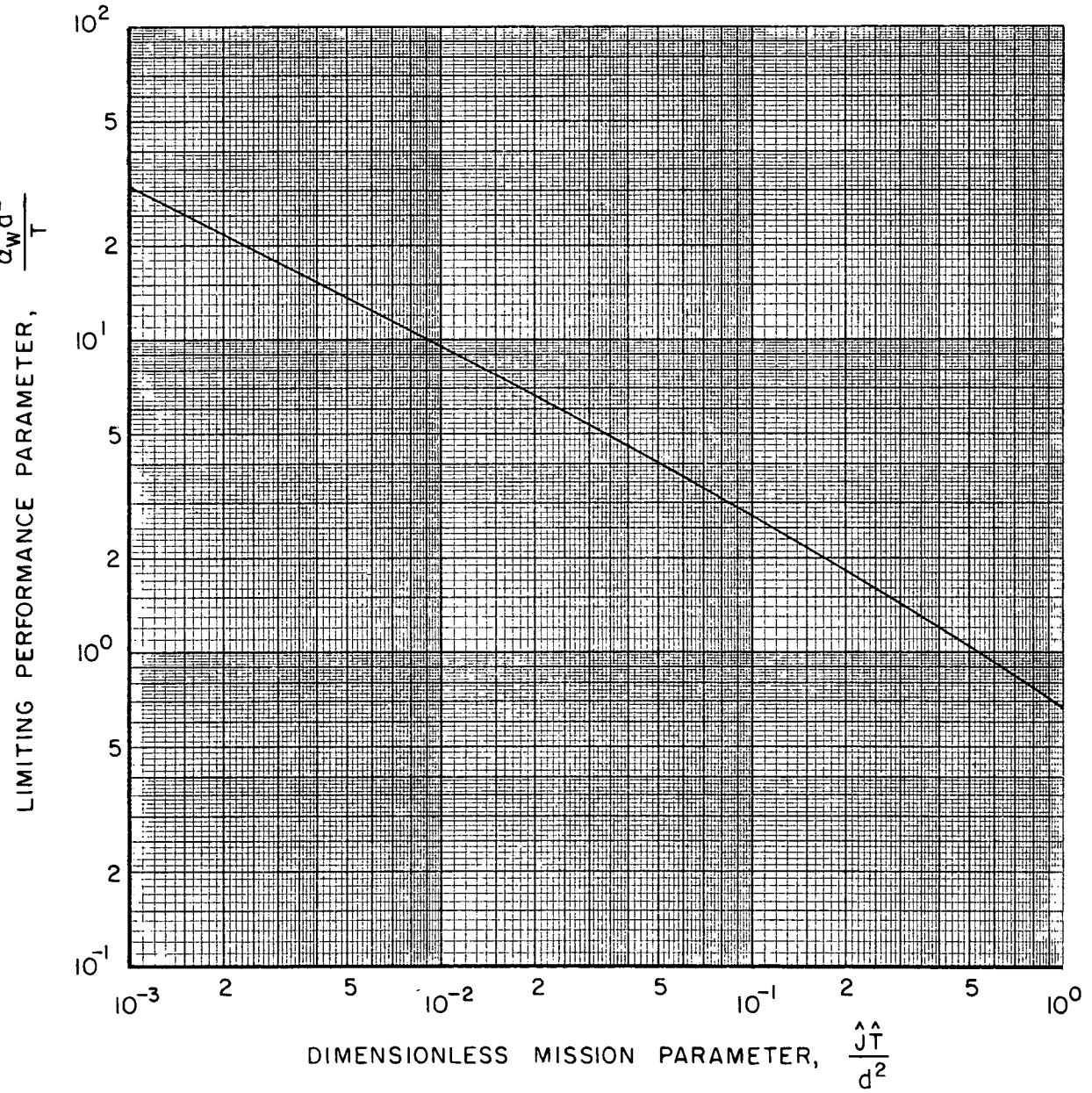

VELOCITY AND POSITION OFFSETS FOR LOW-THRUST HYPERBOLIC TRAJECTORIES DUE TO PLANETARY ATTRACTION

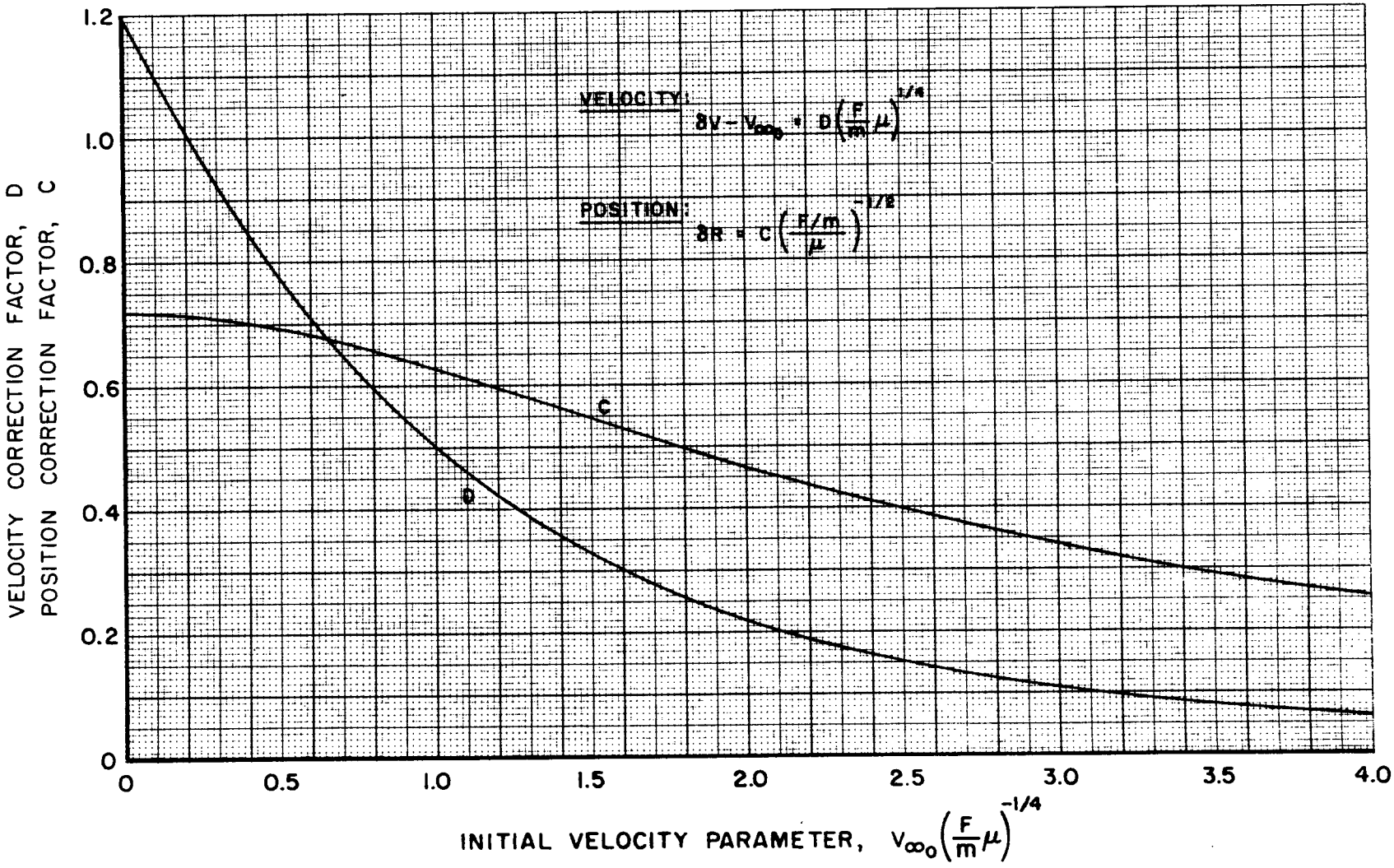

FIG. IX-9

SECTION V

MISSION AND SYSTEMS ANALYSES

The basic insight into the relationships between the trajectory characteristic, J, and the propulsion system parameters, C and μ_W, was presented in Section II, III, and IV with reference to maximum terminal mass fraction and net spacecraft mass fraction. This section is devoted to the application of the previous information in evaluating specific aspects of power-limited propulsion systems when used in certain interplanetary flight modes. The purpose is to develop the system equations for the different flight modes and to present computational aids useful in solving these equations.

In all of the missions to be considered, the flight commences from a low parking orbit about Earth and terminates either on a parking orbit about the planet (for capture missions) or at the time of closest approach to the planet (for flyby missions). Two propulsion modes are presented. The first involves a single electric propulsion system that performs all phases of the flight with no staging of any type. The second consists of mixed high- and low-thrust propulsion with staging of the individual systems. This latter mode requires heliocentric trajectories in which either one or both of the boundaries contain hyperbolic excess speeds that are accommodated by the high-thrust propulsion system. Unfortunately, as of the date of this writing, insufficient mixed high- and low-constant-thrust trajectory data limits the discussion to the development of the appropriate equations.

In the case of the single-stage electric propulsion system, three system variations are treated, all of which require the powerplant specific mass to be given. The first variation is merely that treated in Sections II and III, namely the maximization of net spacecraft mass fraction. The second case assumes that the powerplant mass is given and that the gross vehicle mass and exhaust velocity are to be optimized for maximum net spacecraft mass (not mass fraction). The final variation considers both the powerplant mass and gross vehicle mass to be given and that the exhaust velocity must be optimized to obtain maximum net spacecraft mass.

Single-Stage Electric Propulsion System

Trajectory Optimization

The use of a single-stage propulsion system which operates throughout at most three different gravitational fields requires that the characteristic requirement for such a three-phase trajectory be a minimum. Usually interplanetary missions are specified in part by the allowable overall mission duration. In this case the total duration for the mission, T, is

$$T = T_D + T_H + T_C , \tag{1}$$

where the subscripts D, H, and C denote departure time (from Earth), heliocentric travel time, and capture time, if any, at the planet. From Section IV it was determined that the J for each phase could be written (approximately) as a simple function of travel time. Because only the overall mission duration is specified, it is necessary to determine the constituent times in Eq. (1) which minimize the total J as given by

$$J = J_D(T_D) + J_H(T_H) + J_C(T_C) . \tag{2}$$

That the total J represents the overall trajectory is based on the fact that the final terminal mass fraction is the product of the individual terminal fractions of each phase provided no staging occurs.

$$\mu_I = \mu_{ID}\,\mu_{IH}\,\mu_{IC} \tag{3}$$

Now the mass of the powerplant, m_W, is the same throughout the flight so that the powerplant mass fraction of each phase can be found in terms of the terminal mass fractions.

$$\mu_W = \mu_{WD} , \qquad \mu_{WH} = \frac{\mu_W}{\mu_{ID}} , \qquad \text{and} \quad \mu_{WC} = \frac{\mu_W}{\mu_{ID}\,\mu_{IH}} . \tag{4}$$

Combining the relations of Eq. (4) with the rocket equation (Eq. (1), Section II), and substituting into Eq. (3), the overall terminal mass fraction becomes

$$\mu_I = \frac{1}{1 + \frac{a_W}{2}\,\frac{(J_D + J_H + J_C)}{\eta\,\mu_W}} , \tag{5}$$

where the exhaust velocity is the same for all thrusting phases so that η is constant. Consequently, as expected, the sum of the individual trajectory requirements (parking orbit-to-parking orbit) should be a minimum to ensure maximum final terminal mass fraction.

Strictly interpreted, however, the overall trajectory requirement should be computed as one complete and continuous trajectory accounting for all the perturbing influences of the planet and the sun of the vehicle's motion. The exact solution of this multi-body trajectory problem is not tractable for mission study purposes and therefore the approach is to separately compute the individual planetocentric trajectories while accounting for the transition effects between the planet's and sun's gravitational fields. This permits the Breakwell-Rauch planetocentric trajectory

data of Section IV to be used in conjunction with the appropriate heliocentric data. In addition to the error inherent in the planetocentric spirals about the more massive planets, there is the actual position error of the vehicle which, because of the above approach, is due to the assumption that the spacecraft is at the center of the massless point planet in heliocentric space. This error is neglected in all of the present analysis.

The overall computational approach is to first find the distribution of powered times which minimizes the total J for a specified mission duration. This yields the total minimum J and corresponding total powered time, both of which are required for determining the optimum exhaust velocity and powerplant fraction. These optimum parameters may be found by using either the iterative procedure described in Eq. (15), Section II, or the closed-form expressions in Eqs. (16) to (19), Section II.

The procedure is greatly simplified if the trajectory requirement and powered time equations shown in Tables IV-1 and IV-3 are employed. Assuming for the moment that the heliocentric travel time, T_H, is given, then the total planetocentric time is known from

$$T - T_H = T_D + T_C, \tag{6}$$

where T, the total mission duration, is specified. The total planetocentric trajectory characteristic is

$$J_P = J_D + J_C = \hat{J}_D\left(\frac{T_D}{\hat{T}_D}\right)^{m_D} + \hat{J}_C\left(\frac{T_C}{\hat{T}_C}\right)^{m_C}, \tag{7}$$

where the simplified expressions (Table IV-3) have been substituted. Taking the total derivative of Eq. (7) with respect to T_D and T_C, setting the result equal to zero, and using Eq. (6), the optimum thrusting period for the departure spiral may be found

$$T_D = \left[\frac{\hat{J}_D}{\hat{J}_C}\frac{m_D}{m_C}\frac{T_C^{m_C}}{T_D^{m_D}}\right]^{\frac{1}{1-m_D}} T_C^{\frac{1-m_C}{1-m_D}}. \tag{8}$$

An iterative procedure between Eq. (6) and (8) is required to find T_D and thus the optimum distribution of the given total planetocentric thrusting time.

The overall mission requirement can now be written as a function of the heliocentric and departure travel times.

$$J = \hat{J}_H\left(\frac{T_H}{\hat{T}_H}\right)^{m_H} + \hat{J}_D\left(\frac{T_D}{\hat{T}_D}\right)^{m_D} + \frac{\hat{J}_C}{\hat{T}_C^{m_C}}\left[\frac{\hat{J}_C}{\hat{J}_D}\frac{m_C}{m_D}\frac{\hat{T}_D^{m_D}}{\hat{T}_C^{m_C}}\right]^{\frac{m_C}{1-m_C}} T_D^{m_C\left(\frac{1-m_D}{1-m_C}\right)}, \tag{9}$$

where the entire mission duration is

$$T = T_H + T_D + \left[\frac{\hat{J}_C}{\hat{J}_D} \frac{m_C}{m_D} \frac{\hat{T}_D^{m_D}}{\hat{T}_C^{m_C}} \right]^{\frac{1}{1-m_C}} T_D^{\frac{1-m_D}{1-m_C}} . \qquad (10)$$

Thus the optimum T_H can be determined by setting the derivative of Eq. (9) with respect to T_H equal to zero and keeping in mind that T_D is a function of T_H by Eq. (10). After considerable simplification the equation for optimum T_H is

$$T_H = T - \left[\frac{m_D}{m_H} \frac{\hat{J}_D}{\hat{J}_H} \frac{\hat{T}_H^{m_H}}{\hat{T}_D^{m_D}} \right]^{\frac{1}{1-m_D}} T_H^{\frac{1-m_H}{1-m_D}} - \left[\frac{m_C}{m_H} \frac{\hat{J}_C}{\hat{J}_H} \frac{\hat{T}_H^{m_H}}{\hat{T}_C^{m_C}} \right] T_H^{\frac{1-m_H}{1-m_C}} . \qquad (11)$$

In this form the equation is amenable to solution by successive substitution or, preferably, by the method of false position. The latter method converges to a solution quite rapidly and is very stable.

Equation (11) applies to the general flight mode; namely, planetocentric departure spiral, heliocentric transfer, and planetocentric capture spiral. The second and third terms on the right-hand side of Eq. (11) are, respectively, the contributions of the departure and capture planet-centered spirals. Consequently, if the flight mode under consideration is other than the general one, the appropriate term in Eq. (11) should be omitted. If there is to be no capture at the destination planet, then the third term should be omitted. This implies that the heliocentric trajectory is a flyby and the parameters in the heliocentric J and powered time equations (Table IV-1) must correspond to this type of trajectory. If there is a high-thrust capture at the planet starting from parabolic, i.e., escape, conditions then the third term is omitted and the heliocentric rendezvous trajectory data of Table IV-1, may be used.

If there is a capture spiral but no departure spiral, then the second term must be deleted. The overall flight mode thus consists of a high-thrust departure from the initial parking orbit to parabolic (escape) conditions, a low-thrust heliocentric transfer, and a capture spiral. Under these conditions the rendezvous heliocentric data of Table IV-1 is applicable. However, if more than parabolic conditions are provided by the high-thrust system, i.e., hyperbolic excess velocity greater than zero, then none of the cited heliocentric data are useful. This type of high- and low-thrust mix requires numerous heliocentric trajectory data involving the departure hyperbolic excess speed (and capture if necessary), and insufficient information currently exists to produce a table analogous to Table IV-1. The basic equations for the mixed-thrust system are presented later.

For completeness, it should be pointed out that once the optimum breakdown of mission duration has been determined, then the total thrusting time is known. Since no coast periods occur during the spiral trajectories, then the planet-centered thrusting time is the travel time; for the heliocentric phase the powered-time equation (Table IV-1) yields the heliocentric thrusting time. With the powerplant specific mass (assumed given), the overall J, and the total thrusting time, the optimum exhaust velocity and powerplant fraction can be found from either Eq. (15) or Eqs. (16) and (17) of Section II or from Figs. III-1 to III-8. An estimate of the maximum powerplant specific mass for the mission may be found from Fig. III-9.

System Variations

The variation in the vehicle system operation are merely constraints on the system optimization as fixed by general "real life" considerations. That is, it is not to be expected that a mission will be executed by a space vehicle optimized solely for maximum payload-to-gross mass considerations; a given type of powerplant with definite power output and/or mass may have to be used, a restriction may be placed on the gross mass of the spacecraft by the capability of the launch vehicle, or the payload mass is dictated by the scientific or communications requirements of the flight. Regardless of the variation, the objective of this analysis is to optimally choose the remaining system variables so as to maximize the net spacecraft mass (not necessarily mass fraction). In order to analyze these different variations systematically, the following operating definitions were established.

A. Operation at maximum net spacecraft mass fraction. This is the same case as fully developed in Sections II and III wherein the optimum exhaust velocity and powerplant fraction are required to maximize net spacecraft mass fraction. No further discussion of this variation is presented.

B. Fixed power system (powerplant mass and output power). In this instance a given power system is to be evaluated and, since its mass and output power are known, it is necessary to determine the exhaust velocity and vehicle gross mass which yields maximum net spacecraft mass.

C. Operation with fixed power system and given vehicle gross mass. This situation arises when a particular type of power system is to be used in an electrically propelled vehicle whose gross mass cannot exceed the orbital payload capability of the launch vehicle assigned to the mission. As a consequence, the remaining system parameter available for maximizing net spacecraft mass is the exhaust velocity.

D. Specified powerplant and payload (net spacecraft mass). This case is analyzed under the "Mixed High- and Low-Thrust Propulsion Systems" section below. Under mixed-thrust operation, in which the analysis requires sequential calculation

of masses in each stage, the powerplant and the high- thrust propulsion stage (including mission payload) associated with the electric system must be specified. This implies that the exhaust velocity is to be optimized in order to minimize the gross mass of the electric stage.

Operation with Fixed Power System

A fixed power system implies that the powerplant mass, m_w, and power output, P, are known or that either of these and the specific mass, α_w, are known. In the general case, the exhaust velocity, C, and powerplant fraction, μ_w, are available parameters for optimizing. With the powerplant mass, m_w, known in the present case, this means C and the gross vehicle mass, m_o, are to be optimized.

The net spacecraft mass, m_L, can be written in terms of C and m_o, by using the simplified definition of Eq. (2), Section II:

$$m_L = \frac{1}{\frac{1}{m_o} + \frac{\gamma^2}{\eta}\frac{1}{m_w}} - m_w , \tag{12}$$

where $\gamma^2 \equiv \alpha_w J/2$ and η is some unspecified function of C. Assuming γ^2 is independent of m_o, taking the total derivative of Eq. (12) with respect to C and m_o, and setting the result equal to zero, yields

$$1 + m_o^2 \frac{\gamma^2}{\eta m_w} \frac{\eta'}{\eta} \frac{dC}{dm_o} = 0, \tag{13}$$

where $\eta' = d\eta/dC$. The variation of C with m_o can be found by employing equivalent assumptions to those used in deriving Eq. (15) of Section II. That is, the minimum value of J is independent of m_o, and the average thrust acceleration over a minimum-J trajectory is also independent of m_o.

Now the derivative of C with respect to m_o can be written identically as

$$\frac{dC}{dm_o} = -\frac{\mu_w}{m_o}\frac{dC}{d\mu_w} ,$$

so that the appropriate derivatives in Eq. (14), Section II, may be substituted to obtain

$$\begin{aligned} \frac{dC}{dm_o} &= -\frac{C}{m_o}\left[\frac{1+\mu_1}{2\mu_1} - \frac{\eta' C}{\eta}\right]^{-1} \quad \text{AM} , \\ \frac{dC}{dm_o} &= -\frac{C}{m_o}\left[\frac{2}{1+\mu_1} - \frac{\eta' C}{\eta}\right]^{-1} \quad \text{GM} . \end{aligned} \tag{14}$$

where the notation AM denotes the arithmetic mean case and GM denotes the geometric mean case. Substituting into Eq. (13), the optimum gross mass may be determined.

$$\left.\frac{m_o}{m_w}\right|_{OPT} = \begin{cases} \dfrac{2\eta}{\gamma^2}\left[\dfrac{1-\frac{\eta' C}{\eta}}{2\frac{\eta' C}{\eta}-1}\right] & AM \\ \dfrac{2\eta}{\gamma^2}\left[\dfrac{1-\frac{\eta' C}{\eta}}{\frac{\eta' C}{\eta}}\right] & GM \end{cases} \tag{15}$$

The optimum C and m_o may be computed by iteratively solving between Eq. (15) and the following definitions for average thrust acceleration, $\bar{a}$ (also see Eq. (13) Section II):

$$\begin{aligned} \bar{a}\,\alpha_w C &= 2\eta\frac{m_w}{m_o} + \gamma^2 \qquad AM, \\ \bar{a}\,\alpha_w C &= 2\eta\frac{m_w}{m_o}\left(1+\frac{\gamma^2}{\eta\, m_w/m_o}\right)^{1/2} \qquad GM, \end{aligned} \tag{16}$$

where the dependence of η on C is to be furnished.

If the functional form of the thrustor conversion efficiency is given by (see Fig. II-1):

$$\eta = \frac{1}{1+(d/C)^2}, \tag{17}$$

then closed-form expressions for optimum exhaust velocity may be derived in both the arithmetic- and geometric mean cases.

Eliminating m_o/m_w between the first parts of Eqs. (15) and (16) and substituting Eq. (17) and its derivative, a normal-form cubic in C/d may be obtained:

$$\left(\frac{C}{d}\right)^3 - \frac{C}{d} - \frac{2\gamma^2}{\bar{a}\alpha_w d} = 0 \qquad AM. \tag{18}$$

There is one real root to this equation, provided that

$$\frac{2\gamma^2}{\bar{a}\alpha_w d} > \sqrt{\frac{4}{27}}.$$

This is probably so in most cases, since

$$\frac{2\gamma^2}{\bar{a}\,a_w d} = \frac{J}{\bar{a}d} \approx 0.5 > \sqrt{\frac{4}{27}},$$

for typical values of J, $\bar{a}$, and d. Hence the optimum dimensionless exhaust velocity is

$$\left.\frac{C}{d}\right|_{OPT} = \left(\frac{J/\bar{a}d}{2}\right)^{1/3}\left[\left\{1+\left[1-\frac{1}{27}\left(\frac{2}{J/\bar{a}d}\right)^2\right]^{1/2}\right\}^{1/3}+\left\{1-\left[1-\frac{1}{27}\left(\frac{2}{J/\bar{a}d}\right)\right]^{1/2}\right\}^{1/3}\right] \quad AM, \tag{19}$$

only if

$$\frac{J}{\bar{a}d} > \sqrt{\frac{4}{27}}.$$

The dimensionless quantity $J/\bar{a}d$ encompasses the trajectory requirement, J, the average thrust-acceleration, $\bar{a}$, expected in performing that trajectory, and the parameter d, indicative of the thrustor conversion efficiency. The combination of these parameters is a measure of the entire mission and is termed the mission parameter.

If it should happen that $J/\bar{a}d = \sqrt{4/27}$, then the optimum exhaust velocity is

$$\left.\frac{C}{d}\right|_{OPT} = \frac{2\sqrt{3}}{3} \quad AM.$$

Further, if $J/\bar{a}d < \sqrt{4/27}$ then there are three real and unequal roots to Eq. (18) which are given by

$$\left.\frac{C}{d}\right|_{OPT} = \frac{2\sqrt{3}}{3}\cos\left(\frac{\phi}{3}+120^\circ K\right), \quad K = 0, 1, 2 \quad AM \tag{20}$$

where

$$\cos\phi = \frac{J}{\bar{a}d}\frac{3\sqrt{3}}{2}.$$

For convenience, the optimum exhaust velocity for the arithmetic-mean case is plotted in Fig. V-1 as a function of the mission parameter, $J/\bar{a}d$. It is interesting to note that the optimum exhaust velocity does not depend on the powerplant specific mass. The optimum gross vehicle mass may be found by substituting Eq. (17) into the first part of Eq. (15).

$$\left.\frac{m_o}{m_w}\right|_{OPT} = \frac{2/\gamma^2}{3(d/C)^2-1}\left[\frac{1-(d/C)^2}{1+(d/C)^2}\right] \quad AM \tag{21}$$

Equation (21) is illustrated in Fig. V-2 as a function of the system trajectory characteristic, γ^2, and for a range of values of C/d. The resulting maximum net spacecraft mass may be quickly determined from Fig. V-3.

The use of Eq. (17) in the geometric-mean case results in much simpler expressions for the optimum exhaust velocity and gross mass. Proceeding essentially as in the AM case, the optimum exhaust velocity can be written as

$$\left.\frac{C}{d}\right|_{OPT} = \left[1 + \sqrt{\frac{J T_p}{d^2}}\right]^{1/2} \quad GM \tag{22}$$

where T_p is the total powered time. Again, note that the dimensionless quantity $J\,T_p/d^2$ contains those parameters indicative of the mission as well as the system. Equation (22) is plotted in Fig. V-1 as a function of the mission parameter. Although the GM and AM cases show the same trends, they differ markedly. This discrepancy should not be construed as the actual difference, however, since, for the exact flight, the mission parameters are not expected to have the same values.

The optimum gross vehicle mass may be written explicitly as a function of the mission parameter and the system trajectory characteristic, γ^2.

$$\left.\frac{m_0}{m_w}\right|_{OPT} = \frac{\sqrt{J T_p/d^2}}{\gamma^2}\left[\frac{1 + \sqrt{J T_p/d^2}}{2 + \sqrt{J T_p/d^2}}\right] \quad GM. \tag{23}$$

Figure V-4 displays this equation.

Because of the simplified expressions obtained in the GM case, it is convenient to write the maximum net spacecraft mass in terms of γ^2 and JT_p/d^2.

$$\left.\frac{m_L}{m_w}\right|_{MAX} = \frac{1/\gamma^2}{1 + \dfrac{2}{\sqrt{JT_p/d^2}}} - 1 \quad GM \tag{24}$$

This result is illustrated in Fig. V-5.

In using the foregoing results it is important that appropriate units be used so as to render the mission parameter dimensionless. In practice, the geometric-mean case is much more expedient to use because of the information presented in Section IV and the fact that the optimum exhaust velocity and gross mass equations are quite simple. Although the arithmetic mean yields slightly more accurate results, this improvement does not appear justified for overall system study purposes.

Operation with Fixed Power System and given Gross Mass

The additional restriction of a given gross vehicle mass means that the powerplant mass fraction, $\mu_W = m_W/m_o$, is fixed, leaving only the exhaust velocity to be optimized. Since the net spacecraft mass fraction is

$$m_L = m_o \mu_L ,$$

the problem is to determine the best C given μ_W such that μ_L is a maximum.

For any known power-limited trajectory which has been optimized for minimum J and maximum net spacecraft mass fraction, there corresponds an average thrust acceleration and optimal value of powered time, exhaust velocity, and powerplant fraction. If either the exhaust velocity or powerplant fraction is changed and the entire trajectory again optimized for minimum J and maximum μ_L, practically the same values for J, and $\bar{a}$ will be obtained. The near-constancy of these quantities along the maximum μ_L line is shown in Table V-1 for a 200-day Earth to Mercury rendezvous trajectory in which μ_W was fixed at the indicated value and the exhaust velocity was optimized for maximum μ_L. Table V-2 shows the same information for a 1000-day Earth to Saturn rendezvous. As was found in practically all trajectories so analyzed, the powered time does differ somewhat from the overall optimum value at very low values of μ_W. As expected this influences the geometric-mean thrust acceleration so that it too is noticeably different at the lower μ_W's.

Thus, if information such as given in Tables V-1 and V-2 was available for the trajectory of interest, it is a matter of interpolating for the particular powerplant fraction to obtain the optimum exhaust velocity and corresponding maximum net spacecraft mass fraction. However the necessary trajectory information is time-consuming to obtain even by computer. An approximate analytical technique, sufficiently accurate for system study purposes, may be developed by using the assumption that the average thrust acceleration is invariant with μ_W for a given trajectory. Using the arithmetic- and geometric-mean definitions as before, Eq. (13), Section II and its expanded form, Eq. (16) above, the optimum exhaust velocity may be written

$$\begin{aligned} \bar{a}\alpha_W C &= 2\eta\mu_W + \gamma^2 \quad \text{AM}, \\ \bar{a}\alpha_W C &= 2\eta\mu_W \left(1 + \frac{\gamma^2}{\eta\mu_W}\right)^{1/2} \quad \text{GM}, \end{aligned} \tag{25}$$

where the function $\eta(C)$ must be given to solve for C. If η depends on C according to Eq. (17), then using the dimensionless mission parameters as before, Eq. (25) becomes

$$\frac{C}{d} = \frac{J/\bar{a}d}{\gamma^2/\mu_W}\left[\frac{(C/d)^2}{1+(C/d)^2} + \frac{\gamma^2}{2\mu_W}\right] \quad \text{AM},$$

$$\frac{C}{d} = \left\{\frac{1}{2}\left(1+\frac{\gamma^2}{\mu_W}\right)\frac{JT_P/d^2}{(\gamma^2/\mu_W)^2}\left[1+\sqrt{1-\left(\frac{\gamma^2/\mu_W}{1+\gamma^2/\mu_W}\right)^2\frac{4}{JT_P/d^2}}\right]-1\right\}^{1/2} \quad \text{GM}. \tag{26}$$

Figures V-6 and V-7, respectively, display the optimum exhaust velocity for the arithmetic mean and geometric mean as a function of the system trajectory characteristic, γ^2/μ_W, and a range of values of the appropriate dimensionless mission parameter. As an additional aid, Fig. V-8 presents the terminal mass fraction, μ_1, for various values of the exhaust velocity. Figure V-8 is actually a general plot and is applicable to any values of C/d and γ^2/μ_W, which are not necessarily in the same relation as that implied by Figs. V-6 and V-7. The difference between μ_1 and μ_W thus gives the maximum net spacecraft mass fraction. As implied previously, the results of the analysis are valid as long as the given μ_W is reasonably close to the overall optimum value for the trajectory.

If it is desired to utilize the AM part of Eq. (26), then an initial guess for the iteration on C/d may be obtained by setting $JT_P/d^2 = J/\bar{a}d$ in the GM equation. Since the mission parameters are quite close, the GM equation will yield a starting solution that will increase the convergence rate.

Mixed High- and Low-Thrust Propulsion Systems

In all of the heliocentric trajectories presented previously, the boundary conditions imposed on the vehicle's motion are the departure and arrival planet's heliocentric position and velocity, the planets being considered as point masses. In an overall flight mode evaluation sense, speeds other than the implied parabolic one should be included, as parabolic speed is a special case of zero hyperbolic speed. From an operational viewpoint, these hyperbolic excess velocities require high-acceleration devices for planetary departure or capture. In general, therefore, the analysis of system performance, which in a majority of instances is concerned with minimum gross vehicle mass, should include these high-acceleration systems and their interaction on the intervening heliocentric low-acceleration propulsion system.

The present discussion is a limited attempt to provide the necessary information so that a preliminary evaluation, at least, could be made in optimizing the combination of high- and low-acceleration systems. Because of the many different possible combinations of the departure and arrival hyperbolic speeds for a given trip time and corresponding date, very little trajectory information as such is presented. The required data as outlined below may be computed by the heliocentric power-limited trajectory program described in Section VII.

Mixed-Thrust System Equations

The analysis of the combined high- and low-acceleration systems assumes that each of the thrusting phases is independent of the other. For planetary departure from a parking orbit, it is assumed that after high-thrust burnout and staging the interplanetary vehicle (electric system) commences operation at the heliocentric position of the massless planet with the initial heliocentric velocity consisting of the planet's velocity and the hyperbolic excess velocity provided by the high-thrust system. The same assumption holds for the high-thrust capture onto a planetary parking orbit.

The above assumption neglects the effect of electric system operation within the planet's activity sphere; in actuality the thrusting and staging phases would be sequential. An analysis of the effects of the foregoing assumptions is presented in Appendix B and the results are briefly discussed below.

The formulation of the overall net spacecraft mass-to-vehicle gross mass fraction must account for the propulsion and trajectory parameters for both the low- and high-acceleration systems. For a flight profile consisting of a high-thrust departure from a parking orbit, a low-thrust heliocentric transfer, and a high-thrust capture onto a parking orbit, and where staging is employed, the overall net mass fraction is just the product of the net mass fractions of the individual stages. Thus

$$\mu_L = \mu_D \mu_H \mu_C \tag{27}$$

where subscripts D, H, and C denote departure, heliocentric, and capture, respectively for the net mass fraction μ. Equation (27) would also hold for a flight profile ending in a flyby if μ_C is set identically equal to 1.0. It is assumed that after use each propulsion system is staged.

For a given fixed-time mission, the maximization of Eq. (27) depends solely on the hyperbolic excess speeds of departure, V_D, and capture, V_C. As would be expected, increasing either of the hyperbolic speeds would lower the corresponding J for the heliocentric flight leading to a higher μ_H. But this also results in a lower value for μ_D or μ_C. Consequently, the high-thrust net mass fractions are a function of either V_D or V_C and are opposite in dependence to that of μ_H which is a function of both V_D and V_C.

The optimum values that the pair (V_D, V_C) would take on depend in part on the powerplant specific mass and power output, the specific impulses and inert mass of the high-thrust systems, and the net mass (or payload) to be delivered. Given all of these characteristics, the exact actual determination of the optimum (V_D, V_C) requires that at any trial (V_D, V_C) the mass of each propulsion system, and hence the gross vehicle mass, must be determined. A totally analytical, dimensionless mass ratio approach is not possible since the high-thrust step mass actually depends

on the optimum thrust-to-mass ratio (to minimize velocity loss) and the relationship of inert mass to incremtnal velocity and accelerated mass. The payoff here is taken to be minimum gross vehicle mass for the given net delivered mass.

A reasonable simplification of the procedure implied by the optimization of Eq. (27) may be obtained by eliminating the velocity loss and thrust-to-mass optimization aspect of the high-thrust system and by neglecting the dependence of the inert mass of the high-thrust step on incremental velocity (hyperbolic excess speed) and accelerated mass. Using this approach, Eq. (27) becomes

$$\mu_L = \left[\frac{1 - \mu_1\delta_1}{(1-\delta_1)\mu_1}\right] \mu_H \left[\frac{1-\mu_2\delta_2}{(1-\delta_2)\mu_2}\right], \tag{28}$$

where

$$\mu_{1,2} = \exp\left[\sqrt{\left(\frac{V_{D,C}}{C_{D,C}}\right)^2 + \left(\frac{V_e}{C}\right)^2_{D,C}} - \left(\frac{V_r}{C}\right)_{D,C}\right], \tag{29}$$

and

$$\mu_H = \mu_H(V_D, V_C).$$

The terms multiplying μ_H in Eq. (28) are the high-thrust stage net mass-to-gross mass fractions, and the expression for μ, Eq. (29), is the ideal (no velocity loss) mass ratio for the high-thrust system at departure from (subscript 1) or arrival onto (subscript 2) a circular parking orbit. The high-thrust step inert mass fraction, denoted by δ, is defined as the ratio of the step inert mass to the mass of the entire step (propellant plus inerts). The rocket exhaust velocity is C, and the escape velocity, V_e, is evaluated at the parking orbit radius where the circular velocity is V_r. Again, Eqs. (28) and (29) may be made applicable to a flyby flight profile by setting the third factor in Eq. (28) identically equal to 1.0 which implies that the ideal mass ratio for capture propulsion, Eq. (29), is also identically 1.0.

From limited cases using variable-thrust heliocentric trajectories and certain Mars and Venus missions it was found that the optimum hyperbolic excess speeds usually occurred at 50 to 80% of the corresponding speeds for the all-impulsive heliocentric transfer. These two-impulse hyperbolic speeds may be determined from the trajectory program briefly described in Section VII. A suggested procedure, therefore, would be to initially assign 50 to 80% of the impulsive hyperbolic speed to the appropriate high-thrust system in order to obtain an estimate for δ_1 and δ_2. Holding these values fixed, Eqs. (28) and (29) are sequentially evaluated for a series of values for V_D and V_C. A plot of μ_L versus V_D for various V_C's should

provide sufficient information to interpolate for the optimum (V_D, V_C). If deemed necessary μ_L may then be reevaluated by updating δ_1 and δ_2 using the previously obtained estimate for optimum (V_D, V_C).

The foregoing "compute and plot" approach could be replaced by a computer program which uses a direct search procedure on (V_D, V_C) wherein the dependence of μ_H on (V_D, V_C) would be given in tabular form. This basic search routine, described in Section VII and Appendix C, is useful for the restricted case presented above in which nondimensional ratios are employed throughout. This also means that the powerplant in such an analysis is a "general" one whose characteristics are not known until a solution is obtained; i.e., a specific type of powerplant cannot be evaluated.

A major problem, however, regardless of the approach used in determining the optimum hyperbolic speeds, is the requirement that the intervening heliocentric, electric stage's net mass fraction must be known as a function of V_D and V_C (V_D only for flybys). As of this writing, there are insufficient data available to present a number of plots suitable for a mission analysis; the multiplicity of planets, trip times, and range of hyperbolic speeds, and the associated computing time and expense preclude that possibility. Figure V-9 presents a sample case of a 160-day Mercury rendezvous. Since the propulsion system characteristics are required under the optimum conditions, the exhaust velocity and powerplant fraction are also required.

Optimization of Electric Stage

In the exact determination of optimum (V_D, V_C) wherein the actual masses associated with each propulsion system is computed, the electric system must be optimized under the restrictions of a known powerplant mass and net mass (the mass of the payload and the high-thrust capture propulsion, if there is one). This in essence represents the fourth electric system variation mentioned earlier in paragraph D of "System Variations". The restrictions imposed on the electric propulsion system imply that an exhaust velocity must be found which minimizes the resultant gross vehicle mass. Because the parameters usually available for maximizing the net mass fraction are exhaust velocity and powerplant fraction, with both the net mass and powerplant mass fixed, this leaves the exhaust velocity to be optimized. This optimum exhaust velocity produces minimum gross vehicle mass which in turn assures maximum net mass fraction under the given conditions.

Using the simplified definition, the net mass, m_L, is the terminal mass, m_1, less the powerplant mass, m_W.

$$m_L = m_1 - m_W \tag{30}$$

This means that m_1 is specified. But m_1 can be written

$$\frac{m_1}{m_0} = \frac{1}{1 + \frac{\gamma^2}{\eta}\frac{m_0}{m_W}} , \tag{31}$$

where the gross mass of the electric stage is m_o, and γ^2 and η are defined in the usual manner. Substituting Eq. (31) into (30), the corresponding powerplant fraction may be found.

$$\frac{m_W}{m_0} = \frac{1}{1 + \frac{m_L}{m_W}} - \frac{\gamma^2}{\eta} . \tag{32}$$

This yields the gross mass for a given trip, represented in part by γ^2, and a given exhaust velocity, represented by η.

At any given μ_W, an optimum exhaust velocity may be found which maximizes μ_L for the given heliocentric trajectory. By varying μ_W the conditions for an overall maximum μ_L may be determined. Along this locus of maxima, as previously explained, the average thrust acceleration and J are practically constant. Thus for a given μ_W the optimum exhaust velocity is given by Eq. (25). Consequently Eqs. (32) and (25) must be simultaneously solved to obtain the optimum exhaust velocity.

Eliminating the powerplant fraction between these two equations and assuming $\eta = 1/1 + (d/C)^2$, then

$$\frac{C}{d} = \frac{J/\bar{a}d}{\gamma^2\left(1 + \frac{m_L}{m_W}\right)} \left[\frac{1}{1 + (d/C)^2} - \gamma^2\left(1 + \frac{m_L}{m_W}\right)\right] \quad \text{AM,}$$

$$\frac{C}{d} = \left\{\frac{1}{2}\frac{JT_P}{d^2}\left[\frac{1 - \gamma^2\left(1 + \frac{m_L}{m_W}\right)}{\left[\gamma^2\left(1 + \frac{m_L}{m_W}\right)\right]^2}\right]\left[1 \pm \sqrt{1 - \frac{4}{\frac{JT_P}{d^2}}\left[\frac{\gamma^2\left(1 + \frac{m_L}{m_W}\right)}{1 - \gamma^2\left(1 + \frac{m_L}{m_W}\right)}\right]^2}\right] - 1\right\}^{1/2} \quad \text{GM,} \tag{33}$$

which are similar in some respects to the AM and GM parts of Eq. (26). Instead of the parameter γ^2/μ_W as in Eq. (26), here the system trajectory characteristic is $\gamma^2(1+m_L/m_W)$ which involves all of the known quantities concerning the low-thrust trajectory and propulsion system.

Figures V-10 and V-11 present the optimum exhaust velocity, respectively, for the arithmetic mean and geometric mean as a function of the system-trajectory

characteristic and a range of values for the appropriate mission parameter. With these figures it can be immediately determined if it is possible to perform the mission as required by the system-trajectory characteristic and mission parameter, i.e., if there is an optimum C/d under the given conditions.

Note that if a solution exists both the AM and GM plots yield double values for the optimum exhaust velocity. The desired value to use is, of course, the higher one since the higher specific impulse lead to a lower gross vehicle mass. This may also be seen by rewriting Eq. (32) to

$$\frac{m_L + m_W}{m_O} = 1 - \left[1 + \left(\frac{d}{C}\right)^2\right]\left[\gamma^2\left(1 + \frac{m_L}{m_W}\right)\right] . \qquad (34)$$

The mass fraction on the left-hand side of Eq. (34) is plotted in Fig. V-12 against the system trajectory characteristic. As can be seen, the lower values of exhaust velocity at a given characteristic lead to low values of the mass fraction, i.e., high initial gross mass.

The above approach requires that the average thrust acceleration and J for the AM case or the powered time and J for the GM case be known at each value of (V_D, V_C) in order to determine the minimum gross mass of the entire vehicle. This is in contrast to the previously discussed simplified method of analyzing the mixed-thrust problem wherein dimensionless mass ratios are used throughout and the low-thrust net mass fraction is required as a function of (V_D, V_C). Regardless of the method employed, the problem as stated in either method is amenable to solution by the direct search procedure noted previously.

TABLE V-1

DEPENDENCE OF PARAMETERS ON POWERPLANT MASS FRACTION

200-DAY EARTH-MERCURY RENDEZVOUS*

μ_W	C_{opt} km/sec	μ_L	J m^2/sec^3	T_P days	$\bar{a}$ (AM) 10^{-3} m/sec^3	$\bar{a}$ (GM) 10^{-3} m/sec^2
0.40	111.15	0.4419	29.11	146.64	1.525	1.516
0.38	105.94	0.4547	29.08	147.08	1.523	1.513
0.36	100.72	0.4667	29.04	147.59	1.520	1.509
0.34	95.47	0.4780	29.00	148.15	1.516	1.505
0.32	90.21	0.4882	28.96	148.80	1.512	1.501
0.30	14.92	0.4973	28.91	149.55	1.510	1.496
0.28	79.61	0.5051	28.86	150.43	1.505	1.490
0.26	74.27	0.5111	28.80	151.48	1.500	1.476
0.24	68.90	0.5150	28.74	152.75	1.495	1.476
**0.22118	63.80	0.5164	28.68	154.22	1.489	1.467
0.20	58.00	0.5143	28.61	156.34	1.481	1.455
0.18	52.48	0.5078	28.55	159.01	1.470	1.442
0.16	46.89	0.4953	28.51	162.72	1.460	1.424
0.14	41.23	0.4740	28.52	168.25	1.446	1.401
0.12	35.54	0.4399	28.70	177.21	1.432	1.369
0.110455	32.83	0.4170	28.91	183.62	1.425	1.350
0.097865	29.30	0.3779	29.47	195.76	1.417	1.320

* $d = 20$ km/sec in $\eta = 1/1+ (d/C)^2$

** overall optimum for the trajectory

TABLE V-2

DEPENDENCE OF PARAMETERS ON POWERPLANT MASS FRACTION

1000-DAY EARTH-SATURN RENDEZVOUS*

μ_W	C_{opt} km/sec	μ_L	J m^2/sec^3	T_P days	$\bar{a}$ (AM) $10^{-3} m/sec^2$	$\bar{a}$ (GM) 10^{-3} m/sec^2
0.40	227.42	0.4393	30.41	609.29	0.76008	0.7650
0.38	216.59	0.4520	30.44	608.47	0.76089	0.7661
0.36	205.74	0.4640	30.46	607.56	0.76182	0.7674
0.34	194.88	0.4753	30.50	606.56	0.76285	0.7688
0.32	184.00	0.4856	30.54	605.44	0.76403	0.7706
0.30	173.10	0.4948	30.58	604.17	0.76540	0.7725
0.28	162.17	0.5027	30.63	602.74	0.76698	0.7749
0.26	151.21	0.5090	30.70	601.11	0.76882	0.7775
0.24	140.21	0.5135	30.78	599.23	0.77102	0.7807
0.22	129.17	0.5157	30.88	597.04	0.77369	0.7849
**0.21439	126.07	0.5158	30.91	536.36	0.77454	0.7862
0.20	118.07	0.5150	31.01	594.45	0.77698	0.7901
0.18	106.90	0.5106	31.18	591.37	0.78112	0.7966
0.16	95.63	0.5013	31.41	587.62	0.78651	0.8056
0.14	84.24	0.4856	31.74	583.03	0.79378	0.8178
0.12	72.66	0.4606	32.25	577.31	0.80407	0.8363
0.11	66.79	0.4433	32.62	573.96	0.81101	0.8490
0.10	60.84	0.4217	33.11	570.31	0.81975	0.8657
0.09	54.80	0.3946	33.81	566.48	0.83111	0.8884
0.08	48.65	0.3601	34.84	562.86	0.84650	0.9214
0.07	42.49	0.3171	36.32	561.11	0.86555	0.9674
0.06	36.14	0.2574	39.56	563.79	0.90119	1.0563

* d = 20 km/sec in $\eta = 1/1 + (d/C)^2$

** overall optimum for the trajectory

EXHAUST VELOCITY FOR MAXIMUM NET SPACECRAFT MASS

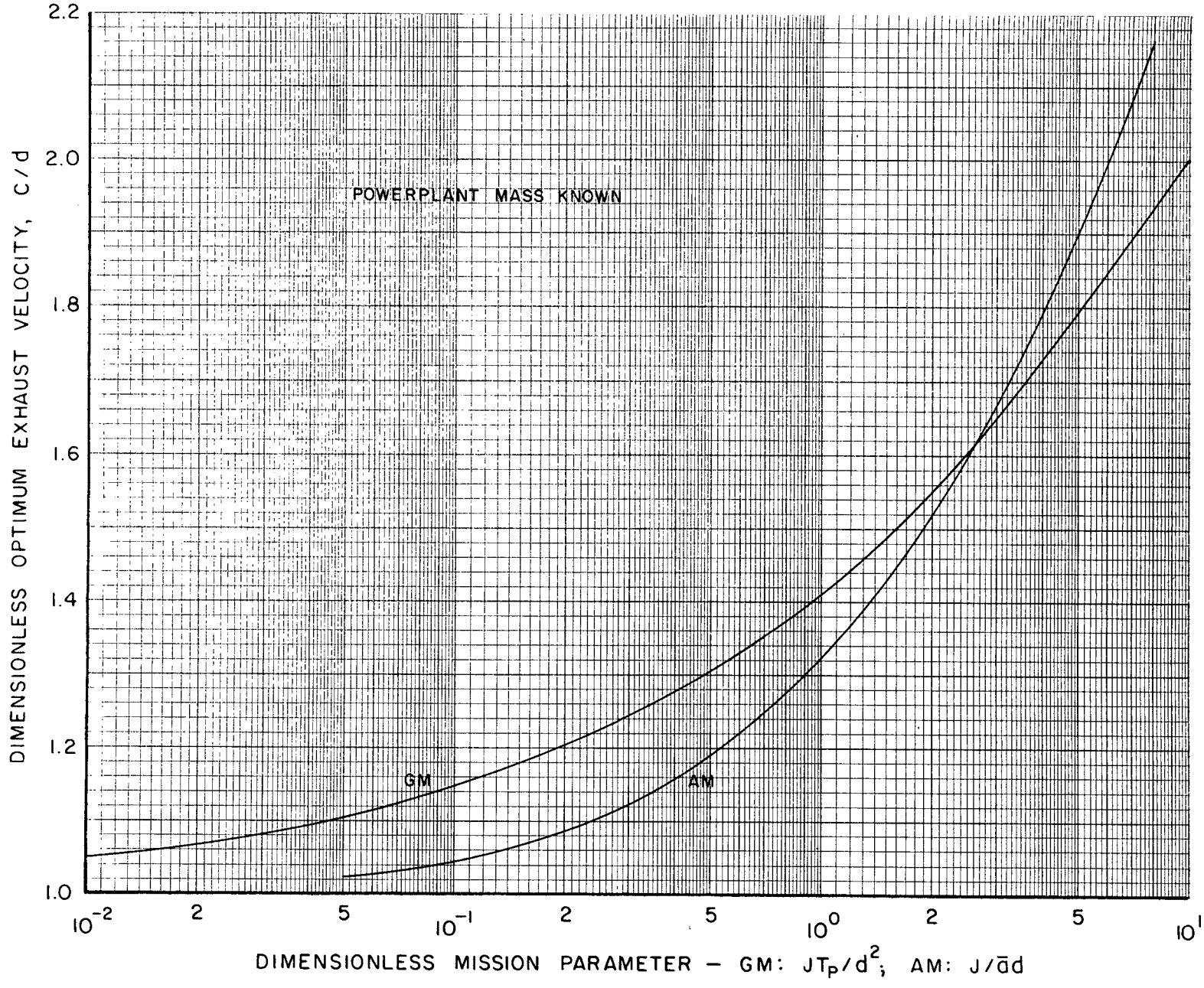

OPTIMUM GROSS VEHICLE MASS FOR GIVEN POWERPLANT MASS

ARITHMETIC MEAN

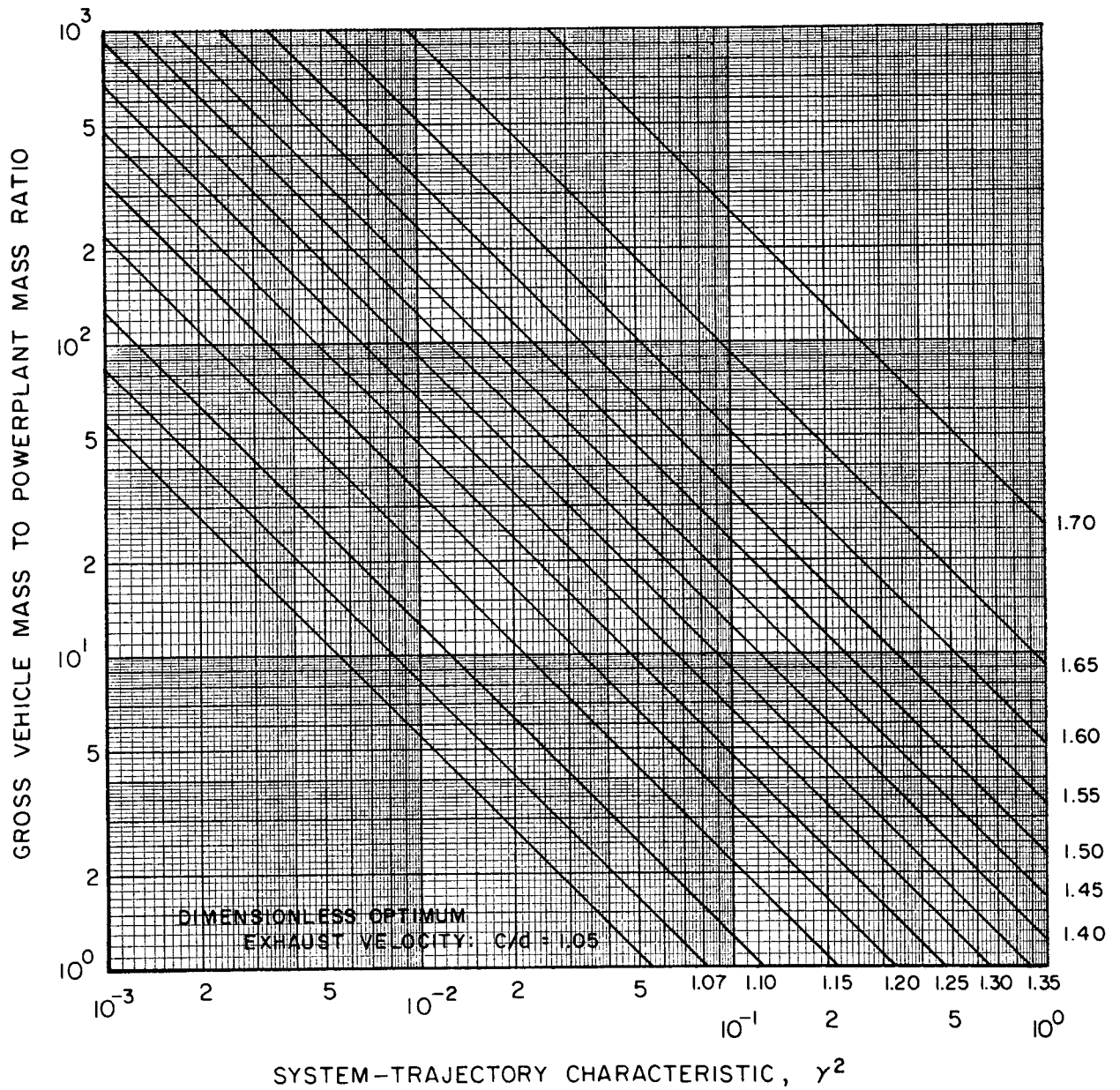

FIG. V-3

MAXIMUM NET SPACECRAFT MASS FOR FIXED POWERPLANT MASS

ARITHMETIC MEAN

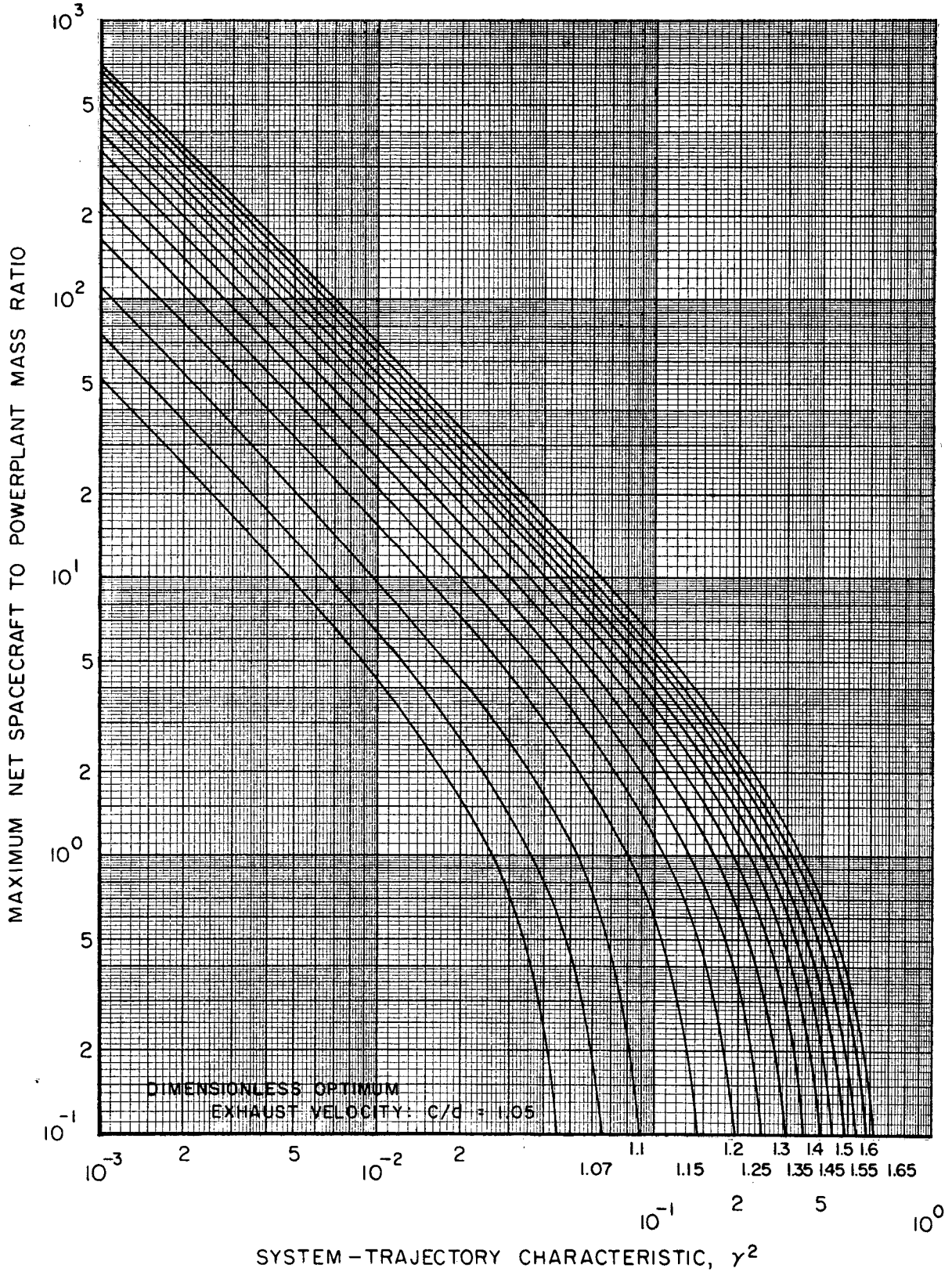

OPTIMUM GROSS VEHICLE MASS FOR GIVEN POWERPLANT MASS

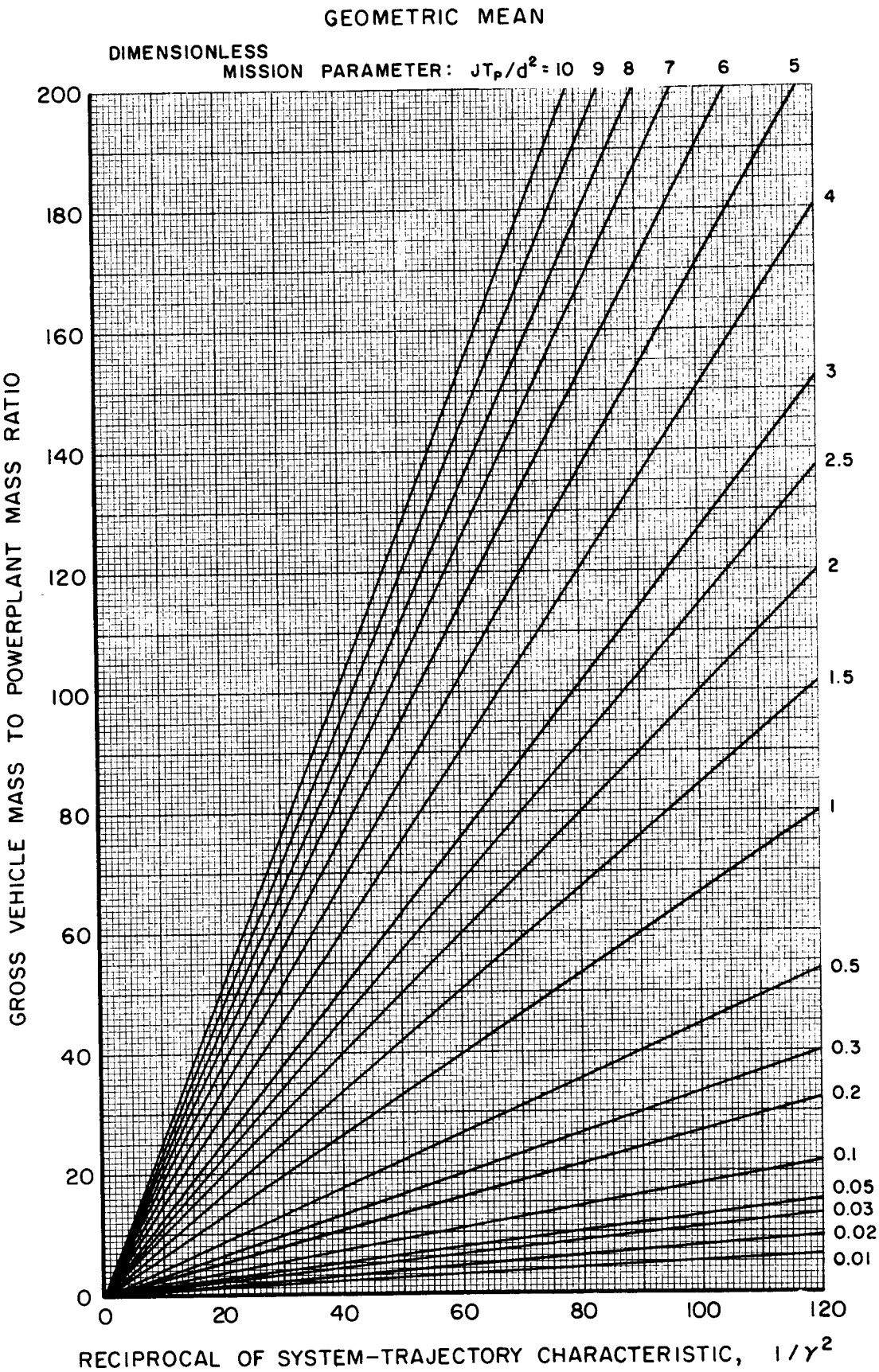

MAXIMUM NET SPACECRAFT MASS FOR FIXED POWERPLANT MASS

GEOMETRIC MEAN

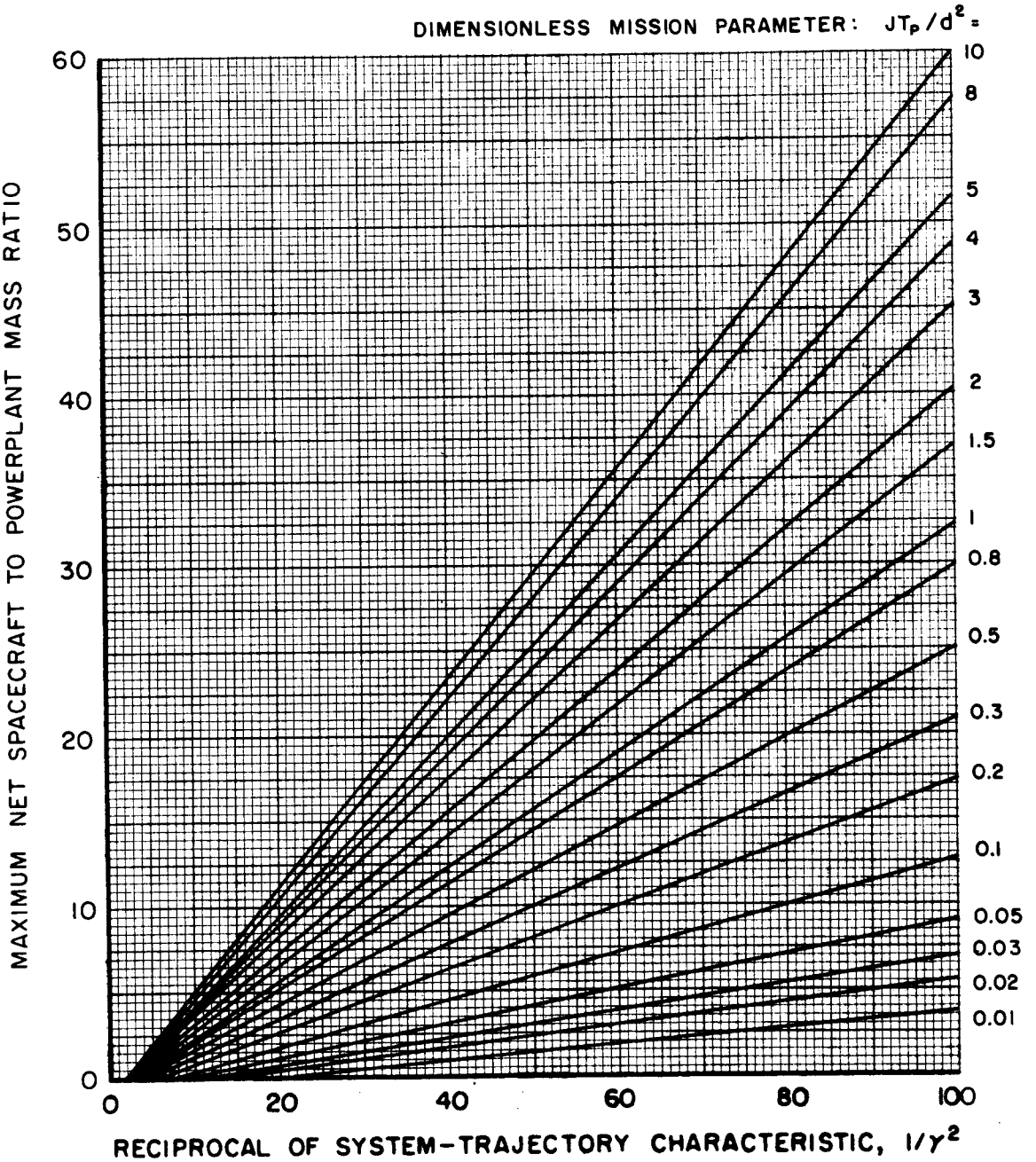

EXHAUST VELOCITY FOR MAXIMUM NET SPACECRAFT MASS FRACTION

ARITHMETIC MEAN

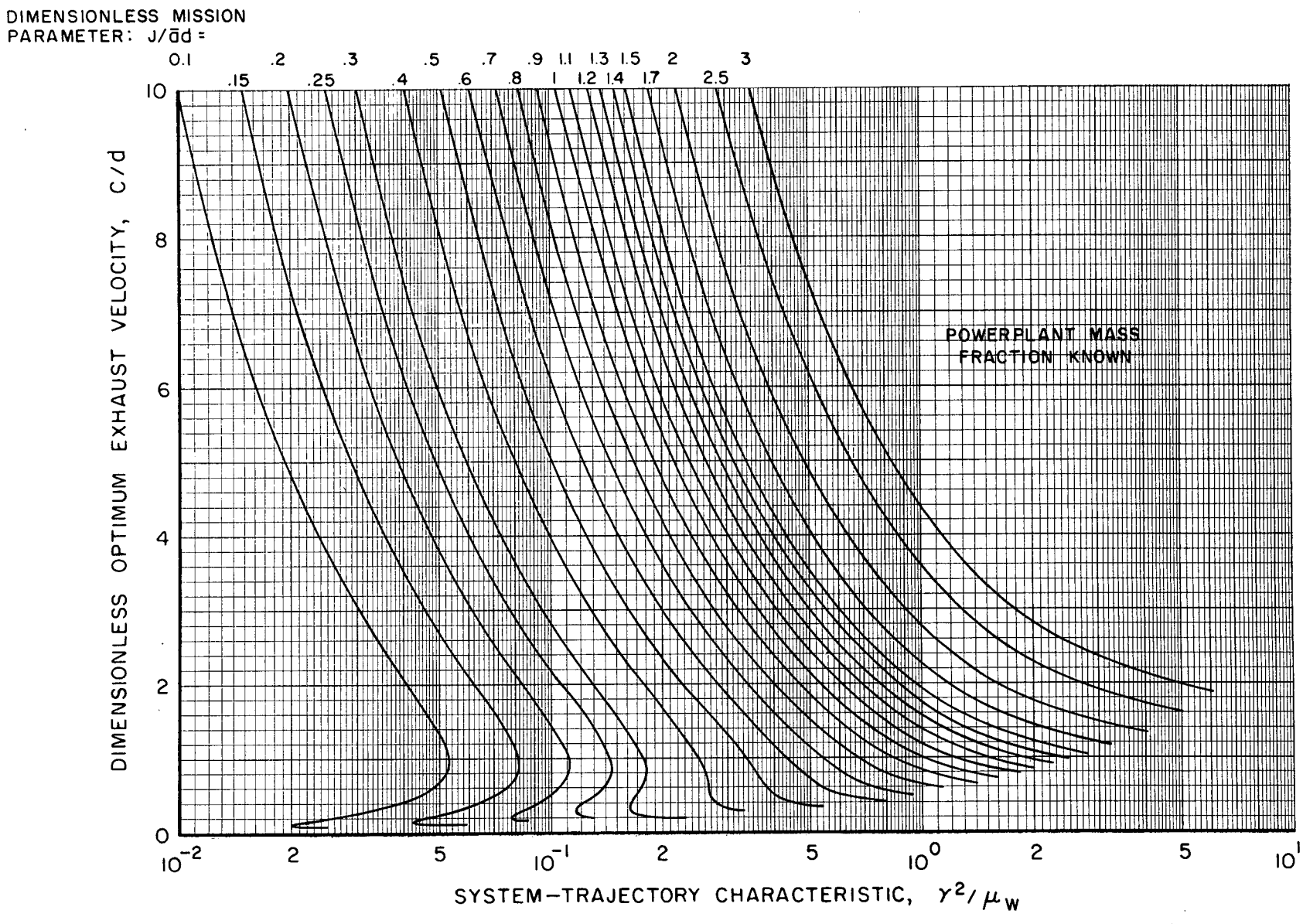

G-110058-28

FIG. IV-6

EXHAUST VELOCITY FOR MAXIMUM NET SPACECRAFT MASS FRACTION

GEOMETRIC MEAN

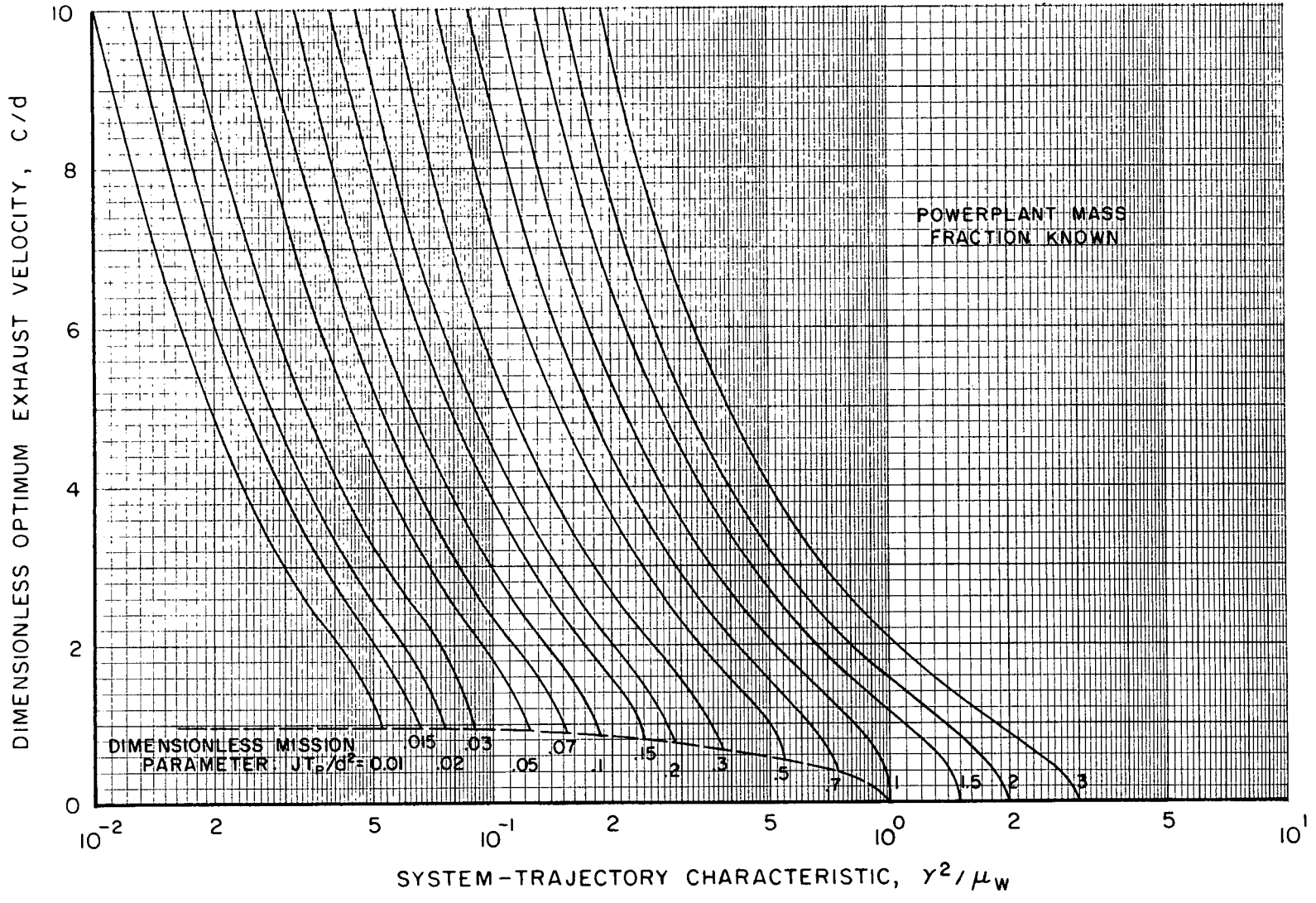

G-110058-28

FIG. IV-7

TERMINAL MASS FRACTION

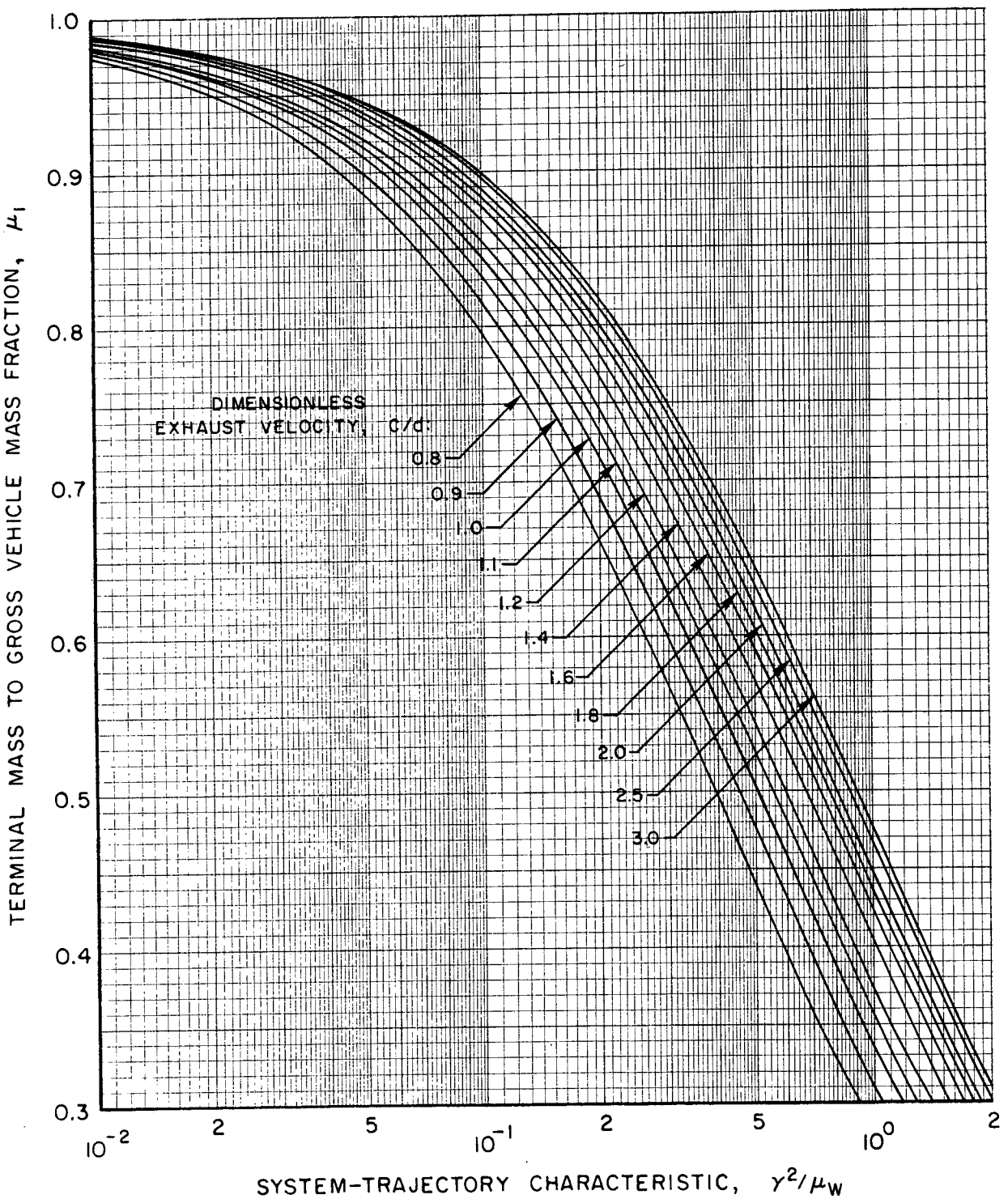

VARIATION OF J WITH HYPERBOLIC EXCESS SPEED

160-DAY EARTH-MERCURY RENDEZVOUS

EMOS: EARTH'S MEAN ORBITAL SPEED

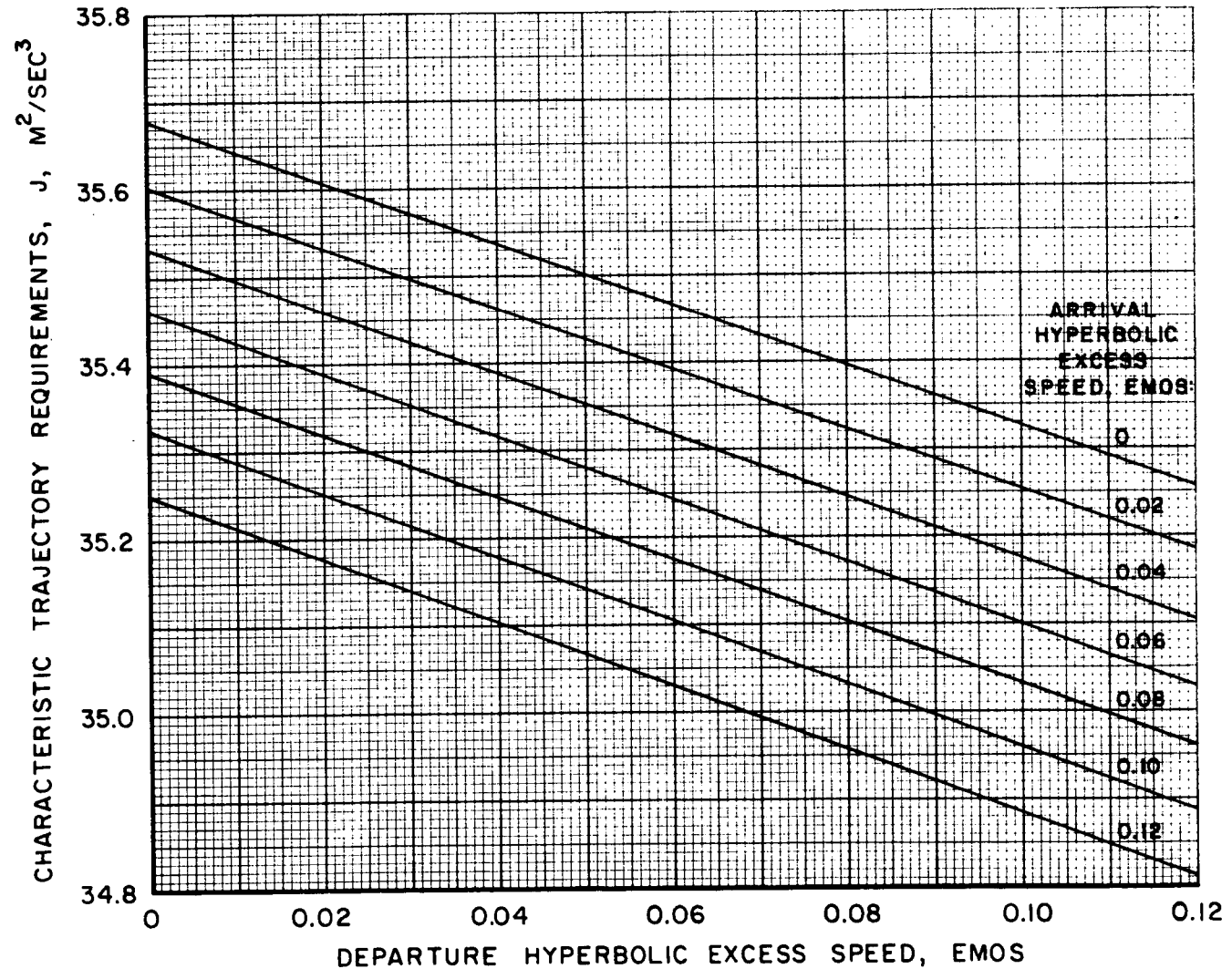

EXHAUST VELOCITY FOR MINIMUM GROSS ELECTRIC SPACECRAFT MASS

ARITHMETIC MEAN NET MASS AND POWERPLANT MASS KNOWN

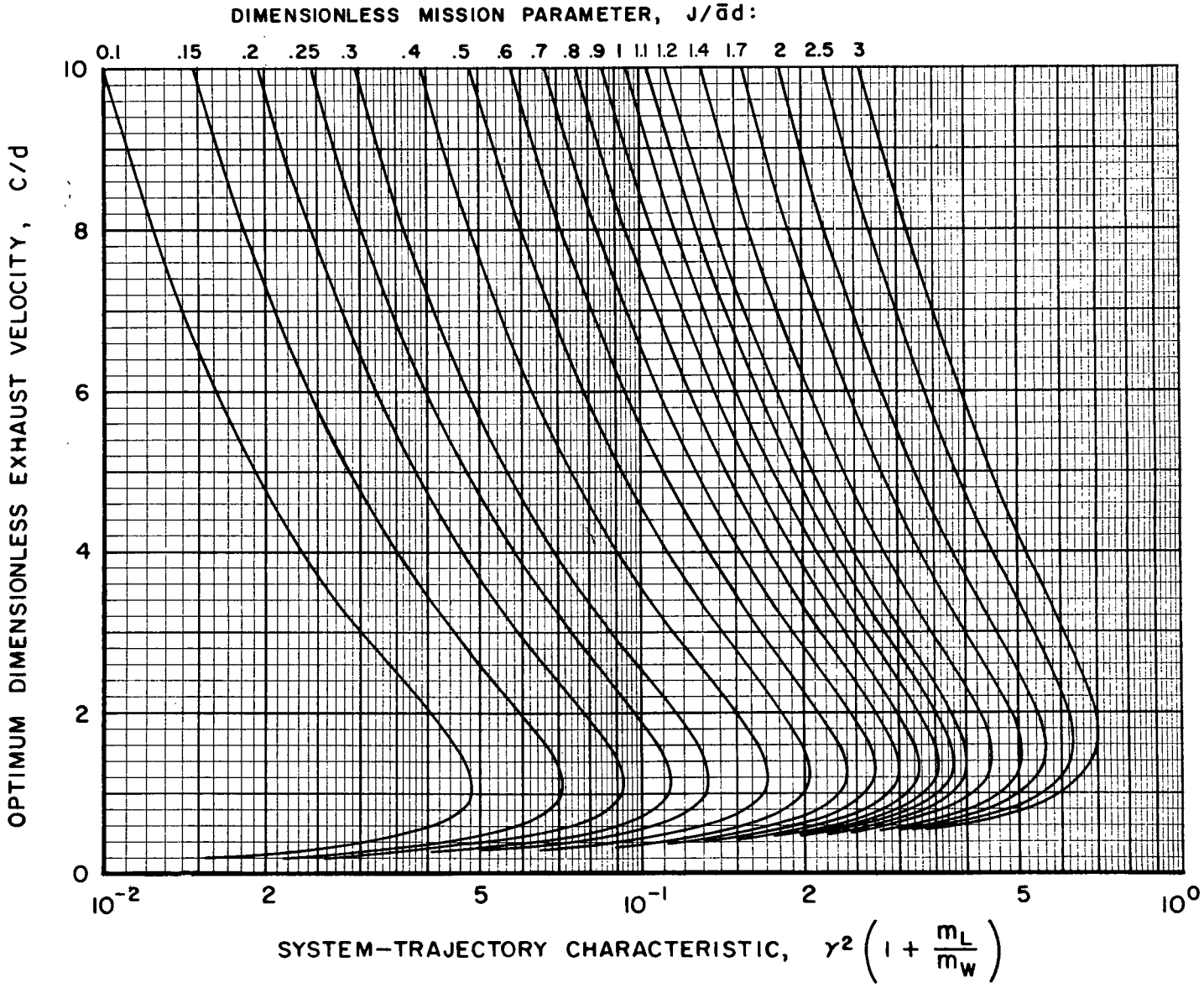

FIG. IV-10

EXHAUST VELOCITY FOR MINIMUM GROSS ELECTRIC SPACECRAFT MASS

GEOMETRIC MEAN — NET MASS AND POWERPLANT MASS KNOWN

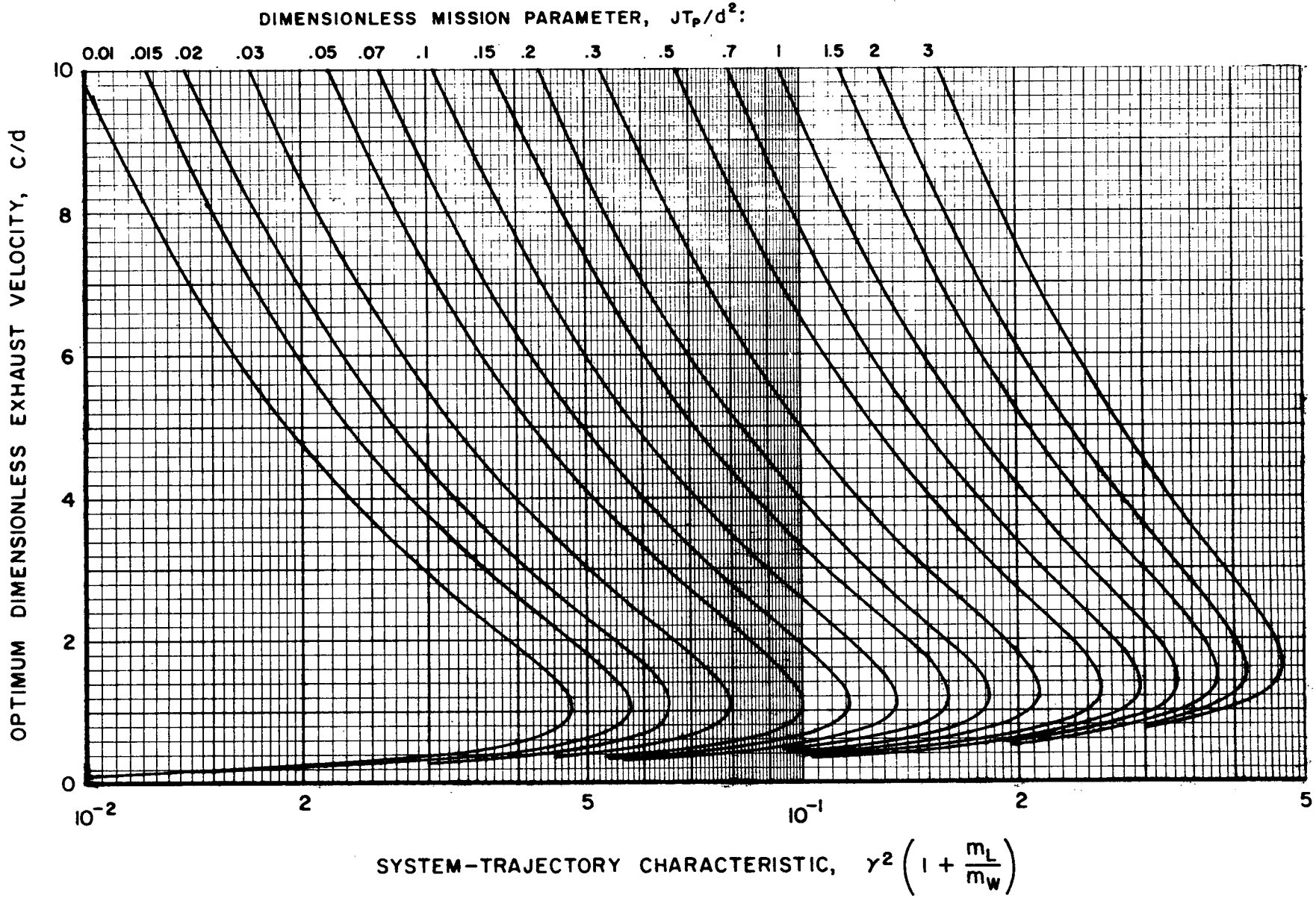

G-110058-28

FIG. IV-11

MINIMUM GROSS ELECTRIC SPACECRAFT MASS

NET MASS AND POWERPLANT MASS KNOWN

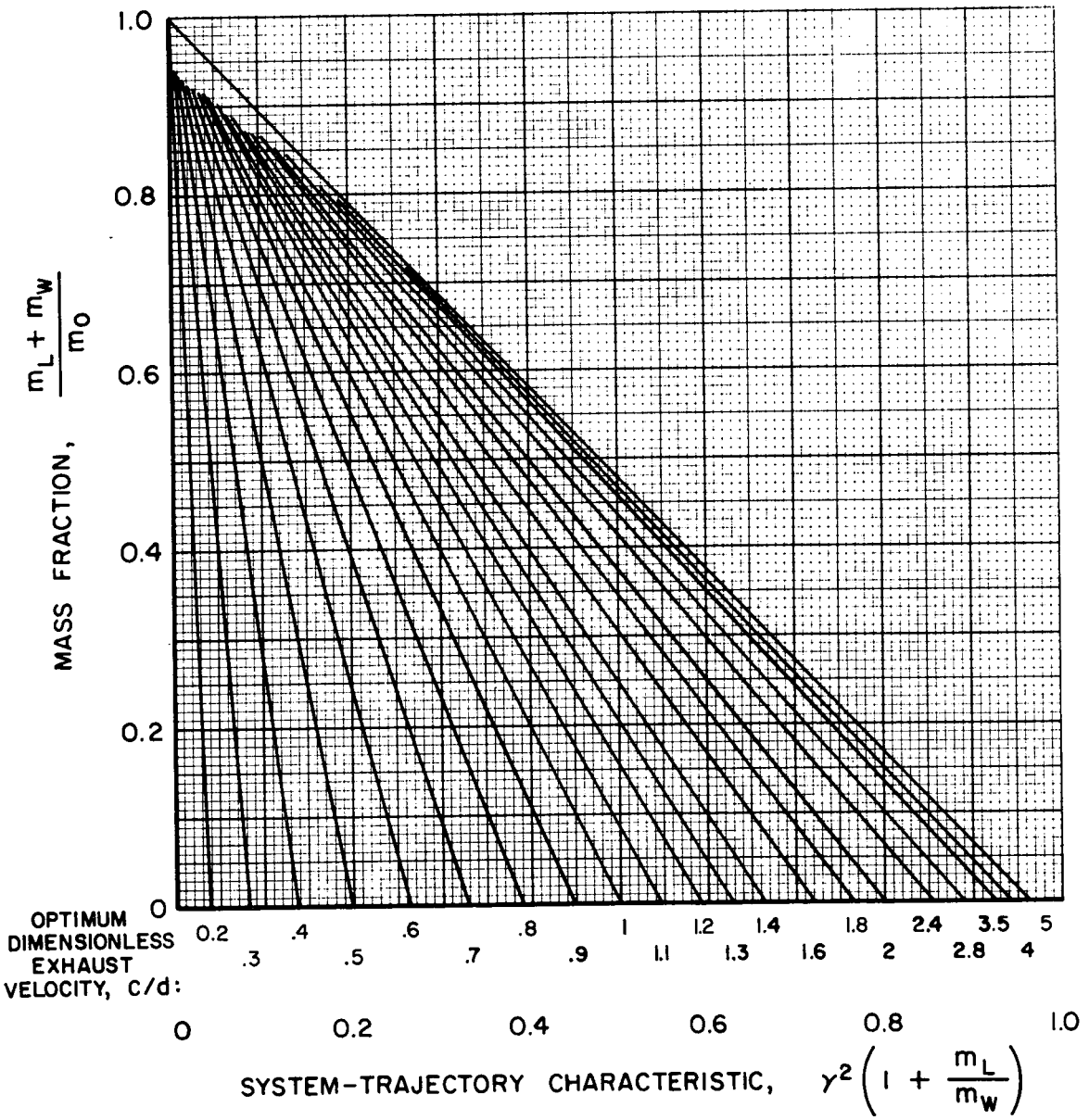

SECTION VI

SAMPLE SYSTEMS ANALYSES

In order to demonstrate the application of the procedures and data presented in the preceding sections, several typical cases of electric propulsion system analysis are discussed herein. The examples presented are not meant to be exhaustive but merely to illustrate the methods and to confirm their utility.

Flyby and capture missions to selected planets are used as a basis for the system calculations. The flight profile that the vehicle executes is basically a constant-thrust, single-stage operation wherein one propulsion system (complete with powerplant, thrustors, tanks, structure, etc.) is used to spiral out from an Earth parking orbit, transfer heliocentrically to the planet and either capture onto a parking orbit about the planet or fly by. The variations in the vehicle system are those listed in Section V under "System Variations". The majority of the following numerical results were obtained from UARL G-110474-1, "The Influence of Power Systems and Launch Vehicles on Electrically Propelled Interplanetary Probes", June 1968.

A. Operation at Maximum Net Spacecraft Mass Fraction

Consider a 1000-day flyby to Saturn powered by a SNAP-50 type power system with a mass of 5750 kg and a power output of 300 kw for a specific mass of 19 kg/kw. The initial parking orbit at Earth is 1.05 radii.

From Tables IV-1 and IV-3, the appropriate parameters for the heliocentric and planetocentric equations are obtained. Thus for the flyby:

$$\hat{T}_H = 600 \text{ days} \qquad \hat{T}_{HP} = 321.034 \text{ days}$$

$$\hat{J}_H = 30.230 \text{ m}^2/\text{sec}^3 \qquad m_{HP} = 0.887848$$

$$m_H = -2.06470$$

and for the Earth departure spiral:

$$\hat{J} = 13.588 \text{ m}^2/\text{sec}^3 \qquad m = -0.89256$$

Equation (11), Section V, may now be solved iteratively (or by use of the single-stage optimization program, Section VII), by setting T = 1000 days and omitting the third term on the right, to obtain T_H = 884.73 days, the optimum heliocentric travel time. The corresponding heliocentric powered time is 453.20 days. Since there is no capture phase at Saturn the optimum departure spiral thrusting time

at Earth is obtained from Eq. (6), Section V, with $T_c = 0$; thus $T_D = 115.27$ days. This means that the total powered time for the entire mission is 115.27 + 453.20 = 568.47 days out of a total 1000 days of travel.

The planetocentric J is 4.0865 m^2/sec^3 while for the heliocentric phase it is 13.558 m^2/sec^3, giving a total J of 17.645 m^2/sec^3. This total J and the total powered time are used in Eqs. (16) to (20), Section II, with $\alpha_W = 20$ kg/kw (instead of 19 to allow for additional mass) and d = 20 km/sec, to obtain

$$\mu_L = 0.30279 \qquad C = 56.268 \text{ km/sec}$$

$$\mu_I = 0.59607 \qquad \eta = 0.88783$$

$$\mu_W = 0.29328 \qquad \alpha_{W\,MAX} = 48.054 \text{ kg/kw}$$

These mass fraction values are to be used in evaluating the SNAP-50 type power system for powering the vehicle under maximum net mass fraction conditions. Because the power system mass is known the gross vehicle mass is immediately found:

$$m_0 = \frac{m_W}{\mu_W} = \frac{5750}{0.293} = 19600 \text{ kg},$$

and the net mass delivered is

$$m_L = \mu_L m_0 = 0.303(19600) = 5940 \text{ kg}.$$

Note that if this net mass is insufficient for the mission objectives, a possible approach, if technically feasible, would be to use two power systems. This in effect doubles the vehicle gross mass and approximately doubles the net mass.

If the mission is a capture onto a planetary parking orbit, essentially the same procedure is followed except that Eq. (11), Section V, will involve the third term on the right-hand side. Once T_H is found an iteration between Eqs. (6) and (8), Section V, will give T_D and T_c.

Sample results of a series of calculations for missions to selected planets are presented in Figs. VI-1 to VI-4. The optimum total J and powered time is given in Fig. VI-1 as a function of total mission duration for both planetary orbiters and flybys. A breakdown of the powered times for various mission durations is shown in Fig. VI-2 for Jupiter missions. Figures VI-3 and VI-4 present variations of the optimum exhaust velocity and powerplant fraction with powerplant specific mass for Mercury and Saturn missions.

B. Fixed Powerplant Mass and Output Power

In the preceding analysis the net mass so computed is a maximum only with respect to the gross mass assuming that the powerplant is characterized only by its specific mass. If, in addition, the powerplant mass is known, then the net mass (not mass fraction) should be maximized by properly choosing the exhaust velocity and gross mass.

Using the above flyby mission as a model along with the SNAP-50 type power system, the following calculations demonstrate the approach. For simplicity, the geometric mean of the average thrust acceleration is employed. Thus Eqs. (22) and (23), Section V, may be solved using the GM mission parameter (assume d = 20 km/sec):

$$\frac{JT_P}{d^2} = 0.0864\,\frac{(17.645)(568.47)}{20^2} = 2.165.$$

Thus

$$\left.\frac{C}{d}\right|_{OPT} = 1.572 \quad \text{and} \quad C = 31.44 \text{ km/sec.}$$

For $\alpha_W = 20$ kg/kw, $\gamma^2 = \alpha_W J/2000 = 0.17645$, so that Eq. (23), Section V, yields

$$\left.\frac{m_0}{m_W}\right|_{OPT} = \frac{\sqrt{2.165}}{0.1764}\left[\frac{1+\sqrt{2.165}}{2+\sqrt{2.165}}\right] = 5.94,$$

whereupon

$$m_0 = 5.94(5750) = 34200 \text{ kg.}$$

The maximum net mass is found from Eq. (24), Section V,

$$\frac{m_L}{m_W} = \frac{1}{0.1764\left(1+\frac{2}{\sqrt{2.165}}\right)} - 1 = 1.402,$$

and

$$m_L = 1.402(5750) = 8070 \text{ kg.}$$

Instead of the equations, Figs. V-1, V-4, and V-5 may be used although the accuracy would be reduced.

C. Operation with given Gross Mass and Power System

Assume that an uprated Saturn IB using a two-thirds length 260-in. solid-propellant first stage is the launch vehicle which places the electric spacecraft on a 1.05-radii Earth parking orbit. The approximate payload of this launch vehicle is about 27,400 kg. If this restriction is combined with the use of the SNAP-50

type power system, then the powerplant fraction is known immediately:

$$\mu_w = \frac{m_w}{m_0} = \frac{5750}{27400} = 0.210.$$

The exhaust velocity which maximizes the net mass is found from Eq. (26), Section V, or by use of Figs. V-6 or V-7. The system trajectory characteristic for the previous Saturn flyby mission is

$$\frac{\gamma^2}{\mu_w} = \frac{0.17645}{0.210} = 0.841.$$

By Eq. (26), geometric mean, the optimum dimensionless exhaust velocity is C/d = 2.03, so that the thrustor efficiency is

$$\eta = \frac{2.03^2}{2.03^2 + 1} = 0.805$$

Consequently, the terminal mass fraction is

$$\mu_1 = \frac{1}{1 + \frac{\gamma^2}{\eta \mu_w}} = \frac{1}{1 + \frac{0.841}{0.805}} = 0.489,$$

and the net mass fraction is

$$\mu_L = \mu_1 - \mu_w = 0.489 - 0.210 = 0.279,$$

which results in a net mass of

$$m_L = 0.279\,(27400) = 7650 \text{ kg}.$$

TOTAL TRAJECTORY REQUIREMENTS FOR PLANETARY MISSIONS

——— J_T – – – – – T_P

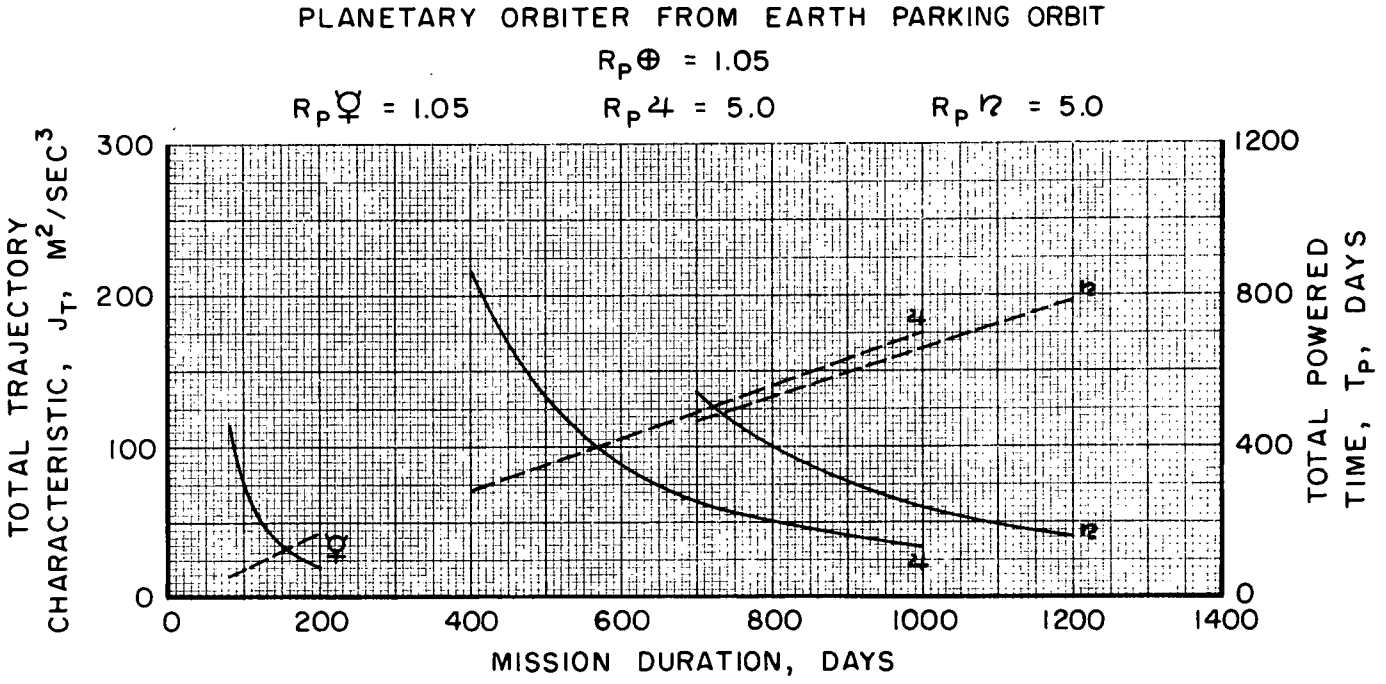

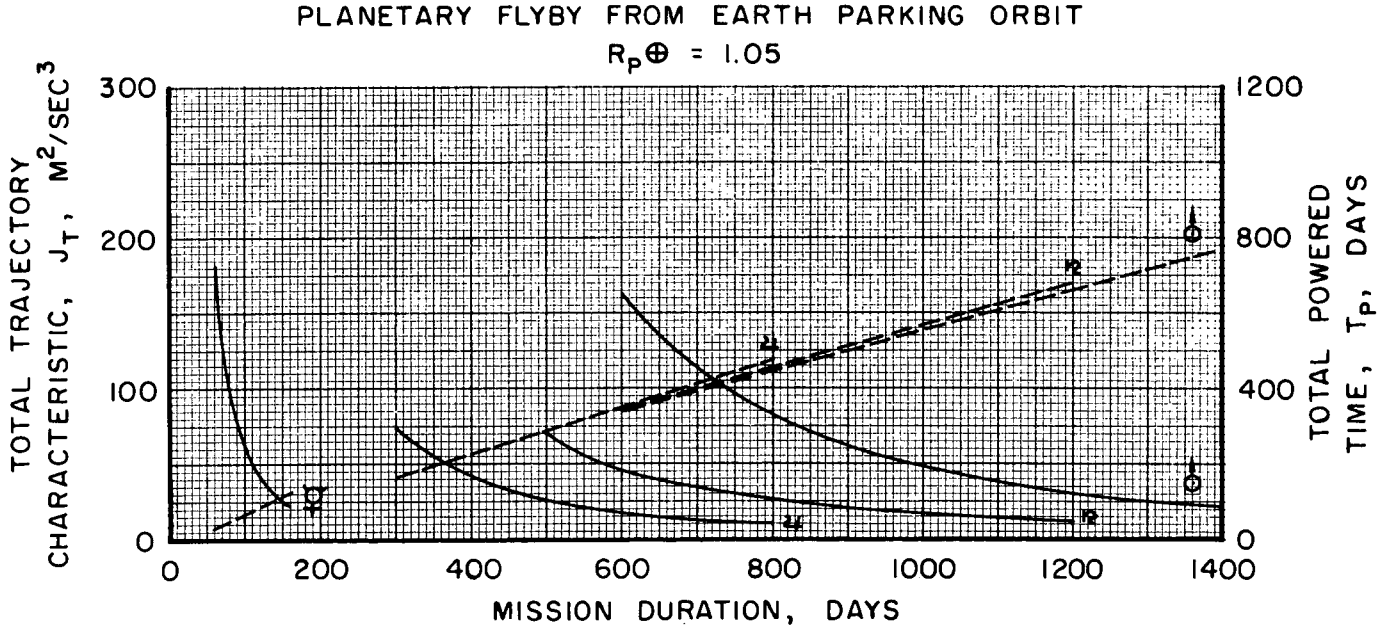

OPTIMUM DISTRIBUTION OF POWERED TIMES FOR JUPITER MISSIONS

——— FLYBY FROM EARTH PARKING ORBIT
$R_P\oplus$ = 1.05

— — — ORBITER FROM EARTH PARKING ORBIT
$R_P\oplus$ = 1.05
$R_P\mathcal{4}$ = 5.0

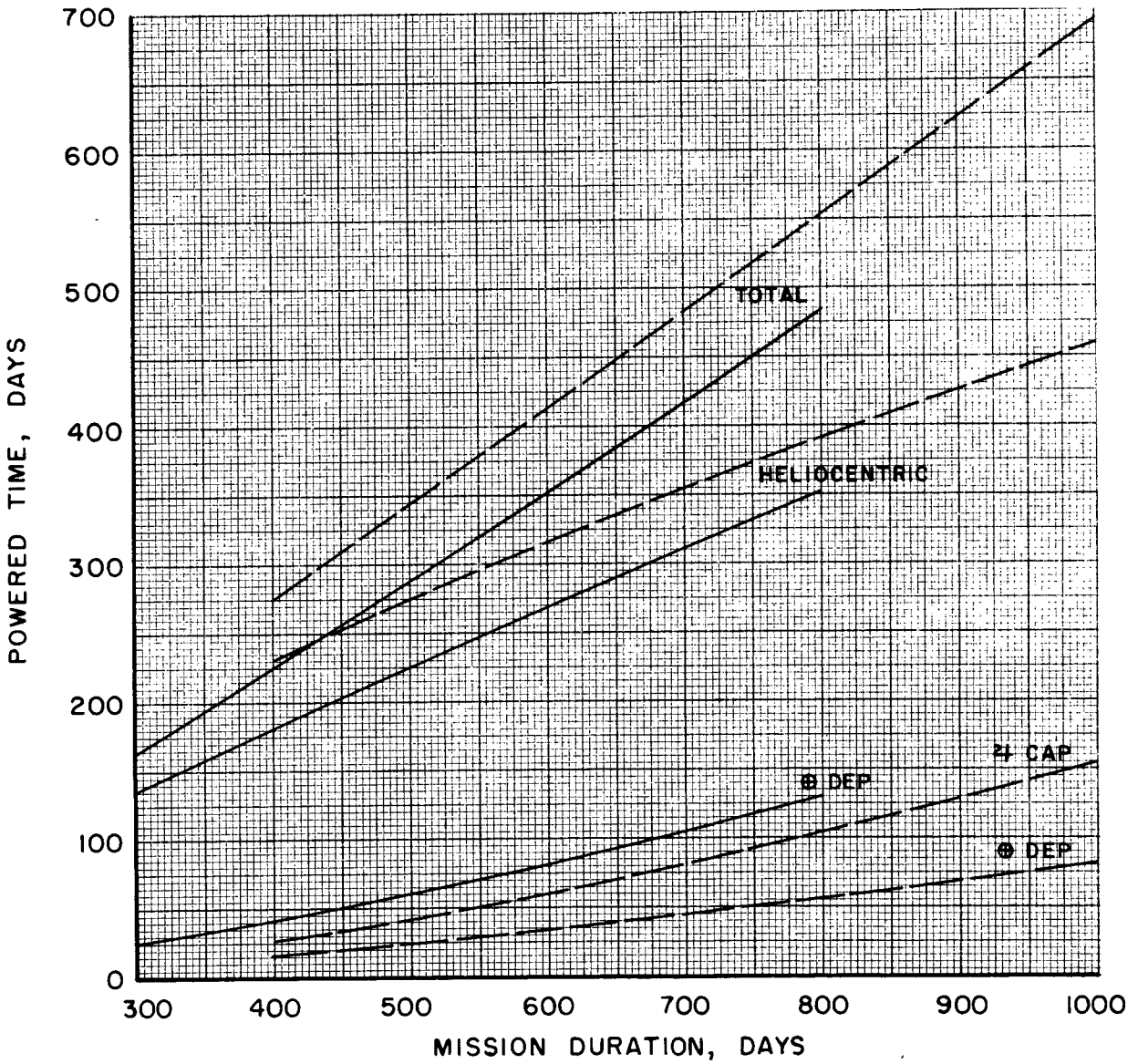

FIG. VI-3

OPTIMUM EXHAUST VELOCITIES AND POWERPLANT FRACTIONS FOR MERCURY ORBITER AND FLYBY

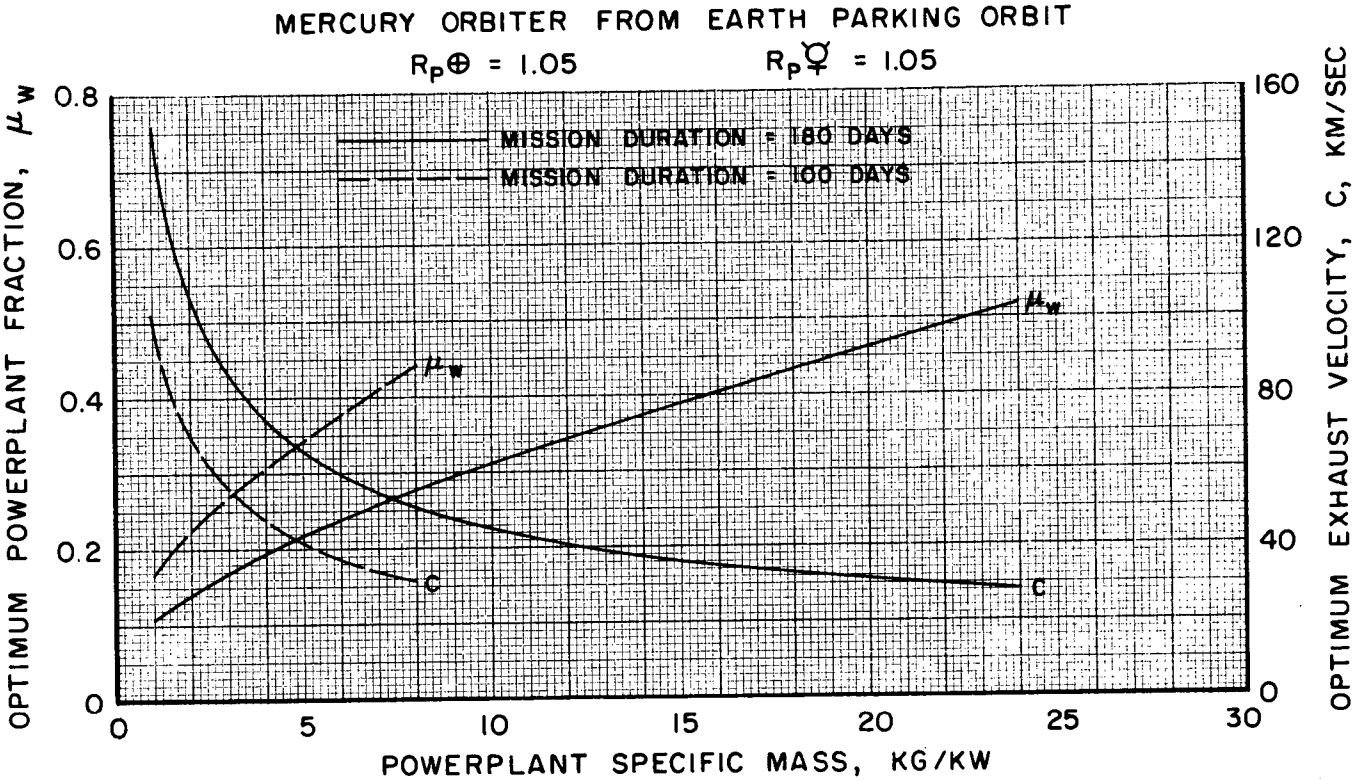

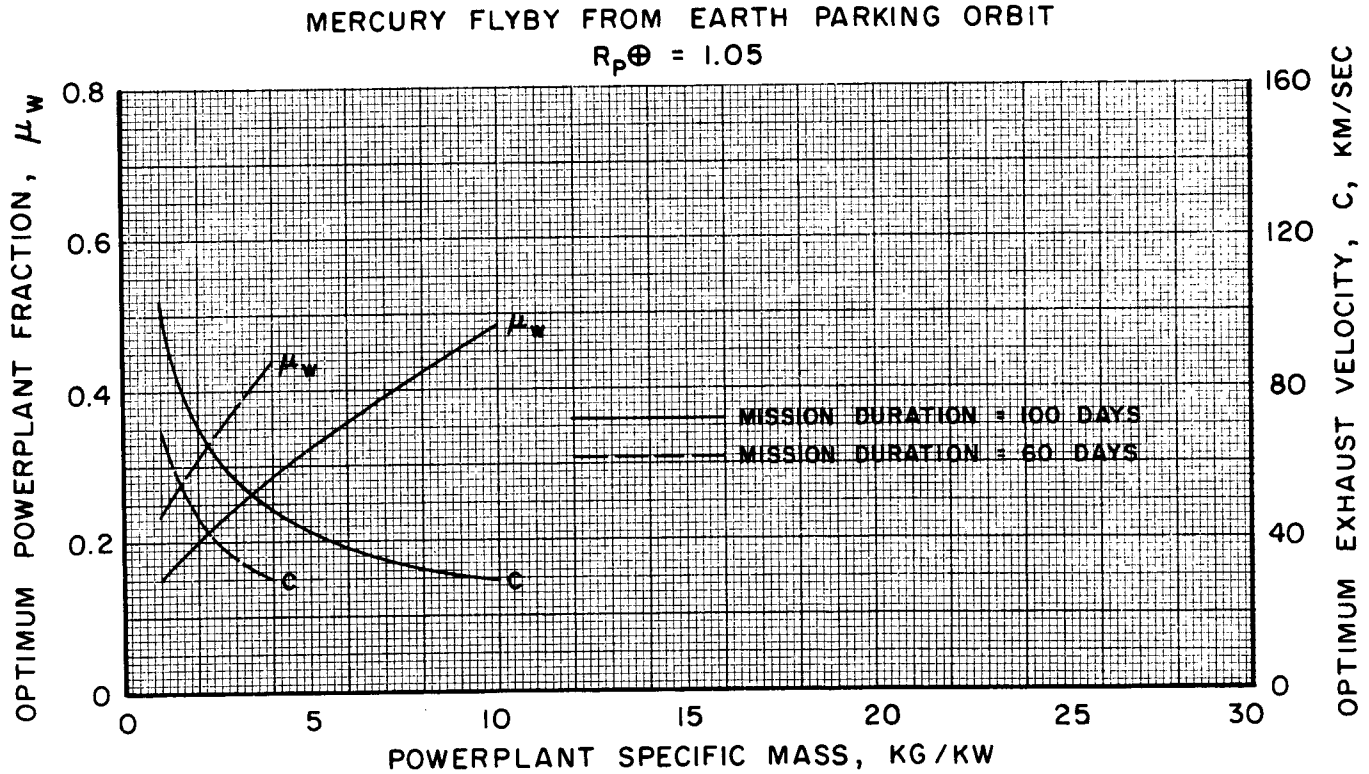

FIG. VI-4

OPTIMUM EXHAUST VELOCITIES AND POWERPLANT FRACTIONS FOR SATURN ORBITER AND FLYBY

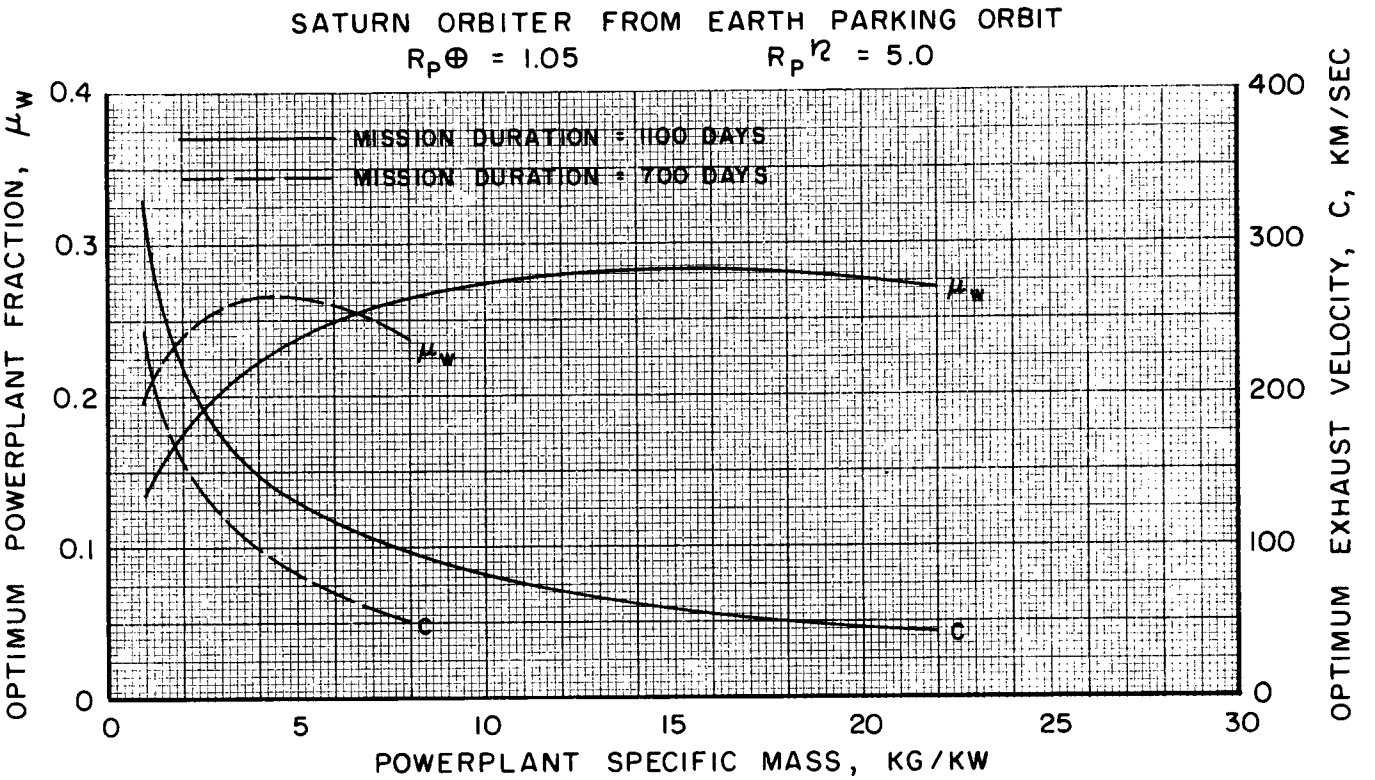

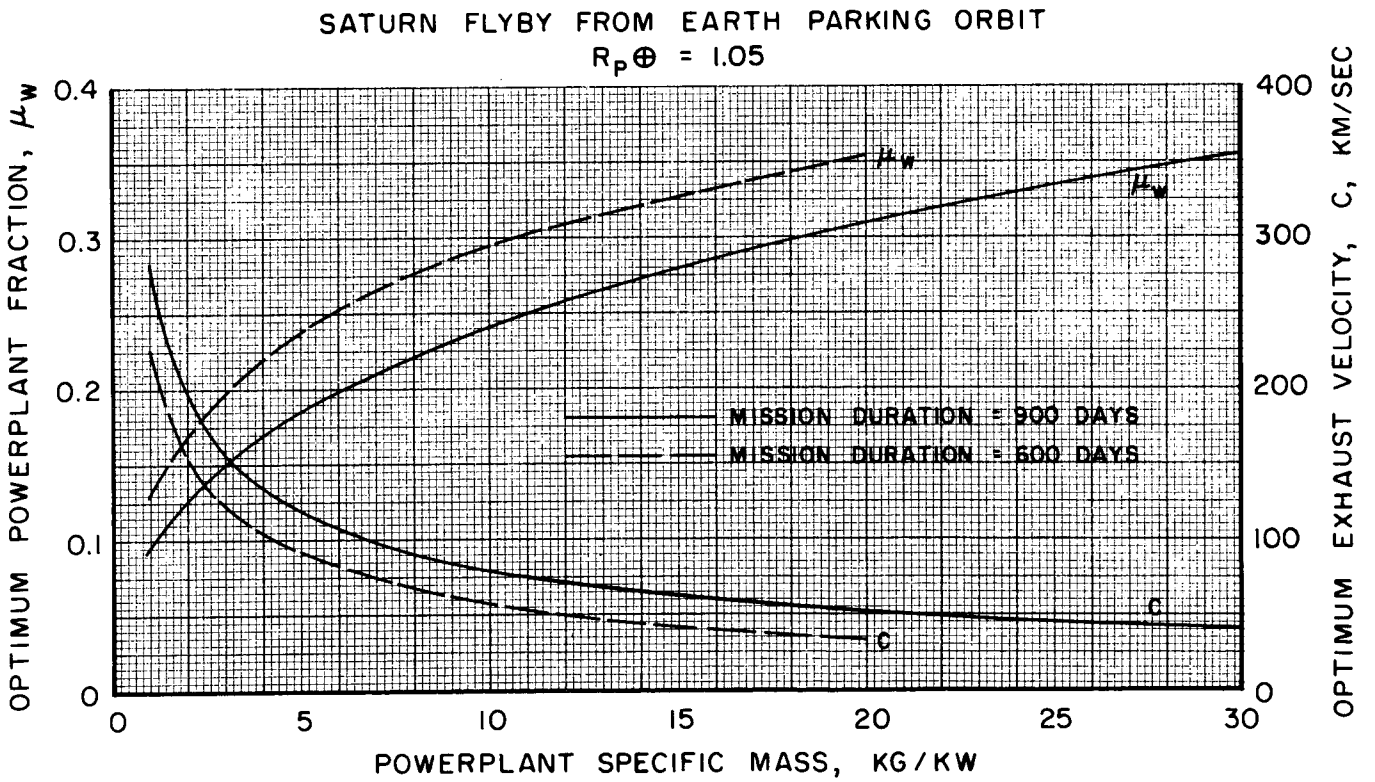

SECTION VII

DESCRIPTION OF RELATED COMPUTER PROGRAMS

Presented below are brief explanatory descriptions of the computer programs developed either under NASA contract or as part of UAC's corporate funded research. Typically, the programs were developed as required for the study of power-limited systems and employ the notation and nomenclature used throughout this handbook. All were programmed in Fortran V, for use on the UNIVAC 1108 computer. The UARL deck numbers are given.

Four programs are discussed: 1) heliocentric, power-limited trajectory optimization, 2) planetocentric trajectory computation, 3) optimization of single-stage electric propulsion systems and 4) direct search routine.

Heliocentric Trajectory Optimization (F615)

The steering program which minimizes J is determined for a constant-power, constant-thrust heliocentric trajectory. Up to two coast periods are allowed in the computation and the occurrence and duration of these are optimized as part of the overall optimization. Flyby and rendezvous trajectory options are available with initial hyperbolic excess speed (zero or nonzero) a specified input; for flybys the final hyperbolic excess speed is a computed quantity resulting from the minimization of J, while for the rendezvous case it is specified.

System options are: (1) optimize both exhaust velocity, C, (i.e., specific impulse) and powerplant fraction, μ_W; (2) optimize C for a fixed μ_W; (3) optimize μ_W for a fixed C; or (4) fix both C and μ_W. In all cases the optimization of the system is performed simultaneously with the trajectory optimization. Either two- or three-dimensional trajectories are allowed.

The basic input consists of the Julian dates for departure and arrival, the specification of the planets (as numbers starting from the sun outward with Mercury as 1), the hyperbolic excess speeds, the powerplant specific mass, α_W, and the efficiency parameter, d, in the thrustor efficiency function (see Section I on the hypothetical thrustor efficiency function). The output includes the trajectory time history, exhaust velocity, powerplant fraction, net mass fraction (μ_L), J, and the powered times (the times of occurrence and duration).

Planetocentric Trajectory Computation (F628)

The trajectory requirements and propulsion system parameters are computed between the planetocentric parking orbit and the switch point for a constant-power, constant low-thrust spiral. The trajectory options include either optimal steering

or tangential thrusting as well as outward or inward spirals. The planet is specified by a number (as in F615 above) which automatically produces the appropriate gravitational parameter and planetary radius. The initial (for departure) or final (for capture) parking orbit radius is input in terms of the planetary radius.

The planetary spiral equations as presented in Section IV (Edelbaum, Breakwell-Rauch) are solved for a given input thrusting time, T, and a given range of exhaust velocities, C. Also to be specified is the thrustor efficiency parameter, d. For each (T, C) pair, the output consists of the time, exhaust velocity, terminal mass fraction, μ_1, the ratio of powerplant fraction to powerplant specific mass μ_w/α_w, the trajectory characteristic, J, the initial thrust acceleration, and the average thrust acceleration (arithmetic and geometric means).

Optimization of Single-Stage Electric Propulsion System (F668)

The thrusting times and propulsion system parameters are determined which maximize the net spacecraft mass fraction of a single-stage electric vehicle. The single-stage aspect means that only one electric propulsion system (complete with power supply, thrustors, propellant, tanks, etc.) is used for all of the powered phases of the mission. For a fixed flight profile the computations are carried through for a given input total mission duration, T, and a range of powerplant specific masses, α_w. For each pair (T, α_w) the optimum distribution of powered time, the consequent minimum J, and all of the propulsion system parameters are determined.

The major input parameters required are the total mission duration, the range of powerplant specific mass, the thrustor efficiency parameter, the parking orbit radius (if necessary) at the departure and arrival planets, and the constants in the J and powered time equations. These latter constants are m, $\hat{J}$, and $\hat{T}$ for the appropriate phases of the overall trajectory and are listed in Table IV-1.

The sequence of computation involves two parts. First, with the given input, the optimum distribution of powered time is determined (see Section V) which holds for the fixed total mission duration. The resulting minimum total J and total powered time remains the same regardless of the powerplant specific mass. Second, with the minimum total J and powered time, the closed-form equations for the system parameters (see Section II) are serially solved for each value in the range of powerplant specific mass. This entire procedure is basic to three flight options: (1) heliocentric low-thrust transfer with an initial hyperbolic excess speed and final planetary spiral capture; (2) low-thrust spiral departure, heliocentric transfer, and planetary flybys; and (3) spiral departure, heliocentric transfer, and planetary spiral capture.

The output consists of all the related input, the optimum distribution of powered time and J's, the total powered time and J, the initial and final thrust acceleration, and the average thrust acceleration (AM and GM). The system parameters

that are output for each α_W are the maximum net spacecraft mass fraction μ_L, the terminal mass fraction, μ_1, the optimum exhaust velocity, C, and corresponding thrustor efficiency, η, the optimum powerplant mass fraction, μ_W, and the maximum powerplant specific mass that produces zero net spacecraft mass fraction, $\alpha_{W\ max}$. This latter quantity is computed to avoid needless computation if the current input α_W is larger than $\alpha_{W\ max}$.

Direct Search Techniques (F365)

The basic concept of the direct search procedure is presented in Appendix C. The purpose here is to discuss the several applications of this technique which were found useful in the particular study of low-thrust systems. These applications, in fact, are actually of general utility and the programming of the deck was oriented in this way.

In brief, the program requires an input function which is to be minimized, and starting guesses for the variables in the function. In addition, the increments or step changes in these variables must be given as well as the tolerances in these variables to which corresponds the accuracy of the final solution. That is, the tolerances are the ultimate incremental changes in the variables for which one deems the consequent accuracy in the corresponding solution to be adequate. The output includes the input along with the initial value of the function and its variables. The final value of the function is listed together with its inverse (for maximization problems) and the corresponding values of the variables.

Aside from the direct extremization of a function of several variables, the method has been found useful in several variations of the basic approach. The first example is in curve fitting according to the least-squares criterion. Here it is desired to fit a curve of the form

$$y = f(a, b, r, s, x)$$

to a given set of n data points (x_i, y_i). The problem is to determine the constants a, b, r, and s. Usually the form desired has a and b as linear constants but with r and s occurring in x^r, e^{rx^2}, or r^x; for example,

$$y = ae^{rx^2} + be^{sx^2}.$$

The problem is greatly simplified by the direct search procedure since a, b may be determined by the least-squares criterion as explicit functions of the r, s, and the data points x_i. This approach is advantageous since a and b are not usually known but r and s may be estimated from the form of the curve. The function to be used in this case for the program is the sum of the squares of the residuals,

$$R^2 = \sum_i (y_i - f_i)^2,$$

which is to be minimized. The parameters r and s can usually be guessed from the shape of the curve so that at each trial value of r and s, a and b are computed and all are substituted into f. The procedure then actually minimizes R^2 which is a function of the "variables" r and s.

The solution of unwieldy nonlinear equations of several variables is handled rather well by the deck. If there are n equations in n unknowns

$$f_i(x_1, \ldots, x_n) = 0 \qquad i = 1, \ldots, n$$

and if the starting values for each of the x_i are reasonably well known, then the solution may be obtained by requiring the following function to be minimized:

$$F(x_1, \ldots, x_n) = \sum_i \left[f_i(x_1, \ldots, x_n) \right]^2 .$$

At the solution, F should be zero to the accuracy implied by the tolerance on each increment.

In the case of minimizing a function subject to certain constraints on the variables, the "penalty function" approach of Appendix C could be used. However, because of the difficulty in choosing the K's in the penalty function (at the present time) and the fact that most of the problems encountered have reasonably tractable algebraic expressions for the constraints, it has been found advantageous to use the following procedure. If the function to be minimized is

$$y = f(x_i) \qquad i = 1, \ldots, n$$

subject to the m constraints

$$g_j(x_i) = 0 \qquad j = 1, \ldots, m < n$$

then each of the constraint equations are solved for a variable as a function of the other variables (a different variable for each constraint equation). The remaining variables not solved for in the "constraint" set are then the independent variables preferably those that have known starting values. Thus the problem becomes a straightforward one of minimizing $f(x_i)$ where some of the x_i are given by the equations from the constraint set.

It sometimes occurs that a minimization problem could be treated semi-analytically by first setting the partial derivatives of each independent variable equal to zero and attempting to solve the resulting (usually nonlinear and cumbersome) set of equations by the approach discussed previously. This is a reasonable procedure provided no mistakes are made in obtaining the partial derivatives and in the subsequent algebraic manipulations. It is advantageous to employ the search procedure, instead, to avoid these errors unless there is a compelling reason for investigating the equations describing the minimum conditions.

As noted in Appendix C, a final solution as obtained by the direct search procedure ideally occurs at or near the minimum solution. However because no sufficiency conditions are available for the success of the method nor, indeed, for the uniqueness of the solution obtained, it is always necessary to check the answer, at least for reasonableness, or recompute certain cases by alternative means.

SECTION VIII

APPENDICES

The following appendices discuss in detail several topics related to low-thrust systems analysis. They are intended to present additional relevant information and some insight, although the information given is not of itself necessary to apply the results of the previous sections. Appendix A develops the low-thrust planetocentric equations for departure or capture spirals and planetary orbit-to-orbit changes. The matching of planetocentric and heliocentric low-thrust hyperbolic trajectories is discussed in Appendix B. The basic notions of the very useful direct search procedure is given in Appendix C.

APPENDIX A

Planetocentric Low-Thrust Trajectories

Melbourne's Method*

For a vehicle being accelerated tangentially to its flight path about a planet, the rate of change of the total orbital energy per unit mass of the vehicle, U, is

$$\frac{dU}{dt} = av, \tag{A-1}$$

where a and v are the thrust acceleration and velocity, respectively, of the vehicle. The total orbital energy of an elliptical orbit is given by

$$U = -\frac{\mu_P}{2r}, \tag{A-2}$$

where μ_P is the planet's gravitational parameter and r is the semimajor axis of the osculating ellipse. Combining Eqs. (A-1) and (A-2), the growth rate $\dot{r}$, of the osculating ellipse is given by

$$\dot{r} = \frac{2r^2 av}{\mu_P}. \tag{A-3}$$

Since the vehicle is experiencing a thrust acceleration which is very much lower than the local gravity, the orbit of the vehicle does not differ from a circular orbit so that the vehicle velocity is essentially the orbital velocity, $v = (\mu_P/r)^{1/2}$. Substituting this expression into Eq. (A-3) yields

$$\dot{r} = \frac{2r^{3/2} a_0}{\mu_P^{1/2}\left(1 - \frac{a_0 t}{C}\right)}, \tag{A-4}$$

where the thrust acceleration, a, is given by

$$a = \frac{a_0}{1 - \frac{a_0 t}{C}},$$

for an initial thrust acceleration, a_0, and constant exhaust velocity, C. Integrating Eq. (A-4) from an initial orbit, r_0, and zero time to some final orbit, r_1, and terminal time, t_1, there results

* See Ref. IV-1

$$\frac{a_0 t_1}{C} = 1 - \exp\left\{-\frac{V_c}{C}\left[1 - \left(\frac{r_0}{r_1}\right)^{1/2}\right]\right\}. \qquad \text{(A-5)}$$

Given the exhaust velocity, initial thrust acceleration, and the initial and final orbits, the time required to transfer between orbits may be found. For the routine calculation of performance in the study of orbit-to-orbit transfers about a given planet, it is convenient to compute J at varying orbits and times. From the mass flow considerations and a given time, T, it can be seen that the exponential term of Eq. (A-5) is the terminal mass fraction, μ_1. Using the normalizing quantities characteristic of the planet, μ_p and radius, R_p, μ_1 may be written

$$\mu_1 = \exp\left[-\frac{\sqrt{\mu_P / R_P}}{C}\left(\frac{1}{\rho_0^{1/2}} - \frac{1}{\rho_1^{1/2}}\right)\right], \qquad \text{(A-6)}$$

where ρ is the nondimensional initial (final) radius referenced to R_p. The trajectory requirement may be computed by

$$J = \frac{C^2}{T}\,\frac{(1-\mu_1)^2}{\mu_1}, \qquad \text{(A-7)}$$

which was obtained by combining the rocket equation (see Eq. (1), Section II) and Eq. (A-5). It should be noted that from the dynamics of the problem the terminal mass fraction is fixed immediately by Eq. (A-6) for tangential steering. Consequently, the trajectory requirement, represented by J, is actually a secondary quantity which assumes its usefulness here only after it has been shown that it is relatively independent of the propulsion parameters for a given trajectory, (see Table IV-4 and corresponding text).

For the problem of a spiral to escape conditions, the corresponding time is found from Eq. (A-5) by setting $r_o/r_1 = 0$, i.e., the terminal radius goes to infinity. The escape time becomes $1/a_o \sqrt{\mu_p/r_o}$ which is high compared to exact numerical solutions. An empirical correction factor, Γ, is employed based on the numerical data and is derived as a function of the initial thrust acceleration. In terms of specific parameters, the escape time is

$$T = \frac{C^2}{2\eta}\,\frac{\Gamma}{\mu_w / a_w}\left(1 - e^{-V_c/C}\right), \qquad \text{(A-8)}$$

where Γ is shown in Fig. IV-4 and given by Eq. IV-2.

Edelbaum and Breakwell-Rauch Method

The planetocentric motion of a vehicle thrusting along a spiral about a planet can be described by its radial, $\ddot{r}$, and tangential accelerations, $\dot{v}$.

$$\ddot{r} = \frac{v^2}{r} - \frac{\dot{r}^2}{r} - \frac{\mu_P}{r^2} + \frac{F}{m}\frac{\dot{r}}{v}, \qquad \dot{v} = \frac{F}{m} - \frac{\mu_P}{r^2}\frac{\dot{r}}{v}, \tag{A-9}$$

where the mass rate of change is

$$\dot{m} = -\frac{F}{C}. \tag{A-10}$$

A nondimensional position, X, velocity, Y, exhaust velocity, Z, and time, T, may be defined according to

$$X = \left(\frac{F/m_E}{\mu_P}\right)^{1/2} r \qquad Z = \left(\frac{F}{m_E}\mu_P\right)^{-1/4} C$$

$$Y = \left(\frac{F}{m_E}\mu_P\right)^{-1/4} v \qquad T = \left[\frac{(F/m_E)^3}{\mu_P}\right]^{1/4} t \tag{A-11}$$

where all of the parameters are referenced to the mass of the vehicle at escape, m_E.

Substituting these parameters into Eq. (A-9) yields

$$\ddot{X} = \frac{Y^2}{X} - \frac{\dot{X}^2}{X} - \frac{1}{X^2} + \frac{m_E}{m}\frac{\dot{X}}{Y}, \qquad \dot{Y} = \frac{m_E}{m} - \frac{\dot{X}}{X^2 Y}. \tag{A-12}$$

The mass ratio m_E/m may be eliminated by introducing the dimensionless characteristic exhaust velocity, W,

$$W = Z \ln \frac{m_E}{m}, \tag{A-13}$$

which is interpreted as the characteristic velocity developed by the propulsion system between any point where the mass of the vehicle is m and the escape point. By differentiating Eq. (A-13) with respect to T and using Eq. (A-10), the time rate of change of W may be found.

$$\dot{W} = \frac{m_E}{m} = e^{W/Z}. \tag{A-14}$$

It is desirable to solve the differential equations of motion in terms of W since this represents the requirements of the trajectory on the vehicle. Thus the independent variable in Eq. (A-12) is changed from T to W using Eq. (A-14).

$$e^{2W/Z}\left(X'' + \frac{X'}{Z} - \frac{X}{Y}\right) = \frac{Y^2}{X} - \frac{(X')^2}{X} - \frac{1}{X^2}\,, \qquad (A\text{-}15)$$

$$Y' = 1 - \frac{X'}{X^2 Y}\,.$$

where a prime indicates differentiation with respect to W. These equations are completely general and any solution will represent a family of solutions of the initial Eqs. (A-9) corresponding to different values of thrust-to-mass ratio, exhaust velocity, parking orbit, and gravitational parameters.

The fact that the vehicle essentially maintains circular orbit conditions throughout most of its flight can be determined by noting that with thrust-to-mass ratios of about 10^{-3}, the value of X and its derivatives becomes small and the first of Eqs. (A-15) becomes $Y^2 = X^{-1}$, or in dimensional terms, $V = \sqrt{\mu_p/r}$, which is the circular velocity at radius r. Consequently, the spiral trajectory is quasi-circular as long as the local thrust acceleration is very small. Further, any spiral trajectory will automatically pass through the initial conditions of other low-thrust trajectories until the thrust acceleration becomes large and the orbit ceases to be quasi-circular. A solution of Eq. (A-15) for a given Z will therefore represent all corresponding low-thrust trajectories. Numerical solutions were obtained and are displayed in Figs. A-1, A-2, and A-3. Positive and negative values of Z correspond to departure and arrival trajectories, respectively; a value of infinity represents constant thrust acceleration (equivalently, infinite specific impulse or constant vehicle mass).

Of particular interest is Fig. A-2, wherein the slope of the curves for high circular velocities (left branch) approaches -1 while for high hyperbolic velocities (right branch) it approaches +1. The appropriate equations for each of these asymptotes are given in Fig. A-2, neglecting the small effect of Z. As is evident from Fig. A-2, the (parametric) planetocentric velocity of a thrusting vehicle approaches an asymptotic form as the planet's gravitational field becomes negligible. If this hyperbolic asymptote is extrapolated back to zero parametric velocity, then the requirements on the vehicle may be determined such that the vehicle thrusts only to this zero parametric velocity point and, by definition, this same vehicle commences its heliocentric journey with the massless planet's heliocentric position and velocity. In application, then, one would compute the planetocentric spiral trajectory requirements to the defined zero velocity point, then switch the calculations to the heliocentric frame ignoring the mass of the planet but taking on, as initial conditions, the point planet's heliocentric position and velocity. This is a distinct advantage over the Melbourne procedure since the implicit assumption of attaining infinite radius in finite time need not be made.

Extrapolating the hyperbolic asymptote back to zero velocity, the characteristic velocity is W = -0.941. On the circular asymptote the corresponding parametric velocity is Y = 1.746, the switch point of interest. Now the curves are referenced to escape velocity so that any point on the circular asymptote yields the characteristic velocity required to spiral from some initial circular orbit to escape. The requirements from circular to escape and from switch point (subscript 1) to escape are:

$$\text{circular to escape} \qquad Y_{CE} = -W_{CE} + 0.805$$

$$\text{switch to escape} \qquad Y_{1E} = -W_{1E} + 0.941$$

The difference between these two equations therefore gives the requirements from circular conditions to the switch point.

$$Y_{CE} - Y_{1E} = -W_{CE} + W_{1E}$$

Rewriting into dimensional quantities, and setting $Y_{1E} = 1.746$, there results

$$\left(\frac{F}{m_E}\mu_P\right)^{-1/4} V_C - 1.746 = \left(\frac{F}{m_E}\mu_P\right)^{1/4} \left(-\ln\frac{m_E}{m_C} + \ln\frac{m_E}{m_1}\right),$$

which may be simplified to

$$C \ln\frac{m_C}{m_1} = V_C - 1.746\left(\frac{F}{m_C}\frac{m_C}{m_1}\frac{m_1}{m_E}\mu_P\right)^{1/4}. \qquad \text{(A-16)}$$

The time spent between the switch point and escape is very small in relation to the time of the entire trajectory so that m_1/m_E is practically unity. Introducing the circular velocity equation into Eq. (A-16), setting $m_1/m_E = 1$, and identifying the terminal mass fraction, $\mu_1 = m_1/m_C$, the spiral trajectory requirement may be written as

$$\mu_1 = \exp\left\{-\frac{V_C}{C}\left[1 - 1.746\left(\frac{F/m_C}{\mu_P/R_C^2}\right)^{1/4}\frac{1}{\mu_1^{1/4}}\right]\right\}. \qquad \text{(A-17)}$$

This is identical to Eq. (IV-6) except for the constant. Because of the semi-graphical approach taken above, the constant of 1.746 is not precisely that obtained from a more exact approach which yields 1.757; both of these values represent the case of tangential steering. The first value was obtained by Edelbaum (Ref. A-1) in this analysis while the second was computed by Melbourne in a subsequent study (Ref. A-2).

In the Breakwell-Rauch approach (Ref. A-3), a systematic theory of a low-thrust spiral transferring into heliocentric space was developed based on the idea

illustrated in Fig. A-4. At some time, t_1, the vehicle is assumed to start from rest at the offset point and to be thrusting in the direction of the asymptote to the spiral trajectory. The heliocentric trajectory is then calculated from the offset point at time t_1 with the gravity field of the planet assumed nonexistent. For an approach spiral, the effect of the planet would be to place the vehicle on the spiral at the point shown at time t_1, rather than to reach the offset point at the same time. Thus t_1 is the point at which the computation of vehicle performance for the planetocentric portion of the flight ceases, for departure, or starts, for capture.

It is this point that is sought by the analytical astrodynamic analysis of Breakwell and Rauch so as to make the calculation of performance agree with the actual trajectory profile. The approach taken was to approximate the three-body problem using the method of matched asymptotic expansions. This is a systematic perturbation procedure which can be carried out to various orders of approximation. The basic idea is that the trajectory close to the planet is expanded in powers of a small parameter, such as the mass ratio of the planet to the sun. Another expansion is made of the heliocentric trajectory in the vicinity of the planet, carried out to the same order of approximation in powers of the same parameter. These two asymptotic expansions are then matched in a suitable region near the planet such that both solutions will give the same answer in this intermediate or "boundary layer" region. In this way, a composite solution is obtained for the whole problem, close to the planet, in the boundary layer region, and far from the planet.

The foregoing analysis reduces to a requirement on the characteristic velocity needed to reach the switch point, t_1:

$$\frac{\Delta V_1}{V_C} = 1 - 1.84 \left(\frac{F}{m_1} \mu_P \right)^{1/4}, \qquad \text{(A-18)}$$

which can be easily rewritten into Eq. (A-17). The constant, 1.84, is based on optimal steering.

Consequently, except for the constant, the two approaches to the planetocentric-heliocentric, low-thrust spiral trajectory problem yield identical results. On the one hand, the velocity intercept approach must assume that $m_1/m_\xi \approx 1$, while the analytical technique requires that the mass ratio of the planet to the sun be negligible to powers of $\frac{1}{2}$ or more, which is also a condition on the first approach. In distinction to both of the foregoing is the early Melbourne method employing a correction factor on a strictly planetocentric trajectory.

Comparison of Methods

Table A-1 compares the two methods for outward spirals from Mercury commencing at a parking orbit radius of 1.05 radii. The hypothetical form of the thrustor

efficiency function was used with d = 20 km/sec. The data shown in the table are typical examples and, in general, the results of the comparison hold for all similarly computed planetary spirals.

The Melbourne approach using the planet-centered spirals without asymptotic matching produces higher J's than the Edelbaum equations. This column is labeled with the constant 0.76382 which appears in the correction factor, Eq.(IV-2). The similarity between this equation and Eq. (IV-6), the Edelbaum result, suggests that the concept of asymptotic matching may be introduced into Melbourne's result simply by changing the constant to 1.76382. This result is shown in the second column. The improvement in the data is shown by comparing with the third column, which is from Edelbaum's method. Although the J's are not in exact agreement, the important point is that the terminal mass fractions, the actual indicators of accuracy, differ only in the third decimal place and are in exact agreement if round-off is used in the fourth place.

For an overall comparison, the results from the optimum steering program are indicated in the last column. As expected, the J's are the lowest computed. However the difference between optimal and tangential steering is essentially negligible in terms of the terminal mass fractions. For practical purposes this conclusion holds even for the massive planets and very long thrusting times (up to 240 days).

REFERENCES

A-1. Edelbaum, T. N.: "A Comparison of Non-chemical Propulsion Systems for Round-Trip Mars Missions". UA Research Laboratories Report E-1383-2, October 1960.

A-2. Melbourne, W. G., and C. G. Sauer: "Performance Computations with Pieced Solutions of Planetocentric and Heliocentric Trajectories for Low-Thrust Missions". JPL Space Programs Summary No. 37-36, Vol. IV, December 1965.

A-3. Breakwell, J. V., and H. E. Rauch: "Asymptotic Matching in Power-Limited Interplanetary-Transfers". AAS Preprint 66-114, 1966.

TABLE A-1

COMPARISON OF PLANETOCENTRIC SPIRAL EQUATIONS

Mercury Departure Spirals
R_p = 1.05 d = 20 km/sec

Thrusting Time (Days)	C (km/sec)	Melbourne; Tangential Steering, 0.76382 μ_1	Melbourne; Tangential Steering, 0.76382 J, m^2/sec^3	Melbourne; Tangential Steering, 1.76382 μ_1	Melbourne; Tangential Steering, 1.76382 J, m^2/sec^3	Edelbaum (Breakwell-Rauch), Tangential, 1.757 μ_1	Edelbaum (Breakwell-Rauch), Tangential, 1.757 J, m^2/sec^3	Edelbaum (Breakwell-Rauch), Optimal, 1.840 μ_1	Edelbaum (Breakwell-Rauch), Optimal, 1.840 J, m^2/sec^3
15	40	0.9384	4.998	0.9489	3.398	0.9477	3.562	0.9485	3.453
	80	0.9684	5.014	0.9740	3.422	0.9735	3.569	0.9739	3.460
	120	0.9790	5.019	0.9826	3.430	0.9822	3.572	0.9825	3.463
	160	0.9842	5.022	0.9869	3.434	0.9866	3.573	0.9868	3.464
	200	0.9873	5.024	0.9895	3.436	0.9893	3.574	0.9895	3.465
30	40	0.9371	2.610	0.9461	1.894	0.9450	1.975	0.9457	1.925
	80	0.9680	2.617	0.9726	1.906	0.9721	1.978	0.9724	1.929
	120	0.9785	2.620	0.9816	1.910	0.9813	1.980	0.9815	1.930
	160	0.9838	2.621	0.9862	1.912	0.9859	1.980	0.9861	1.930
	200	0.9871	2.622	0.9889	1.913	0.9887	1.981	0.9889	1.931

MEAN PATH PARAMETRIC VELOCITY AND RADIUS DISTANCE

CONSTANT LOW - THRUST PLANETOCENTRIC SPIRAL

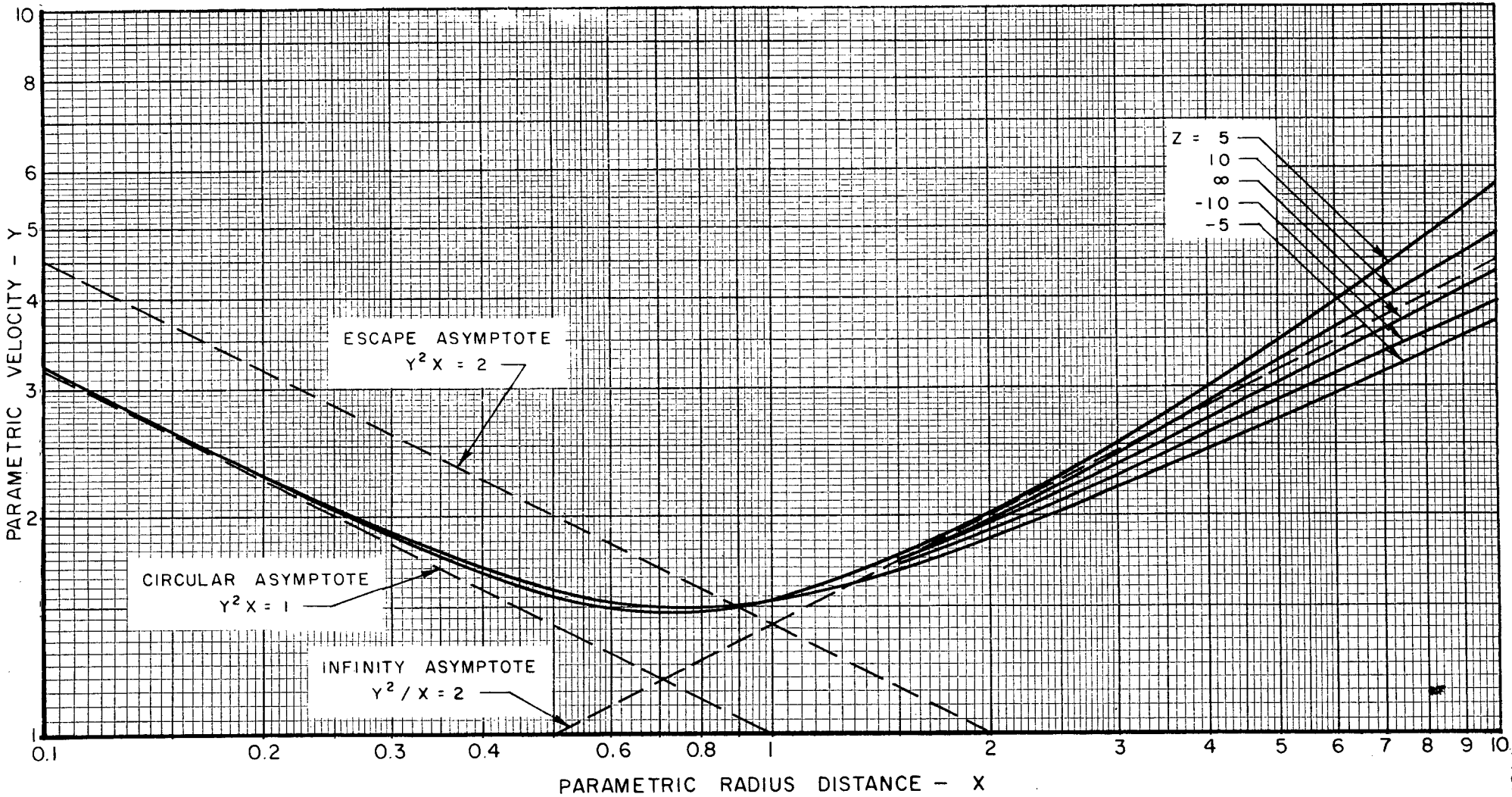

FIG. A-1

DEPENDENCE OF MEAN PATH VELOCITY ON CHARACTERISTIC VELOCITY

CONSTANT LOW-THRUST PLANETOCENTRIC SPIRAL

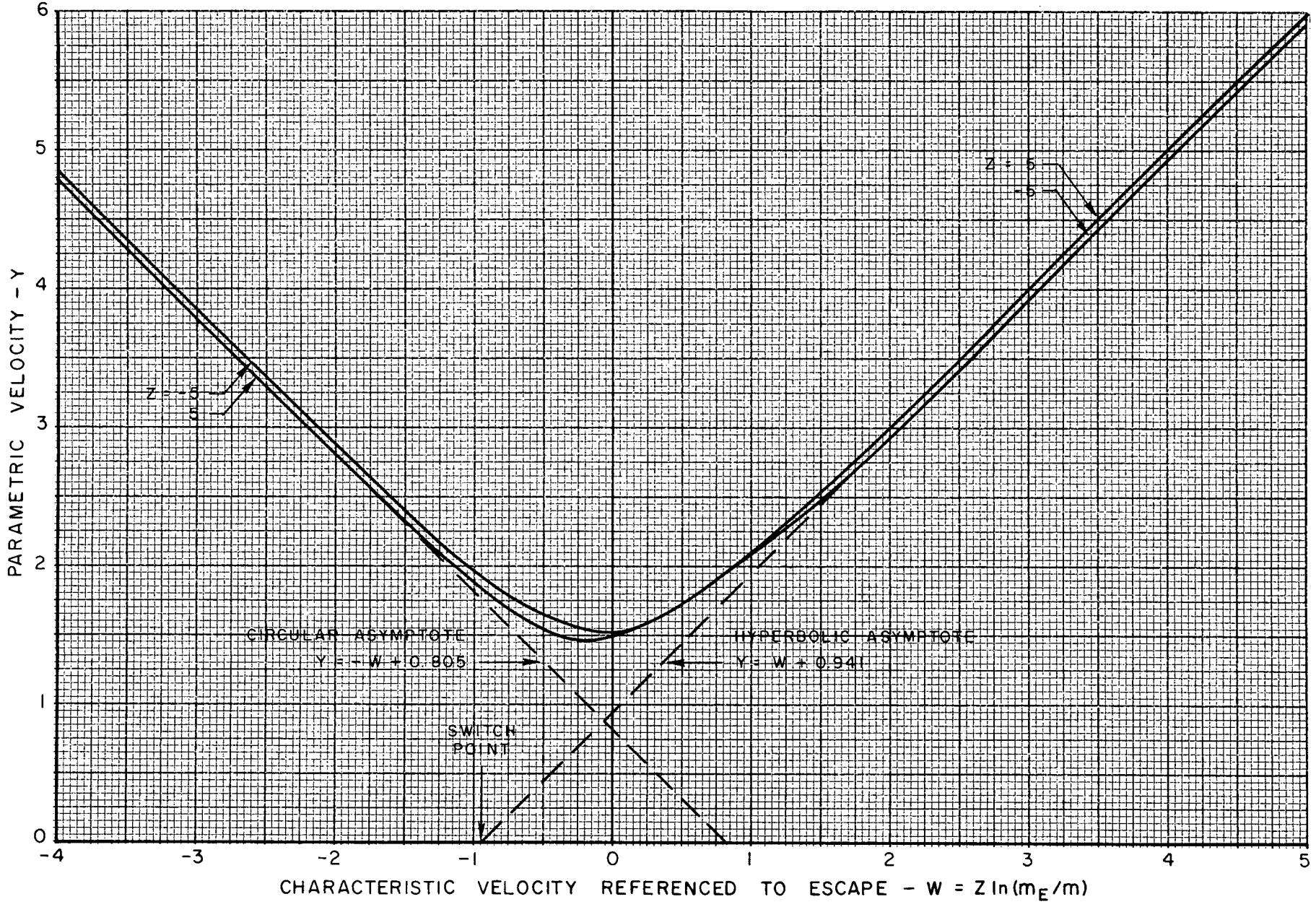

G - 110058 - 28

FIG. A-2

FIG. A – 3

FLIGHT PATH ANGLE AT VARIOUS RADIUS DISTANCES

CONSTANT LOW – THRUST PLANETOCENTRIC SPIRAL

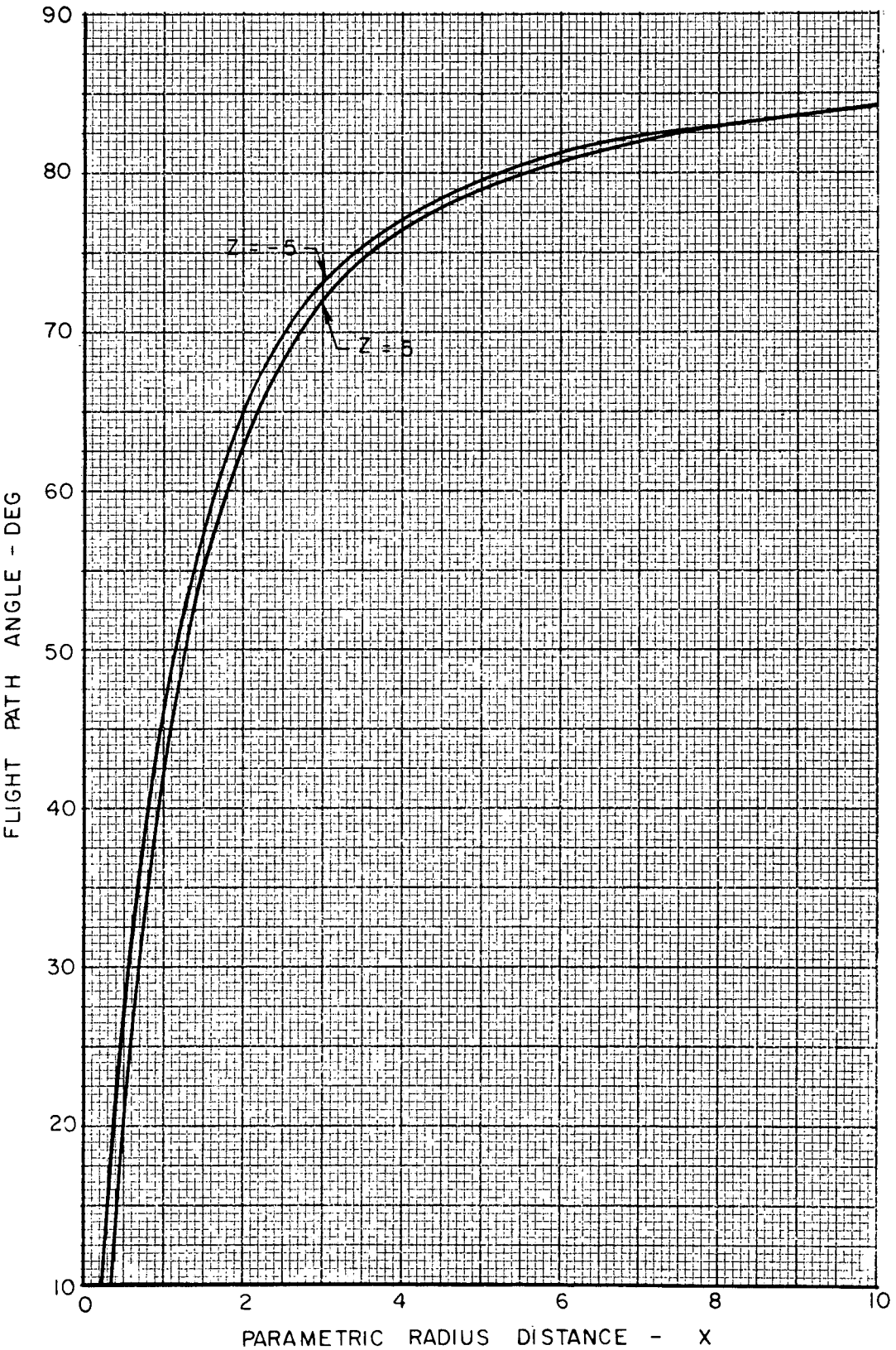

FIG. A-4

EFFECT OF PLANETARY GRAVITATIONAL FIELD ON LOW-THRUST TRAJECTORY

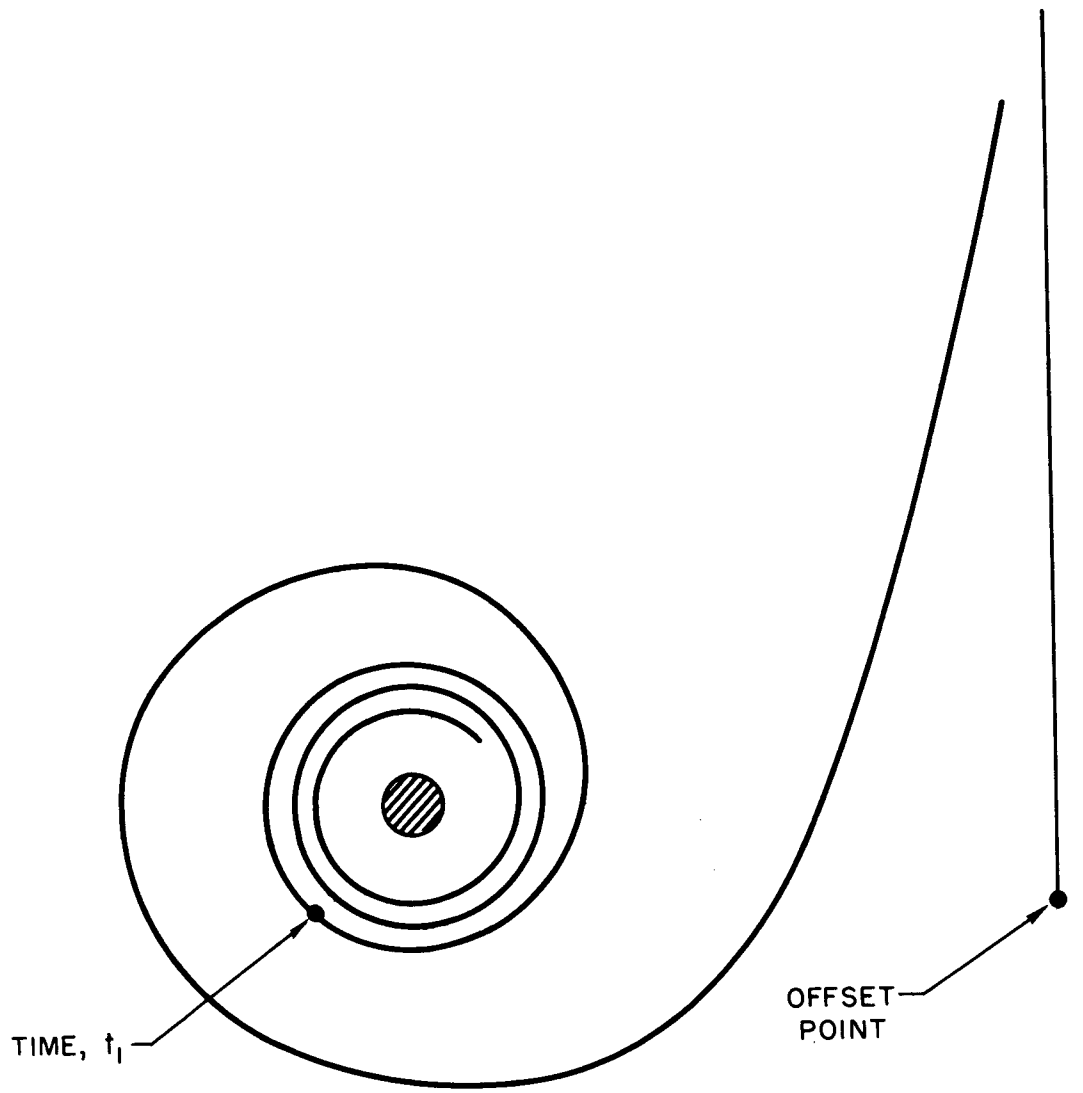

APPENDIX B

Low-Thrust Hyperbolic Trajectories

As mentioned in Section IV, the corrections to the low-thrust trajectory due to initial hyperbolic energy and subsequent thrusting within the planet's sphere of influence may be determined by using the concept of asymptotic velocity intercept. That is, as the vehicle recedes from the planet (with an initial hyperbolic velocity due to high thrust), the planetocentric velocity approaches an asymptotic form as the planet's gravitational field diminishes. This asymptote is extrapolated back to zero planetocentric velocity to identify an intercept time, t_1. By definition, t_1 is the time at which the velocity profile assumes the foregoing asymptotic form. Consequently t_1 is the time on the overall trajectory at which the performance calculations switch to the heliocentric frame, thereby allowing the interplanetary portion of the trajectory to be computed using the massless point planet's heliocentric position and velocity (along with the assumed initial hyperbolic velocity due to high thrust). This general approach is identical to that used in the notion of matching the planetocentric spiral with the heliocentric trajectory as described in Appendix A.

Determination of Intercept Time

The following analysis due to Edelbaum (Ref. B-1) is based on constant thrust acceleration and purely radial motion. Because the vehicle is given an initial parabolic or hyperbolic energy condition, the time spent in the vicinity of the planet is very small and the vehicle quickly assumes radial motion, Fig. B-1. As in Appendix A, the equations are treated in nondimensional form using the following normalized quantities:

$$X = r\left(\frac{F}{M\mu_p}\right)^{1/2}, \qquad Y = V\left(\frac{F\mu_p}{M}\right)^{-1/4}, \qquad T = t\left(\frac{F}{M}\right)^{3/4}\mu_p^{-1/4}. \tag{B-1}$$

Thus the normalized radial acceleration is

$$\ddot{X} = \dot{Y} = 1 - \frac{1}{X^2}. \tag{B-2}$$

Multiplying through by $\dot{X}$ yields

$$\dot{X}\ddot{X} = \dot{X} - \frac{\dot{X}}{X^2}. \tag{B-3}$$

which can be integrated from initial conditions (subscript o) to arbitrary final conditions

$$\frac{\dot{X}^2}{2} = X + \frac{1}{X} - X_0 + \frac{\dot{X}_0^2}{2} - \frac{1}{X_0}. \tag{B-4}$$

The initial energy is

$$U_0 = \frac{\dot{X}_0^2}{2} - \frac{1}{X_0} = \frac{Y_{\infty_0}^2}{2} . \tag{B-5}$$

where Y_{∞_0} is the initial hyperbolic excess speed due to high thrust.

Notice that as the radial distance increases, the retarding acceleration of the gravitational field decreases until the planetocentric velocity becomes a minimum. The radius at which minimum velocity occurs may be found by setting Eq. (B-2) equal to zero:

$$X^2 = r^2 \left(\frac{F}{m\mu_P}\right) = 1, \quad \text{or} \quad r = \left(\frac{\mu_P}{F/m}\right)^{1/2} \tag{B-6}$$

Substituting for U_0 in Eq. (B-4) and setting $X = 1$ and $X_0 = 0$ (the trajectory is assumed to start at the origin), the minimum velocity is obtained.

$$\dot{X}_{MIN} = (4 + 2U_0)^{1/2}$$

$$\text{or} \quad V_{MIN} = \left[V_{\infty_0}^2 + 4\left(\frac{F}{m}\mu_P\right)^{1/2}\right]^{1/2} \tag{B-7}$$

An example of a typical velocity profile having an initial thrust acceleration of 10^{-4} g and initial parabolic energy is illustrated in Fig. B-2. The path for impulsive departure and subsequent ballistic coast is shown; this is the profile resulting from an initial parabolic energy condition and no electric propulsion. The velocity asymptote extrapolated back to zero parametric velocity yields a parametric intercept time of about -1.2.

Continuing the analysis, the differential equation (B-4) can be solved for the differential of parametric time to yield

$$\sqrt{2}\, dT = \frac{dx}{\sqrt{x - x_0 + \frac{\dot{X}_0^2}{2} - \frac{1}{X_0} + \frac{1}{X}}} \tag{B-8}$$

Substituting Eq. (B-5), the initial energy, and integrating from $X = 0$ and $T = 0$ to arbitrary distance X, there results

$$T = \frac{1}{\sqrt{2}} \int_0^X \frac{x^{1/2} dx}{\sqrt{x^2 + U_0 x + 1}} . \tag{B-9}$$

which is an elliptic integral.

The solution of Eq. (B-9) depends on the initial energy and results in two cases of interest.

Case 1: $-2 \le U_0 \le 2$

The integral may be rewritten into tabular form by the following procedure. By adding and subtracting 2X in the denominator, and factoring, the integrand becomes

$$\left(\frac{X}{1 + U_0X + X^2}\right)^{1/2} = \left\{\frac{X}{(1+X)^2} \frac{1}{\left[1 - \frac{4X}{(1+X)^2}\left(\frac{1}{2} - \frac{U_0}{4}\right)\right]}\right\}^{1/2}.$$

Using the definition

$$\sin^2\phi = \frac{4X}{(1 + X)^2},$$

then

$$\cos\phi = \frac{1 - X}{1 + X} \quad \text{or} \quad X = \frac{1 - \cos\phi}{1 + \cos\phi},$$

and

$$dX = \frac{2}{1 + \cos\phi}\left(\frac{1 - \cos\phi}{1 + \cos\phi}\right)^{1/2} d\phi.$$

Thus by letting the modulus $k^2 = \frac{1}{2} - \frac{U_0}{4}$, $0 \le k^2 \le 1$,

Eq. (B-9) becomes

$$\sqrt{2}\, T = \int_0^{\phi}\left(\frac{1 - \cos\phi}{1 + \cos\phi}\right) \frac{d\phi}{(1 - k^2\sin^2\phi)^{1/2}}. \tag{B-10}$$

In terms of elliptic functions, this becomes

$$\sqrt{2}\, T = \int_0^{u} \frac{1 - cnu}{1 + cnu}\, du, \tag{B-10}$$

where

$$cnu = \cos\phi,$$

$$d\phi = \sqrt{1 - k^2\sin^2\phi}\, du.$$

Equation (B-10) is now in the form 239.03 tabulated in Ref. B-2. Simplifying into nondimensional notation, there results

$$\sqrt{2}\, T = F(\phi,k) - 2E(\phi,k) + \frac{2\sqrt{X}}{1 + X}(1 + U_0X + X^2)^{1/2}. \tag{B-11}$$

Now the concept of asymptotic matching of the planetocentric and heliocentric trajectories requires that the time of Eq. (B-11) be evaluated as the radial position goes to infinity. Thus as X becomes very large in relation to unity, the elliptic integrals F and E (first and second kind, respectively) become complete and the third term of Eq. (B-11) reduces to $\sqrt{2X}$. The corresponding velocity at infinity may be found by introducing $X \gg 1$ in Eq. (B-4). Thus

$$\dot{X}_\infty = Y_\infty \simeq \sqrt{2X} .$$

The time as a function of parametric asymptotic velocity is therefore

$$T \approx \sqrt{2}\, K(k) - 2\sqrt{2}\, E(k) + Y_\infty ; \qquad -2 \le U_0 \le 2 . \tag{B-12}$$

Case 2: $U_0 \ge 2$

The denominator of (B-9) may be written as the product of two factors by adding and subtracting $U_0^2/4$ so that

$$\sqrt{2}\, T = \int_0^X \left[\frac{X}{(X-b)(X-c)} \right]^{1/2} dX ,$$

where

$$b = -\left[\frac{U_0}{2} - \sqrt{\frac{U_0^2}{4} - 1} \right] , \qquad c = -\left[\frac{U_0}{2} + \sqrt{\frac{U_0^2}{4} - 1} \right] .$$

This is in the proper form as given by 237.03, Ref. (B-2). In terms of elliptic functions it is

$$\sqrt{2}\, T = \frac{2(-b)}{\sqrt{-c}} \int_0^u tn^2 u\, du ,$$

$$\sqrt{2}\, T = 2 \left[\frac{X(X-c)}{X-b} \right]^{1/2} - 2\sqrt{-c}\, E(\phi, k) , \tag{B-13}$$

where

$$\sin^2 \phi = \frac{X}{X-b}$$

and

$$k^2 = \frac{c-b}{c} ; \qquad 0 \le k^2 \le 1 .$$

For asymptotic matching $X \gg 1$ and $E(\phi, K)$ becomes the complete elliptic integral $E(K)$. Hence Eq. (B-13) gives the time in terms of parametric asymptotic velocity

$$T \simeq Y_\infty - \left[2\left(U_0 + \sqrt{U_0^2 - 4}\right)\right]^{1/2} E(k), \quad U_0 \geq 2, \tag{B-14}$$

where, as before, $Y_\infty \simeq \sqrt{2X}$.

Equations (B-12) and (B-14) are the equations of the asymptotes with initial energy (actually initial velocity) as a parameter. The intercept time is obtained by extending the asymptote back to zero velocity , i.e., $Y_\infty = 0$. For example, if the initial energy were zero (parabolic conditions), then Eq. (B-12) would yield $T_1 = -1.19814$. Because the intercept time is solely a function of parametric energy, a new function $G(U_0)$ may be defined according to $T_1 = G(U_0)$ so that the intercept time may be rewritten in dimensional form using the definition for T, Eq. (B-1).

$$t_1 = \left[\frac{(F/m_0)^3}{\mu_P}\right]^{1/4} G(U_0), \tag{B-15}$$

where

$$U_0 = \frac{Y_{\infty_0}^2}{2} = \frac{V_{\infty_0}^2}{2}\left(\frac{F}{m_0}\mu_P\right)^{-1/2} - \frac{1}{r_0}\left(\frac{F/m_0}{\mu_P}\right)^{-1/2}, \tag{B-16}$$

and

$$G(U_0) = \sqrt{2}\,K(k) - 2\sqrt{2}\,E(k), \quad -2 \leq U_0 \leq 2$$

$$G(U_0) = -\left[2\left(U_0 + \sqrt{U_0^2 - 4}\right)\right]^{1/2} E(k), \quad U_0 \geq 2. \tag{B-17}$$

The function $G(U_0)$ is plotted in Fig. B-3 for various values of initial energy.

As is usually the case in performance analysis, the computation of intercept time is only a small part of the overall analysis. Since the programming of Eqs. (B-12) and (B-14), with $Y_\infty = 0$, involves the evaluation of the elliptic integrals at different values of k^2, it is convenient to approximate Fig. (B-3) by a curve fit. Using the form

$$G(U_0) = aU_0^r + bU_0^s, \tag{B-18}$$

a least-squares fit was employed on the data of Fig. B-3. The results are

$$a = -1.86443 \qquad r = 0.508984$$

$$b = 1.86431 \qquad s = -0.193751$$

Since a and b differ (except for sign) in the fifth place, Eq. (B-18) may be further simplified to

$$G(U_0) = aU_0^r\left(1 - U_0^{s-r}\right).$$

Equation (B-18) is highly accurate, having an error of not more than one unit in the fifth significant figure.

Velocity and Position Offsets

As can be seen from Fig. B-3, for all initial conditions greater than or equal to zero, the intercept time is negative, which means that the intercept time, t_1, must be subtracted from the heliocentric portion of the trajectory. This alters the boundary conditions on the heliocentric trajectory, particularly the position of the point mass planet in space.

A more convenient procedure, which leaves the heliocentric boundary conditions unaffected, would be to use the asymptotic velocity corresponding to T = 0 in Eqs. (B-12) and (B-14). This velocity is termed the velocity offset, δV, and is found from

$$\delta V \equiv Y_\infty = -G(U_0), \tag{B-19}$$

where $G(U_o)$ is defined by Eq. (B-17). In dimensional form this equation becomes Eq. (IV-14) or (IV-16) of Section IV.

The velocity along the flight path as a function of position is given by

$$\frac{\dot{X}^2}{2} = X + \frac{1}{X} + U_0. \tag{B-4}$$

The position displacement, or offset, is found by requiring $X \gg 1$ so that $\dot{X}^2 \to \dot{X}_\infty^2$, the vehicle's velocity at infinity. Thus

$$\frac{\dot{X}_\infty^2}{2} = X + \frac{Y_{\infty_0}^2}{2}. \tag{B-20}$$

Solving for X, the position offset,

$$X = \frac{\dot{X}_\infty^2 - Y_{\infty_0}^2}{2}. \tag{B-21}$$

This may be rewritten into dimensional form by using Eqs. (B-1) and (B-19) and defining δR as the position offset,

$$\delta R = \frac{(\delta V)^2 - V_{\infty_0}^2}{2(F/m_0)}. \tag{B-22}$$

which is Eq. (IV-18).

Correction for Finite Periapsis Radius

The foregoing analysis was based on an approximation that the initial periapsis radius was zero; that is, the trajectory was assumed to start at the center of the planet. The following analysis (Ref. B-3) corrects for this and shows the effect of starting at a finite periapsis radius. The vehicle is assumed to be injected by the high-thrust rocket onto the periapsis of a hyperbolic orbit. At this point, low-thrust propulsion is started. The analysis to follow shows that the effect of the finite periapsis radius is of order μ, the ratio of the mass of the planet to that of the sun. This is a higher-order effect and may be neglected for purposes of performance analysis, along with the other higher-order terms (also of order μ) which were neglected in the analysis given above.

The effect of the initial periapsis radius is analyzed by considering the difference in a linear analysis of having an initial eccentricity of unity or an initial eccentricity corresponding to the actual trajectory which starts at the parking orbit radius. The acceleration due to thrust is assumed to be constant in magnitude and to be directed tangentially. Under this perturbation, the linear theory predicts that the increase in energy of the orbit will be proportional to the arc length of the hyperbola. In the following equations, the unit of distance is the AU and the unit of time is the time required for Earth to traverse one radian in its orbit. Thus the gravitational parameter of the sun is unity and the gravitational parameter of the planet, μ_p, is given in terms of this unit solar gravitational parameter.

The radial position, r, along the hyperbola is given by

$$r = a(e \cosh H - 1) \tag{B-23}$$

and the time is

$$t = \frac{\mu_p}{V_\infty^3} (e \sinh H - H) \tag{B-24}$$

The arc length is

$$s = ae \left[\frac{e^2 - 1}{e^2} F(\phi, k) + e \sin\phi \cosh H \right] \tag{B-25}$$

where the numerical eccentricity of the hyperbola is

$$e = 1 + \frac{r_p V_\infty^2}{\mu_p}$$

and the modulus for the elliptic integrals is

$$k^2 = \frac{1}{e} \qquad \text{with} \qquad \sin\phi = \frac{e \sinh H}{\sqrt{e^2 + e^2 \sinh^2 H - 1}}$$

The semimajor axis, a, is taken to be positive and H is the hyperbolic eccentric anomaly. F and E are the incomplete elliptic integrals of the first and second kind, respectively.

What is of interest is the change in time and the change in arc length (due to the change in periapsis radius) as the vehicle gets far from the origin. Accordingly, the limits of Eqs. (B-24) and (B-25) as given by Eqs. (B-26) and (B-27) are used.

For $H \gg 1$:

$$t \approx \frac{\mu_P}{V_\infty^3} \left[\frac{r + a}{a} - \ln\left(2\frac{r + a}{a}\right) + \ln e \right] \tag{B-26}$$

$$s \approx r + a\left[1 + \frac{e^2 - 1}{e} K\left(\frac{1}{e}\right) - eE\left(\frac{1}{e}\right)\right] \tag{B-27}$$

The effect of the finite planetary radius will be assumed to be reflected in a change in the initial hyperbolic excess velocity of the trajectory. In order to calculate this, consider the difference in hyperbolic excess velocity between a trajectory with unit eccentricity and the actual trajectory. Equation (B-28) considers the changes due to both the time required to get to a given radius and the difference in arc length traveled in getting to that same radius.

$$\delta V_\infty = \frac{F}{m} \frac{1}{V_\infty} (s - s_{e=1}) - \frac{F}{m} (t - t_{e=1}) \tag{B-28}$$

If the values obtained from Eqs. (B-26) and (B-27) are substituted into Eq. (B-28), the result is Eq. (B-29) which gives an approximate indication of the perturbation in initial hyperbolic excess velocity due to a finite periapsis radius. It should be noted that this perturbation is of order μ and will generally be small enough to be neglected for performance calculations.

$$\delta V_\infty = \frac{\mu_P}{V_\infty^3} \frac{F}{m} \left[1 - \ln e + \frac{e^2 - 1}{e} K\left(\frac{1}{e}\right) - eE\left(\frac{1}{e}\right)\right] \tag{B-29}$$

REFERENCES

B-1. Ragsac, R. V., et al: "Study of Low-Acceleration Space Transportation Systems". UA Research Laboratories Report D-910262-3, Appendix A by T. N. Edelbaum, July 1965.

B-2. Byrd, P. F., and M. D. Friedman: Handbook of Elliptic Integrals for Engineers and Physicists. Springer-Verlag, Berlin, 1954.

B-3. Ragsac, R. V., et al: "Study of Trajectories and Upper Stage Propulsion Requirements for Exploration of the Solar System". UA Research Laboratories Report F-910352-12, Vol. II, Section VI, by T. N. Edelbaum.

STRAIGHT LINE TRAJECTORY APPROXIMATION

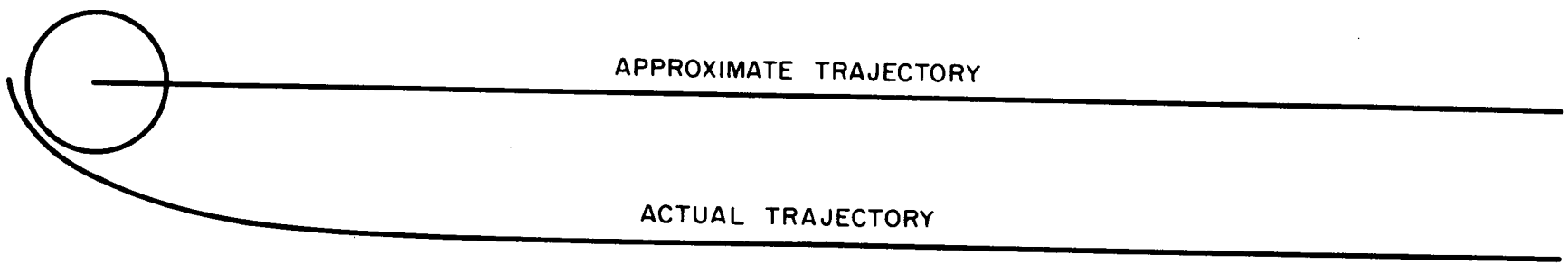

FIG. B-1

ASYMPTOTIC VELOCITY-INTERCEPT METHOD

INITIAL THRUST ACCELERATION = 10^{-4} g

INITIAL PARABOLIC ENERGY CONDITIONS

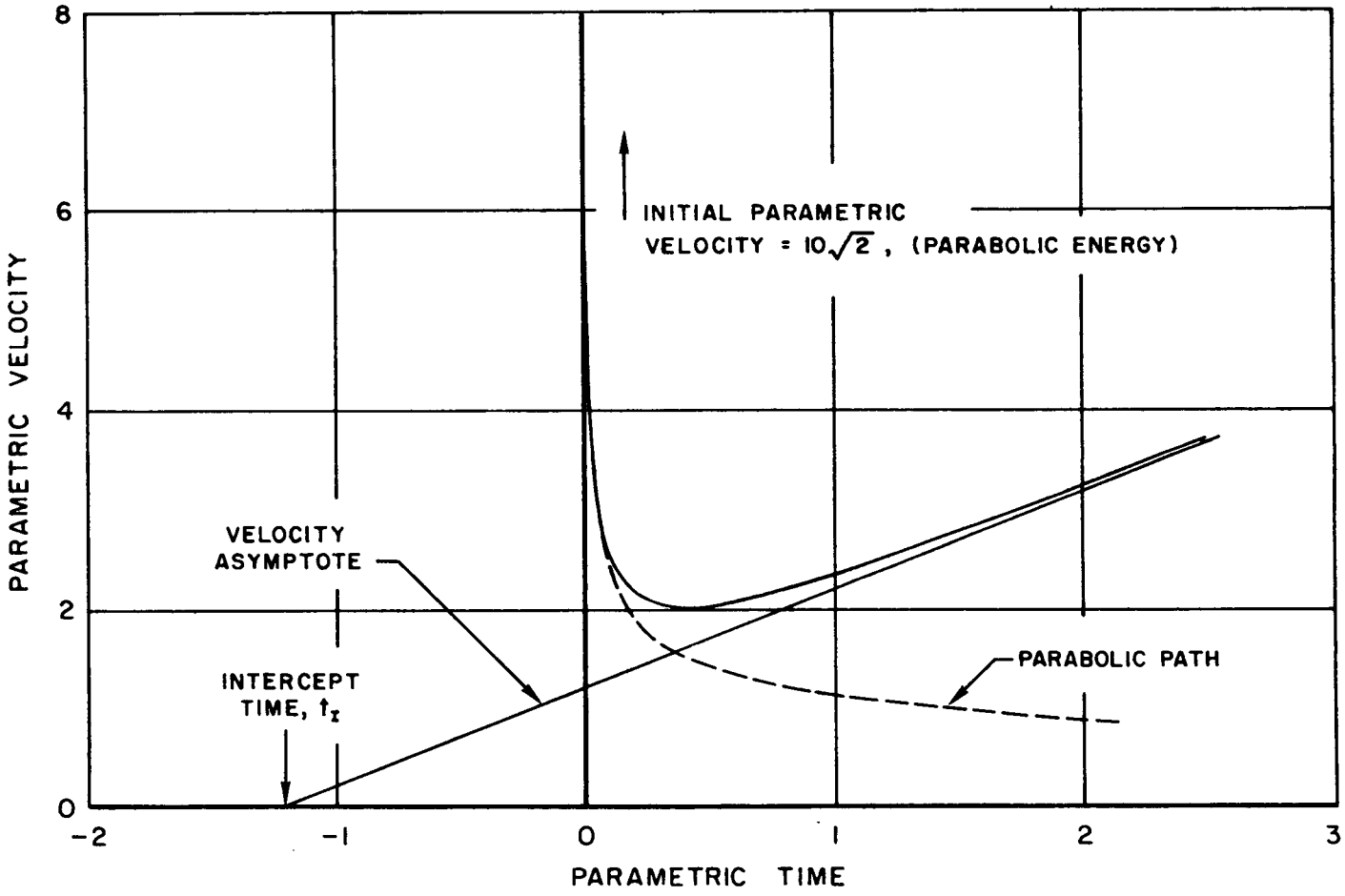

FIG. B-2

INTERCEPT TIME FOR PLANETOCENTRIC LOW-THRUST HYPERBOLIC TRAJECTORIES

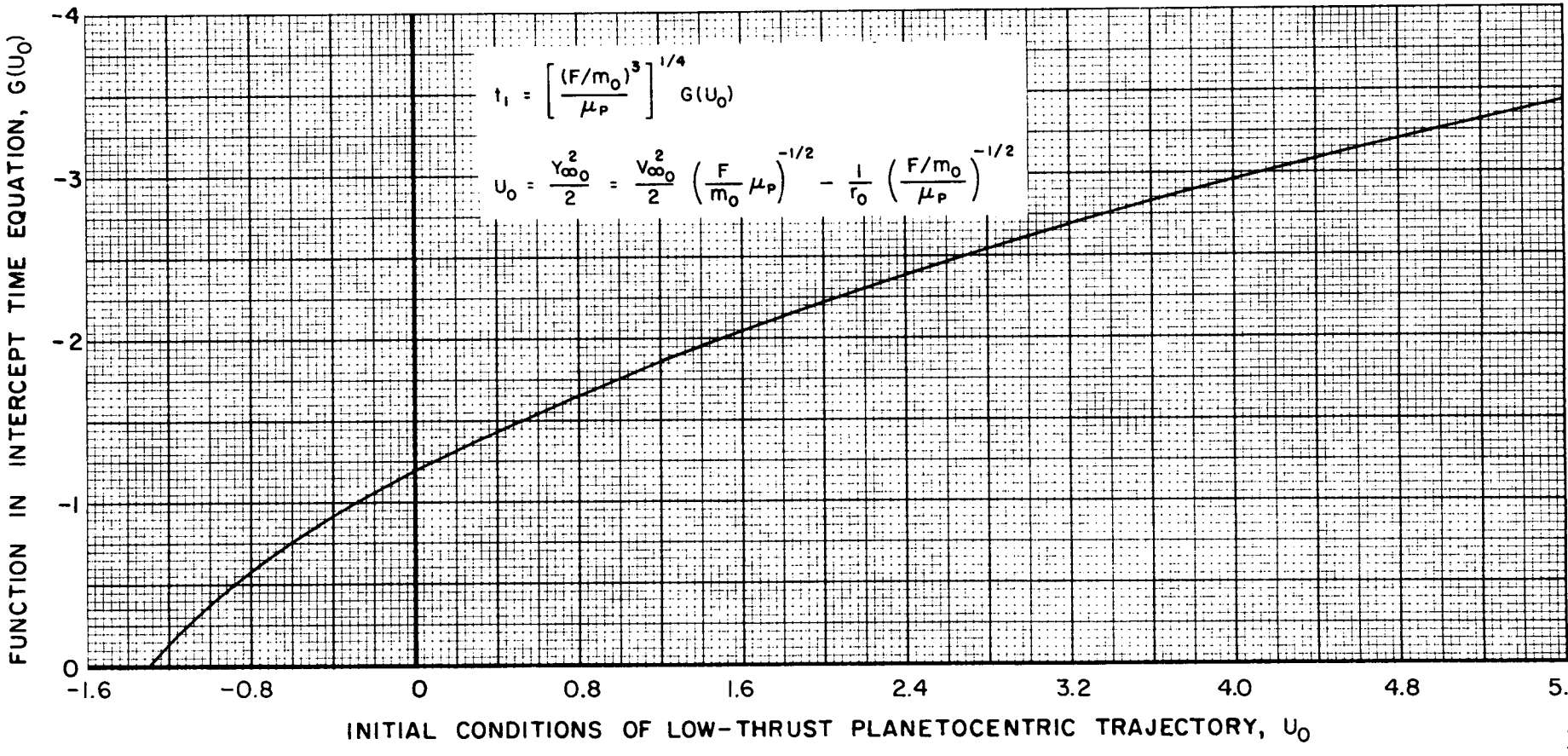

FIG. B-3

APPENDIX C

Systematic Search Technique

The original UARL program for finding the minimum (or maximum) of an n-variable function was prepared under the direction of D. Fridshal (Ref. C-1). Much of the basic theory behind the systematic search method is contained in Ref. C-1. This technique is based on a development by Hooke and Jeeves (Ref. C-2) termed "direct search". According to both Refs. C-1 and C-2, the direct search method has been found to be attractive for the following reasons:

1. No techniques of classical analysis are necessarily involved,
2. repeated arithmetic operations are used with simple logic,
3. an approximate solution, improving continuously, is provided at all phases of the computation, and
4. other classes of problems are readily attacked.

Direct Search

The basic theory of the method is briefly summarized here for the sake of completeness. For an exhaustive treatment of the subject as well as a formalized definition of direct search the reader is referred to Ref. C-2.

The problem is to minimize a function of n variables, $f(x_1, x_2, \ldots, x_n)$. A solution vector or "point" P_i consists of n components $(x_{1_i}, x_{2_i}, \ldots, x_{n_i})$ which when compared to some other solution P_j is better if and only if

$$f(x_{1_i}, x_{2_i}, \ldots, x_{n_i}) < f(x_{1_j}, x_{2_j}, \ldots, x_{n_j}).$$

A base point, B_o, is determined from initial guesses of the values for the n components or coordinates. Using the strategy discussed below, an adjacent point, P_1, is generated and compared to the base point, B_o. If P_1 is an improved solution compared to B_o, then P_1 becomes the new base point B_1, and the "move" which resulted in P_1 is termed a success. If P_1 is not better than B_o, then the move was a failure. A success or failure in a move or step is judged solely by the above inequality.

The next trial point, P_r, is determined relative to B_r by the present state S_r. The states make up part of the logic, since they determine directions for moves in the solution space. They provide new directions if recent moves fail, and they decide when no further progress can be made.

The search procedure employs two types of moves - exploratory and pattern moves. Explorations in the n coordinates are made to determine how the function $f(x_1, \ldots, x_n)$ behaves in the neighborhood of the past point. The pattern move utilizes the behavioral information to provide a substantial reduction of the function.

The exploratory moves are made one coordinate at a time. Thus, x_1 is varied by an increment $+\delta$ while $x_2, \ldots, x_n$ remain fixed. This new vector $(x_1 + \delta, x_2, \ldots, x_n)$ is tested against the base point $(x_1, \ldots, x_n)$. If it is better, the new coordinate value is retained. If it is not, x_1 is varied by $-\delta$ while $x_2, \ldots, x_n$ remains fixed. If this vector yields a smaller f, $x_1 - \delta$ is retained. If both + and - variations do not reduce f, then the original value, x_1, is retained.

The entire procedure is repeated for the remaining coordinates x_2 through x_n. At the completion of the procedure, each coordinate will have associated with it a direction and a slightly reduced value for f if at least one variation succeeded. The set of directions is referred to as a pattern. Hence the pattern move consists of changing all the coordinates simultaneously in the indicated directions or patterns as obtained from the exploratory moves.

The new values of the coordinates after the pattern move form the new base point from which exploratory moves may be made, as discussed above. Alternatively, the same pattern may be used repeatedly with a test for improvement in the value of the function made after each move. Each success updates the base point. In this approach, if a pattern move fails, exploratory moves are then made from the current base point. The present version of the computer program uses this approach. The justification for this approach is based on the fact that, for problems so far encountered, shorter machine times are realized.

If a combination pattern and exploratory move fails and if exploratory moves from the last base point fail, a decrease in the variation, or step size, δ, is required. The criterion for a final solution is when δ is reduced below some input tolerance, ϵ. Ideally, this final solution occurs when the function is at a minimum or near-minimum solution. However, the fact that no further progress can be made beyond the tolerance, ϵ, does not always indicate that a solution has been found. As is characteristic of direct search methods, no sufficiency conditions are available for the success of the method. Thus, Hooke and Jeeves recommend the

search technique for the following types of problems:

1. Problems for which the answers may be tested, and

2. problems consisting of many separate cases, a few of which can be checked by alternative means.

If (1) and (2) are not feasible, partial checks may be obtained by using the method several times, with different starting solutions.

An overall view of the systematic search technique may be obtained from Figs. C-1, C-2, and C-3 which present the basic logic in flow chart form.

Functions Subject to Constraints

The concept of penalty functions arises from approximating a minimum problem subject to constraints by another problem which does not involve constraints. Thus, if the problem is to minimize $f(x_1, \ldots, x_n)$ subject to the m constraints

$$g_j = g_j(x_1, \ldots, x_n), \quad j = 1, \ldots, m < n,$$

one forms the penalty function P:

$$P = f + \sum_{j=1}^{m} k_j g_j,$$

where k_j are positive constants. The summation in this function represents the "penalty" terms which will have the effect of reducing the constraint "violations" to zero since these are non-negative terms. As the k_j becomes large positively, the solution of this minimum problem will approach the minimum solution of the original problem with constraints. This concept is rigorously analyzed in Ref. C-3. The rate at which the k_j is increased positively is important, since too fast an increase will halt the procedure, while too slow an increase will prolong the convergence process.

REFERENCES

C-1. Fridshal, D.: Solution of Minimum Problems Utilizing a Systematic Search Technique. UA Research Laboratories Report B-110058-9, June 11, 1963.

C-2. Hooke, R., and T. A. Jeeves: Direct Search Solution of Numerical and Statistical Problems. Journal of the Association of Computing Machinery, Vol. 8, No. 2, April 1961, pp. 212-223.

C-3. Courant, R.: Lecture Notes on the Calculus of Variations. New York University Institute of Mathematical Sciences, pp. 270-280.

FIG. C-1

DECK F365 SEARCH PROCEDURE

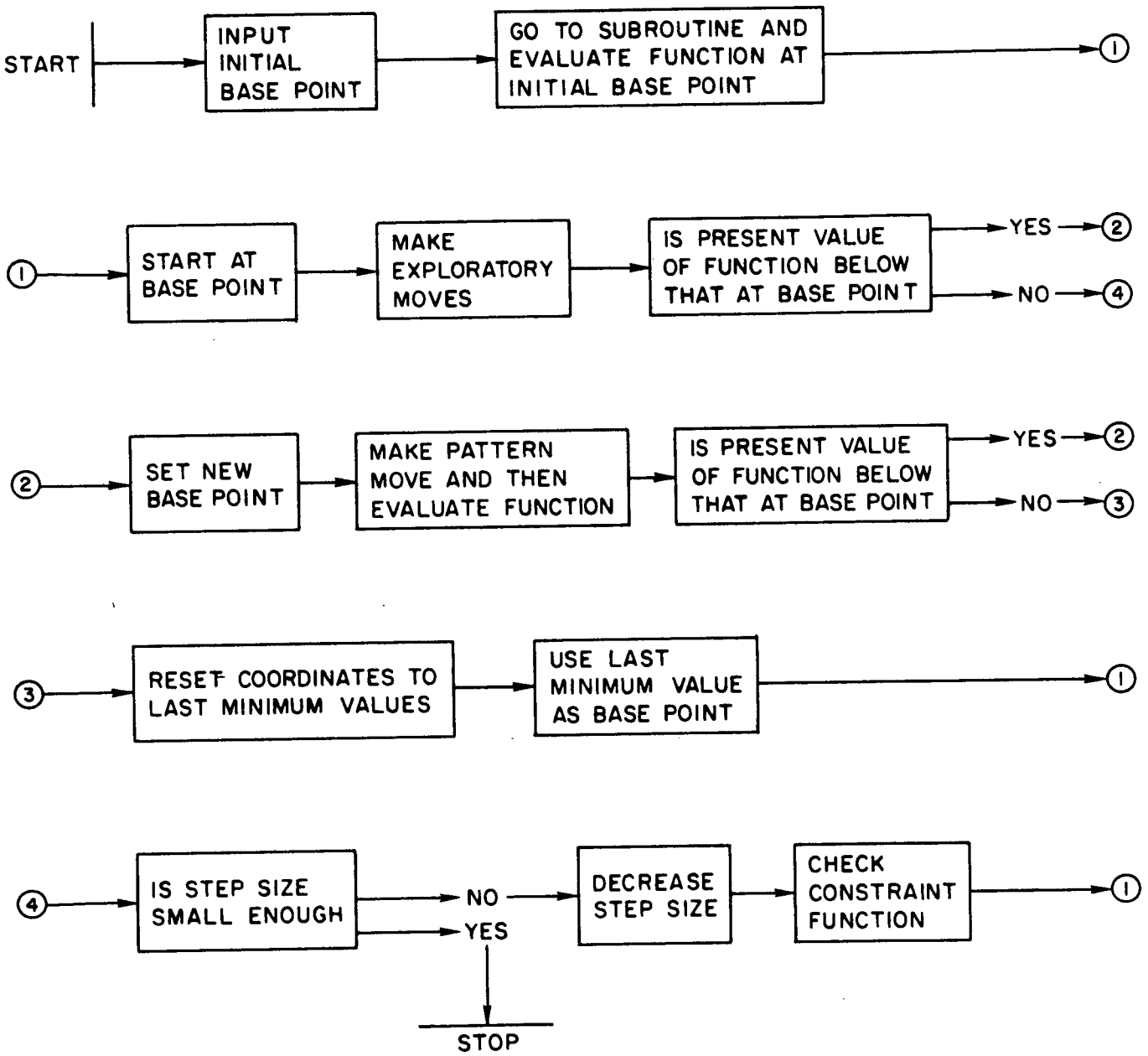

FLOW CHARTS DESCRIBING EXPLORATORY AND PATTERN MOVES ARE DESCRIBED ON THE FOLLOWING PAGES

FIG. C-2

EXPLORATORY MOVES

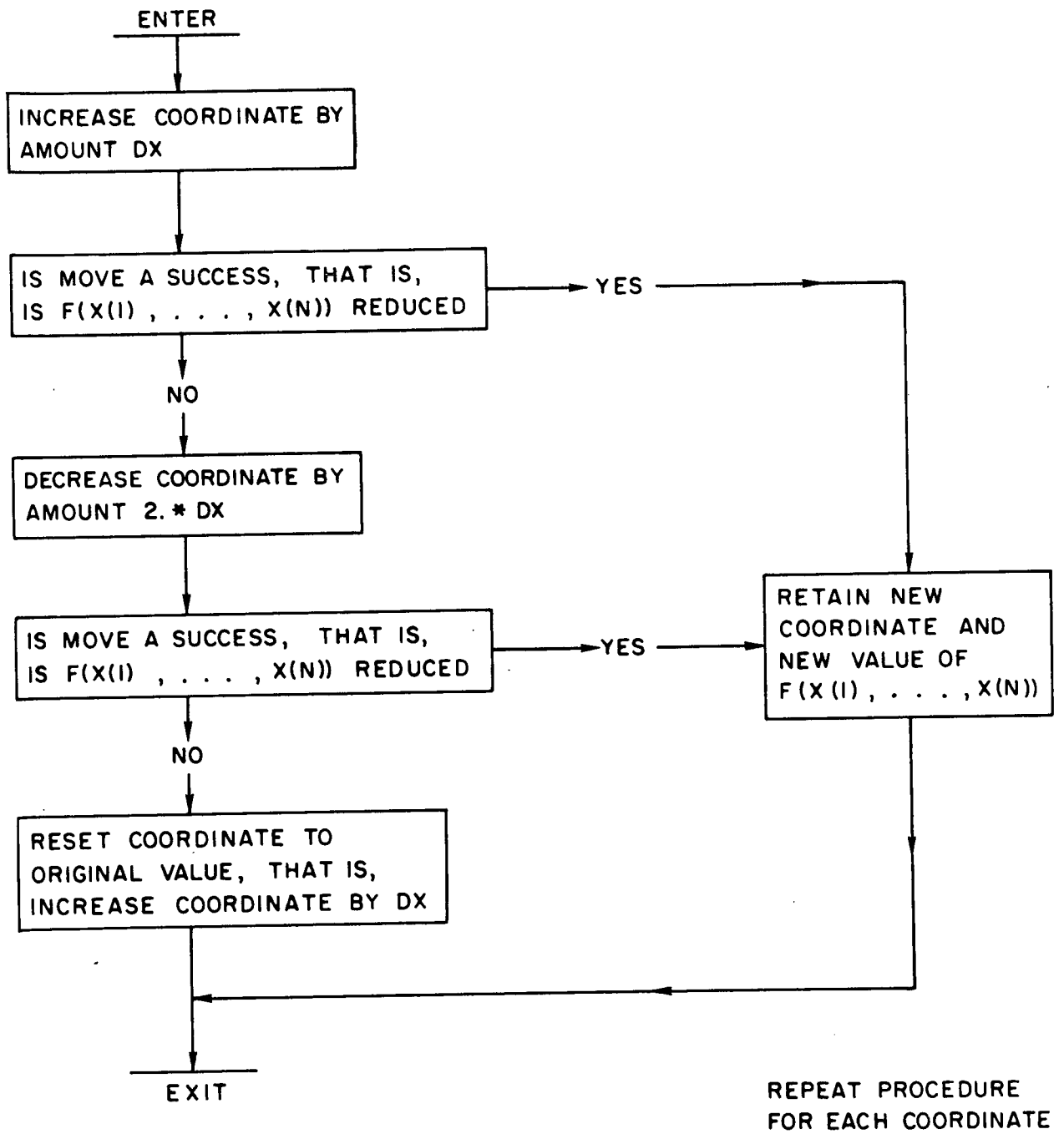

FIG. C-3

PATTERN MOVE